AR-010-389

An Investigation of F/A-18 AMAD Gearbox Driveshaft Vibration

Brian Rebbechi, Madeleine Burchill, Gareth Coco

DSTO-TN-0121

] APPROVED FOR PUBLIC RELEASE

DEPARTMENT ◆ OF DEFENCE
DEFENCE SCIENCE AND TECHNOLOGY ORGANISATION

An Investigation of F/A-18 AMAD Gearbox Driveshaft Vibration

Brian Rebbechi, Madeleine Burchill, Gareth Coco

Airframes and Engines Division
Aeronautical and Maritime Research Laboratory

DSTO-TN-0121

ABSTRACT

The RAAF has experienced several failures of the input bearing of the F/A-18 AMAD (Aircraft Mounted Accessory Drive) gearbox. Two of these failures have resulted in in-flight fires. Measurements of input housing vibration showed very high vibration levels on some aircraft, apparently due to unbalance in the driveshaft assembly. Subsequent measurement of drive-shaft motion confirmed synchronous forward whirl of the driveshaft. The driveshaft system appears to operate below its first critical speed, but there are indications that the first critical speed may not be far above running speed. There is no evidence of significant driveshaft system resonances during the operating speed range of idle to full military power. The unbalance appears to result primarily from clearances in the AMAD gearbox input shaft assembly. These clearances will bring about an initial unbalance of the assembly much greater than specified component tolerances. Partial alleviation of the high vibration has been brought about by rotation of the 19E215-1 driveshaft relative to the input power take-off shaft assembly.

Published by

DSTO Aeronautical and Maritime Research Laboratory
PO Box 4331
Melbourne Victoria 3001 Australia

Telephone: (03) 9626 7000
Fax: (03) 9626 7999

AR-010-389
November 1997

APPROVED FOR PUBLIC RELEASE

An Investigation of F/A-18 AMAD Gearbox Driveshaft Vibration

Executive Summary

Failure of the input bearing of the F/A-18 AMAD (Aircraft Mounted Accessory Drive) gearbox has resulted in two in-flight fires in RAAF aircraft. The first fire was in aircraft A21-045 in February 1993. The second fire, in aircraft A21-022, occurred in November 1993, and caused significant heat damage to the internal bulkhead which necessitated major repair of the airframe at the US Navy Depot San Diego. This report is a summary of the preliminary investigation by AMRL into the vibratory behaviour of the drivetrain.

The conclusions reached at this point in the investigation are as follows:

(a) AMAD gearbox input housing vibration measurements have shown very high vibration levels on some aircraft. The vibration appears to be largely due to unbalance in the driveshaft assembly.

(b) Measurements of drive-shaft motion have confirmed synchronous forward whirl of the driveshaft which couples the engine to the AMAD gearbox. The driveshaft orbits are nearly circular.

(c) The driveshaft system appears to operate below its first critical speed, but the rapid increase in vibration levels at the higher speeds indicates that the first critical speed may not be far above running speed. There is no evidence of significant driveshaft system resonances during the operating speed range of idle to full military power.

(d) The primary cause of unbalance appears to be excessive clearances in the AMAD gearbox input shaft assembly. These clearances will bring about an initial unbalance of the assembly much greater than individual component balance factors.

(e) Rotation of the 19E215 driveshaft relative to the input PTS assembly can bring about significant reductions in vibration levels. This procedure has been incorporated as a routine RAAF maintenance action under STI-H-333 "Vibration Monitoring Program for AMADS".

Contents

1. Introduction

Failure of the input bearing of the F/A-18 AMAD (Aircraft Mounted Accessory Drive) gearbox has resulted in two in-flight fires in RAAF aircraft. The first fire was in aircraft A21-045 in February 1993. The second fire, in aircraft A21-022, occurred in November 1993, and caused significant heat damage to the internal bulkhead which necessitated major repair of the airframe at the US Navy Depot San Diego.

The seriousness of the second fire, and the indication that it was not an isolated occurrence, drew increased attention to the problem. This led the RAAF TFLMSQN to request an investigation by AMRL into the dynamic behaviour of the drive system, and the influence that this may have on bearing failure [1][1]. This report is a summary of the preliminary investigation by AMRL into the vibratory behaviour of the drivetrain. It is intended as an interim report; the investigation is not yet complete. The investigation by AMRL into the metallurgical aspects of the failures has been separately reported [2].

The input bearing is not the only component within the AMAD gearbox to cause problems. Undiagnosed "metal contamination" has been responsible for a higher than expected rate of unscheduled maintenance actions on the gearbox. Aside from the input bearing, other components within the gearbox have displayed problems - loose bearing cage pins, oil pump drive shearing (due to the ingress of debris to the pump) and failure of oil pump drive gears. Deterioration of the gearbox elastomeric top mount, and the semi-spherical metal side mounts has also been a problem. Whilst the gearbox displays a lower than desired reliability for these various reasons, the failure of the aft power take-off shaft (PTS) input bearing is a particular concern because of the resulting in-flight fires.

In general, high speed power transmission shafts can cause problems for several reasons. The high speed offers advantages of reduced size and weight, as the torque is reduced for the same power transmission. However, the disadvantages are a reduced tolerance for balance and misalignment, and a closer proximity to system critical speeds, which may be lower due to the weight reduction that follows the lower torque requirement. With an external shaft it is difficult to closely control alignment. The couplings necessarily need to be sufficiently flexible to accommodate misalignment, and axial movement usually has to be accommodated. Both these factors tend to lower the shaft critical speed.

There are no comparable studies on the F/A-18 AMAD gearbox drive system dynamic behaviour available to the authors at the present time. The vibration surveys that are available relate to the response of the gearbox to external vibratory loads [3]. These loads simulate airframe vibration which is input through the gearbox mounting points,

[1] References are listed at the end of the report.

and are presumably representative of the buffet loading on the horizontal stabilator at high angles of attack.

Although specific references to the F/A-18 system are not available, several similar investigations are relevant [4] - [7]. References [4] and [5] describe the development of a power takeoff system for the X-29A PTO/AMAD, which was powered by the same engine (a General Electric F404), and runs at the same rpm as the F/A-18, but utilised a considerably longer driveshaft. References [6] and [7] describe an unstable subsynchronous vibration encountered in development of the F-16 engine start system power takeoff system. Reference [8] contains relevant general design information for high-speed drive systems. These references show that seemingly quite small design changes can have a large effect on the system dynamic behaviour.

The objective of this report is to describe the results of the AMRL preliminary investigation. With the exception of a set of measurements carried out on the AMAD gearbox post-overhaul test rig at Lucas Aerospace Sydney, all of the measurements were carried out on RAAF aircraft, and include casing vibration, and driveshaft dynamic mode shapes as measured by proximity probes at six locations. Measurements were also undertaken of driveshaft static side-clearances, in order to allow computation of an estimate of bearing dynamic load. Video recordings of shaft strobed motion were also made, and a still frame from these recordings is included in this report.

2. AMAD Gearbox System Description

Figure 1 shows the location of the two AMAD gearboxes in the F/A-18 aircraft. The AMAD gearbox is powered by a high speed drive from the General Electric F404 engine. The drive is geared at a ratio of 1:1 through two right-angled drives from the high-speed engine rotor (16810 rpm being 100% speed). The AMAD gearbox has several accessory pads, and mounted on the front face are the electrical generator, hydraulic pump, fuel boost pump and air turbine starter. Figure 2 shows the overall layout, Fig. 3 a cross-section through the input housing, and Figs. 4-6 show front, top and rear views of the gearbox. When starting, the power flow is in a 'reverse' direction from the air turbine starter through the AMAD gearbox to the engine. A manually-operated free-wheel is incorporated in the AMAD gearbox input to enable disconnection of the drive to the engine so as to permit ground running of the accessories from the air turbine. The gearbox is mounted in two steel spherical mounts each side of the gearbox, with an upper elastomeric mount. The lower inboard mount is fixed, the outer one sliding on the spindle (Fig. 7), as is the practice with the main engine mounts. Additional restraint to the gearbox is brought about by the fuel and hydraulic pipe connections to the fuel boost pump and hydraulic pump.

Gearbox ratios and PTS bearing characteristic frequencies are listed in Table 1. A schematic of the gear train is shown in Fig. 8, and the derivation of the PTS bearing

characteristic frequencies is given in Appendix 1. Figure 9 shows the transmission driveshaft. The driveshaft (which is referred to either as the LAPTC - Lucas Aerospace Power Transmission Company, or simply 19E215-1 shaft), is composed almost entirely of titanium, the only steel components being the drive flange at the engine end, which also incorporates shear bolts, and the captive flange attachment bolts. A manufacturer's drawing could not be obtained for this shaft, and as a result, key dimensions were obtained by direct measurement of the shaft involved in the in-flight fire in A21-022. In addition, the transverse and angular coupling stiffness, and shaft mass parameters were experimentally evaluated, using the same shaft. The dimensions, masses and stiffnesses thus obtained are given in Appendix 2 (the shaft dimensions are also included in Fig. 9).

The PTS input shaft -348 is free (within limits) to move axially within the -347 sleeve (Fig. 10). The -347 sleeve is supported by two identical ball bearings and is isolated from gear side loads, as the drive gear is itself supported on two separate bearings (see Fig. 3). The housing dimension in the axial direction is checked and adjusted before assembly so that there is between 0.002 and 0.004 ins (0.051 to 0.102 mm) end-clearance for the bearing outer races. The bearings are deep-groove plain ball-bearings. The cage is bronze, with steel pins. Ref. [2] provides further details on bearing construction. There is no specific control over bearing axial pre-load. The -348 shaft is located within the -347 sleeve at the diameters A and B in Fig. 10; manufacturing tolerances of the -347 and -348 shafts shown in Fig. 10 result in radial clearances at these two points ranging between 0.0013 in and 0.0028 in (0.033 to 0.071 mm). This clearance is large in comparison with the balance tolerance of the -348 shaft which is 0.002 oz-in at the flange end, equivalent to a centre-of-mass eccentricity of 0.00012 in (0.0031 mm), as the flange end weighs 16 oz. The implications of this clearance is further discussed in Section 10.

3. Test Equipment

3.1 Casing Vibration

The casing vibration was measured by four Endevco 7251-10 Integrated Circuit Piezoelectric (ICP) accelerometers, with a nominal sensitivity of 10 mV/g. A PCB model 483A02 amplifier was used for signal conditioning and amplification. The data were recorded with a SONY PC-204 digital tape recorder, which has a frequency response of DC to 20 kHz on X2 speed. Frequency domain analysis was variously carried out using a Bruel & Kjaer 2034 FFT analyser, a CSI 2400 analyser, or an AMRL-developed vibration analysis system. The signal conditioning system was calibrated before and after use. The input PTS housing vibration measurements were carried out by attaching the accelerometers to a steel or aluminium block glued to the housing using Loctite 324 Speedbonder Structural Adhesive (activator 707) as shown in Fig. 11. The subsequent fleet-wide trials by the RAAF used the faster-drying Loctite 401 (cyanoacrylate 'super-glue') for attachment of this block to the input housing. For

the initial measurements, another location was also used, on the base of the gearbox (Fig. 12), where a bracket was attached to the earth-lug stud. The directions of the accelerometers tri-axially mounted on the block are referred to here as axial, radial and tangential (Fig. 11). The location on the input housing was chosen because of its close proximity to the input bearing, so that the motion would reflect to some extent the environment the bearing was subject to. The accelerometers had an insulated base and were electrically isolated from the gearbox and hence the airframe. For high-power runs, testing was carried out in a dedicated installed-engine runup area; testing up to 80% speed[2] could be carried out on the flight-line.

3.2 Driveshaft Vibration

Driveshaft vibration (displacement) was recorded with eddy-current proximity probes. Initial shaft run-out was recorded with a single Kaman KD2400 eddy-current probe (8mm dia probe tip) mounted at a average gap from the shaft of 0.10 ins (2.5 mm). Later displacement measurements were made with a pair of Indikon AP 1390-2 eddy-current proximity probes (0.38 inch/9.6mm dia tip) which were specifically calibrated for this application to provide a linear sensitivity of 100 mV/mil when used with the titanium driveshaft. Eddy-current probe systems calibrated for steel are unsuitable for titanium, having reduced range and linearity. The AP 1390 probes were operated at a mean shaft gap of around 0.150 ins (3.8 mm). When two probes are used in close proximity on a shaft then a distinct beat frequency is evident at the difference frequency between the probe carrier frequencies, due to electrical cross-talk. This is a problem when using unfiltered time-domain data, but is not a problem in the frequency domain as the beat frequency in this case was around 1600 Hz, well above the shaft frequency. The probes were mounted on a frame fastened to the underside of the aircraft, and the shaft orbit recorded at three axial locations. The included angle between the probes was 90 degrees, and as only two probes were available, successive recordings were made for each axial position, while retaining the same tacho reference position on the driveshaft.

3.3 Vibration Units

Appendix 3 contains a brief description of the relationship between displacement, velocity and acceleration, for a sinusoidal vibration. In this report, vibration is expressed typically in terms of 'g'[3] rms if acceleration, in/sec rms if velocity, and peak-peak mils (1 mil = 0.001 inch) if displacement. Either velocity or displacement are the usual units for specification of aircraft system vibration; displacement is *usually* peak-peak but velocity units may be either average, rms or peak. Vibration units are

[2] For the F404 engine the percentage engine power refers to the percentage of maximum speed of the high-speed rotor - 16810 rpm being 100%. During ground testing, the maximum engine speed obtainable at full throttle 'military power' (max dry) was usually around 94%. The precise figure is a function of ambient air temperature, a lower ambient resulting in a lower speed.

[3] 1 'g' is the acceleration due to gravity, 9.8 m/s^2 (32.2 ft/s^2, 386.4 in/s^2).

sometimes not clearly stated, and can never be assumed to be one or the other. For example, vibration limits for the F404 engine are specified by General Electric in terms of an average velocity, whereas the Chadwick-Helmuth 192A recording equipment gives a peak velocity reading.

The phase convention used in this report is that the signal phase is relative to the tacho, i.e. a positive phase is a phase lead of the vibration signal (which may be from a shaft displacement probe or an accelerometer). This is not necessarily the same as that used elsewhere.

4. Initial Aircraft Vibration Measurements

4.1 Aircraft A21-116 And A21-04

4.1.1 Details of Measurements

4.1.1.1 Aircraft A21-116

Aircraft A21-116 is a two seat aircraft, operated by RAAF 2 OCU Squadron, Williamtown. This aircraft was chosen as the first aircraft on which to carry out vibration measurements, because it was available due to an unrelated unserviceability. The initial measurements were carried out using the tri-axial group of accelerometers (Fig. 11) and an additional accelerometer mounted on the base of the AMAD gearbox (Fig. 12). Due to the presence of the generator, the top of the gearcase was not accessible. The location at the base of the gearbox was chosen to give an indication of vibration levels in other regions of the gear casing, but the position on the input bearing (Fig. 11) was expected to more closely reflect the bearing environment.

The initial tests were repeated in an attempt to increase AMAD gearbox drive torque loading via electrical and hydraulic demand, which would increase accessory drive-power requirements.

A summary of the results from the vibration measurements on the left and right-side gearboxes is given in Table 2. The vibration amplitude vs frequency for the triaxial group of accelerometers is given in Figure 13. The vibration amplitude of the once/per revolution component is plotted vs speed in figs 14 (a)-(c) for the left-side, and Fig. 14(d) for the right-side.

The abnormally high vibration levels observed led to the speculation that large shaft amplitudes may be present. As a result, a test was planned to reveal if the shaft motion could be visually observed with a synchronous strobe-light running at a slight slip frequency, so as to give motion visualisation. The image was video-taped to enable remote observation. The question of how to video-tape a strobed image, and the possible problems due to framing-rate and exposure time were resolved by a simple practical demonstration with a low-speed multi-bladed fan. The results showed that a

standard video camera produced good results (tests with a high shutter speed resulted in gaps in the image). The videoing was then carried out by connecting a timing signal from a shaft tacho to the strobe-unit, and adjusting the slip frequency to produce the desired effect. The shaft was then video-taped from several angles. Figure 15 shows an image from the camera.

In order to quantify this motion, the shaft displacement was recorded with a proximity probe (Kaman KD2400), the probe system being first calibrated on a actual shaft. A tachometer once/revolution signal, using reflective tape on the 19E215-1 shaft, was also obtained. The results from this recording are given in Table 3 and plotted in Fig. 16. Figure 17 shows the positioning of the proximity probe. Slow-roll run-out was not available from these tests, as at this point the tacho had to be disconnected before engine run-down, due to the possibility of the wing flap striking the open AMAD gearbox bay doors.

4.1.1.2 Aircraft A21-04

Due to the extremely high levels of vibration recorded on aircraft A21-116, another aircraft was selected at random to see if this high vibration occurred in more than one aircraft. Aircraft A21-04, a single-seat aircraft, was selected. The measurement system was the same as for the initial tests on A21-116, that is the tri-axial accelerometer mount on the AMAD input housing (Fig. 11), but the accelerometer on the base of the gearcase was deleted. Both left and right-side gearbox vibration levels were recorded. The results for run-up and run-down are given in Figs. 18(a)-(d).

4.1.2 Discussion

The vibration levels recorded during this initial trial were exceptionally high for aircraft A21-116, and lower, but still higher than desirable, for aircraft A21-04. These were the only aircraft for which vibration levels were available, so that at this point it was not known if they were indicative of fleet-wide levels. Several conclusions could be drawn from these initial measurements however, and these were that:

(a) The vibration levels recorded were much greater than considered acceptable for this class of machinery. Levels tolerated in aircraft tend to be higher than that considered acceptable for industrial equipment, however a level of 1.5 in/s peak velocity is generally considered to be an upper limit. For example, levels for the GE F404 engine over 1.0 in/s average, (which is equivalent to 1.57 in/s peak) are considered an upper limit.

(b) The vibration was predominantly at shaft speed, that is a frequency component of once-per-revolution, almost certainly caused by a large unbalance in the rotating assembly.

(c) Misalignment could conceivably be a factor, but in view of the absence of large vibration at twice/rev, and the absence of a large axial component, it is not likely. Also, checks of the alignment of this assembly showed it to be within tolerance.

The video tape provided graphic evidence of sizeable run-out of the 19E215-1 shaft and of the input PTS shaft (-348). During run-up in the region 75-80% the diaphragm coupling flanges passed through several modes. Subsequent analysis of shaft vibration amplitude and phase showed little connection with this mode, so that it appears to have been localised to the coupling assembly. Visual observation suggested that dynamic shaft motion could be as large as 0.060 inches peak-peak, and this was confirmed by the eddy-current proximity probe measurement (Fig. 16).

The shaft motion comprised almost entirely of a once per revolution frequency component over the entire speed range. There was no evidence of any significant non-synchronous vibration, and it is presumed (although this could not be absolutely confirmed at this stage) that the vibration is forward whirl, as there is no reason to expect otherwise.

Notable features of the vibration measurements during engine run-up are:

(a) An absence of resonances in casing or shaft motion, as confirmed by amplitude and phase measurements.

(b) A change in phase of the shaft once per revolution frequency component, and the increasing amplitude with engine rpm suggests that the shaft was approaching its first significant critical speed.

The input housing assembly of the AMAD gearbox on the left-side of aircraft A21-116 was subsequently removed, and the input casing was found to be cracked in two locations, on the housing flange. Also, the housing retaining nuts were found to have low tension, and there was evidence of heavy fretting on the input housing and mating gearcase flange. Later examination of the aft PTS bearing showed loose cage pins, heavy bearing on the cage, and contamination on the raceway.

A factor that may be relevant to the high vibration levels recorded in aircraft A21-116 is that this aircraft had sustained at one time very high 'g' levels (beyond normal flight limits). Whether this is a coincidence or not is a matter for speculation. There is no current misalignment of the input shaft on the left-side.

5. Aircraft A21-51, 114, 06, 21 and 25

To develop an improved data-base of typical fleet aircraft vibration levels, a random sample of 5 aircraft were tested. Initially nine aircraft were to be evaluated, but the time involved in testing precluded this, as they were run to military power (max. dry, typically 94%) - at this power level the aircraft were required to be tested in a specialised run-up area.

5.1 Details of measurements

Vibration was recorded using the block glued to the PTS input housing as in Fig. 11, but using only the radial and tangential accelerometers. The 19E215-1 shaft dynamic motion was recorded using the single Kaman KD2400 probe system as in Fig. 17, and the shaft motion was video-taped using the synchronous strobe (running at a small slip frequency). A once-per-revolution tacho signal was obtained from the 19E215-1 shaft, using a piece of reflective tape and an optical sensor. The accelerometer vibration data, shaft displacement and tacho pulse were again recorded on the SONY PC-204 4-channel tape recorder.

5.2 Results

The maximum shaft displacements of the right-side AMAD gearbox units on aircraft A21-114 and A21-21 were found to be higher than for the other units tested. The maximum shaft displacement for both gearboxes was 0.069 inches peak-peak at military power (96% and 94% respectively). The shaft displacements on the other units tested was found to be in the region of 0.040 to 0.050 inches peak-peak at military power. The results of peak shaft displacement and tangential vibration (on the AMAD gearbox input housing) are summarised in Table 4. In Table 5, shaft dynamic displacement versus speed is given for run-up and run-down. These results are also plotted in Figs. 19 (a)-(e). Figure 20 is a plot of the frequency spectra of the RHS shaft displacement for aircraft A21-06. Table 6 summarises the harmonic content of the casing vibration.

6. Analysis of Aircraft A21-39 and A21-52 with AMRL Equipment and Chadwick-Helmuth 192A Analyser, and Effect of Shaft Rotation

In view of the likely correlation between high AMAD gearbox input housing vibration levels and susceptibility of PTS bearing failure, the decision was taken by the RAAF TFLMSQN to introduce fleet-wide vibration checks. Additionally, it was proposed to investigate the possibility of introducing a procedure to rotate the 19E215-1 drive-shaft relative to the input PTS, to minimise vibration, and hence bearing loads. The 19E215-1 driveshaft is attached to the input PTS by three bolts at equal radius, at an even circumferential spacing of 120 degrees. There is no restriction on the driveshaft being attached in any of the three possible positions. Accordingly, a trial was carried out to compare the Chadwick-Helmuth 192A analyser readings (using the tangential location on the input housing), with that obtained using AMRL equipment, and rotate the driveshaft. The Chadwick-Helmuth analyser was selected for this trial as it was already in service with the RAAF, and it was anticipated that it would be used for the fleet-wide survey.

6.1 Details of Measurements

The vibration transducers were mounted in the tangential direction (as in Fig. 11). The Endevco 7251-10 accelerometer and the Chadwick-Helmuth 192A transducer (termed a Velometer by Chadwick-Helmuth, as the transducer incorporates charge conversion and integration), were mounted alternately on the same block, using an adaptor to convert from the 1/4 inch UNF thread of the velometer to the 4mm ISO thread of the Endevco accelerometer. As in earlier trials, a once per revolution shaft tacho-pulse and the shaft displacement were also recorded. The tests were carried out on the aircraft flight-line, and as a result the engine speed was restricted to 80% (226Hz, 13448 rpm of N1) for environmental and safety reasons. The time taken overall for the testing was much reduced in comparison with high-power runs, which necessitated towing of the aircraft to a specialised area well removed from the flight-line.

6.2 Discussion of results

The results, summarised in Appendix 4, showed close agreement between the Chadwick-Helmuth 192A analyser and the Endevco equipment, as could be expected. An interesting result from the run of A21-039 was that the casing vibration phase of the once/revolution vibration relative to the once/revolution shaft tacho pulse remained substantially constant relative to input PTS (-348) position, as evidenced by the fact that the phase lagged by approximately an additional 120 degrees each time the shaft was rotated 120 degrees CW (in the direction of rotation), the reflective tape for the tacho remaining in the same position on the 19E215-1 shaft. The phase convention used here is that the signal phase is relative to the tacho pulse, i.e. a positive phase is a phase lead.

Rotation of the 19E215-1 shaft relative to the AMAD input PTS can have a significant effect on vibration levels, as evidenced by measurements on A21-39 left-side AMAD gearbox. Here the variation between maximum and minimum was 1.2 in/s to 0.69 in/s peak (Appendix 4). The subsequent fleet wide survey by the RAAF [9] has shown the results to be repeatable in nearly all cases, and reductions of over 50% on some aircraft have been achieved by this technique.

7. Comparison of Vibration Levels between Left and Right Side Gearbox, and 80/94% Engine Speed

For routine testing of AMAD gearbox vibration it is desirable for the tests to be carried out on the flight-line, where engine rpm is restricted to 80%. Accordingly, a survey was carried out of all the vibration results obtained to date to see if a consistent relationship between values at 80% and 94% existed, so that a factor could be arrived at to estimate peak values from the lower speed 80% testing. In addition, the left and

right-side values were compared, as were the outputs from the three transducers of the tri-axial transducer mount (Fig 11).

7.1 Discussion of results

The results of this survey are given in Tables 7(a)-7(b), with the overall findings summarised in Appendix 5. The decision was made to use the tangential direction accelerometer for the subsequent fleet-wide monitoring programme, because of several factors:

(a) The tangential levels were higher.
(b) The tangential direction was the most accessible on both sides of the aircraft for the Chadwick-Helmuth 192A transducer.

It should be noted that the term tangential accelerometer refers to the position of the accelerometer on the tri-axial mount (Fig. 11). It is to be expected that input housing displacement recorded by this accelerometer will be effectively the same as a radial accelerometer located 90 degrees around the input housing from the mount location.

The overall conclusions were that a comparison factor of vibration at 80% rpm to vibration at 94% rpm of 0.35 was appropriate to the right-side AMAD gearbox, and 0.48 was appropriate to the left-side. During most of the testing to date, speeds above 94% were not attained due to ground ambient conditions.

8. Aircraft A21-035

Further analysis of gearbox vibration was carried out for aircraft A21-035 stationed at RAAF Tindal. The left-side AMAD had vibration levels, using the standard RAAF Special Technical Instruction procedure, that were close to the maximum considered desirable. The results of the analysis carried out by AMRL are shown in Fig. 21, and are interesting for the increase around 80%; in this instance the ratio between 80% and 94% engine speeds being, at 0.48, almost exactly the average ratio proposed in Section 7.

9. Drive System and AMAD Gearbox Dynamic Behaviour

9.1 Aircraft Installation Drive system Dynamic Behaviour A21-102

9.1.1 Details of Test Equipment

Initial recordings of the 19E215-1 driveshaft motion were limited to measurements at one location (Fig. 17). In order to gain a more complete picture of the driveshaft dynamic behaviour, in particular the shaft orbits at various axial locations, a new fixture was constructed as shown in Fig. 22. This fixture was attached to the airframe as in Fig. 23 (a)-(b). Two Indikon AP 1390-2 eddy-current proximity probes were mounted successively at each of the three axial positions. An additional mount point close to the input PTS was found to be unusable due to the close proximity of the coupling diaphragm. The probe system was specially calibrated by Indikon to provide a sensitivity of 100 mV/mil when used with the titanium tube. The probes were check-calibrated on a shaft upon receipt and found, within the limits of very small non-linearity, to have this sensitivity.

The probe layout is sketched in Fig. 24, and the axial mounting dimensions are shown in Fig. 9. The probes were mounted at 90 degrees relative to one another, and the probes were quite large at 9.5 mm (0.375 in) tip diameter so as to enable a sufficiently large gap from the driveshaft to prevent the possibility of tube damage. This relatively large clearance was important for two reasons - the frame was not able to be precisely located relative to the drive-shaft, and the tests were carried out on operational aircraft. Accelerometers were mounted adjacent to the displacement probes, so as to monitor absolute probe motion in case of resonances of the mounting frame which would change the displacement measurement. Initially there were concerns over the possibility of the relatively close proximity of the balance rings affecting the probe response, but this was found not to be a problem.

For all the recordings the reflective tape used with the optical tacho remained in the same position on the 19E215-1 shaft, so as to enable consistent phase relationship as the probes were shifted to the different axial locations. Additionally, AMAD gearbox input casing vibration for the radial and tangential directions was recorded.

9.1.2 Results and Discussion

The shaft dynamic orbits (1X component, slow-roll[4] corrected) are plotted in Figs. 25 (a)-(g). A line is drawn joining each orbit to indicate the point where the reflective tape on the shaft is co-incident with the optical tacho probe. Orbit directions are shown with the arrow. Notable features are the circularity of the orbits at the

[4] slow-roll refers to the shaft run-out errors evident at very slow speed, as a result of features such as shaft eccentricity and mounting errors.

AMAD gearbox end, and the small change in phase of the shaft amplitude with increasing speed, indicating that the critical speed is significantly higher than the speed reached during these tests. These plots also confirm the forward whirl of the orbits. Figure 26 shows the input PTS casing orbit (1X component) at maximum rpm. The small circle on the orbit indicates the point where the reflective tape was co-incident with the optical tacho probe. Appendix 6 provides a summary of shaft displacement (1X) amplitude and phase for each of the probe positions; Tables 8(a) and 8(b) list the casing vibration for the radial and tangential directions.

To indicate the harmonic content of the shaft orbits, the 1X, 2X and 3X data for one displacement probe position is summarised in Table 9. This shows the very low harmonic content of shaft motion. Also, from examination of dynamic shaft displacement frequency spectra there was no evidence of significant non-synchronous vibration, other than at the engine end of the drive-shaft. It was presumed that at this end, where amplitude is lower, that there is influence from the engine vibratory behaviour.

Further examination of the casing orbits was carried out for the earlier runs on A21-51 and A21-06, on left and right sides (see Sect 5). This was carried out to look further at the casing mode shapes, at the PTS input housing, and to compare the left and right side gearboxes. The resulting casing 'orbits' are plotted in Figs 27 (a)-(d), for the 1X component only. Notable is the similarity between left and right side, despite the mirror-image nature of the mounting configuration (about the aircraft centre-line) of the gearbox lower side mounts, where the inboard mount is fixed, and the outboard is sliding. These figures indicate that the casing vibration mode, at least at these frequencies, is more affected by the local gearbox configuration, such as the presence of the large and heavy generator (34 kg, 75 lbm) on the front face of the gearbox. The right and left side gearboxes are interchangeable, other than the lower mounts referred to above which are readily exchanged from one side to the other of the casing. The casing response (Table 8) shows significant harmonic content, to a greater degree than the shaft orbits.

9.2 Lucas Aerospace Test Stand Drive System Dynamic Behaviour

Further observations of drive-shaft dynamic behaviour and casing vibration were made on the AMAD gearbox post-overhaul test stand at Lucas Aerospace Sydney. The test stand is run up to an AMAD gearbox input speed of 18,000 rpm during acceptance tests, a significantly higher speed than possible in the aircraft (typically limited to 94% speed - 15800 rpm). Tests were carried out with the standard test rig shaft (a Kamatic shaft with single flexible coupling at each end), and with the F/A-18 19E215-1 shaft, which as far as could be ascertained, had not been used previously in the test rig.

9.2.1 Test Equipment

The test rig instrumentation comprised a tangentially-mounted accelerometer (Endevco 7251-10), as in the aircraft installation, and, for tests of the 19E215-1 shaft, two eddy-current displacement probes oriented at 90 degrees to each other. For the tests with the standard Kamatics test rig shaft, a single probe was used. The gearbox used for the test was Serial no. 1396, which had been returned for overhaul because of high vibration. Tests were carried out with the original PTS housing, and with a reconditioned housing, with new bearings as is prescribed standard overhaul procedure. Additionally, the shaft motion was video-taped with a synchronous strobe, as in the previous aircraft tests.

9.2.2 Results and Discussion

The test results are summarised in Table 10, and Nyquist plots for shaft run-up of the 19E215-1 shaft given in Fig. 28. Notable from Table 10 are the larger casing vibration levels and shaft amplitude with the 19E215-1 shaft. From the Nyquist plots (Fig. 28) the large increase in amplitude at the higher speeds, together with the phase change (lag) of vibration relative to the tacho signal, indicates that the critical speed would appear not very much beyond the 18000 rpm reached in testing. Why the 19E215-1 shaft exhibits a much larger vibration amplitude than the Kamatics shaft is not clear. Balance checks subsequent to these tests [10] showed the two 19E215-1 shafts to have a similar unbalance to the 'silver' Kamatics shaft, which was found to be 0.024 oz-inch at one end and 0.027-0.031 oz-inch at the other. The balance limits prescribed at the time of manufacture of the 19E215-1 shafts was 0.05 oz-inch at each end [11]. There are significant constructional differences between the two shafts, which could influence this behaviour. For example the 19E215-1 flexible coupling is further from the AMAD gearbox flange than for the 'silver' Kamatics shaft.

10. AMAD Gearbox Input PTS Assembly Clearances

The requirement for axial movement in the coupling from the engine to the AMAD gearbox has necessitated a sliding spline input PTS shaft (Fig. 3). The associated radial clearances can have a detrimental effect on PTS assembly balance, not just of the -348/-347 assembly, but also of the 19E215-1 driveshaft. Figure 29 shows an exaggerated view of the tilting that results from these clearances. The effect on a high-speed assembly is potentially quite large. For example, the clearance will cause a centre-of-mass eccentricity far in excess of the balance tolerance - the balance criterion for these components is 0.002 oz-inch, and the clearances (if at their maximum manufacturing tolerance), will result in an unbalance 10 times that figure. In addition, the clearance is magnified at the driveshaft flexible diaphragm, to the extent that side clearance at the coupling of 0.014 inch peak-peak was measured on an operational aircraft. This clearance effectively introduces a large initial unbalance into the drivetrain, which cannot be properly corrected by component balancing.

Manufacturing tolerances result in clearances at points A and B (Fig. 10 and Fig. 29), which range from a minimum of 0.0013 in to a maximum of 0.0028 in (0.033 - 0.071 mm). Measurements of in-service components indicate that clearances are within these tolerances, but can be expected to fall anywhere within this range.

Measurements of the clearances of the left and right assemblies on Aircraft A21-109 gave the results listed below (see also Fig.30). These clearances were assessed by rocking the shaft from side-to-side. Whilst subjective to some extent, the point at which the -348 comes into contact with the -347 sleeve can usually be clearly felt. The 'O' ring tends to centralise the -348 shaft in the -347 sleeve.

		PTS input	19E215-1	Casing
		p-p inches	p-p inches	Displ. p-p
		(fig. 30)	(fig. 30)	(fig. 30)
RHS A21-109	absolute	0.009 inches	0.016 inches	0.006 inches
RHS A21-109	Rel. casing	0.003	0.010	0.000
LHS A21-109	absolute	0.010	0.018	0.004
LHS A21-109	Rel. casing	0.006	0.014	0.000

These clearances have several implications:

(a) When in operation, the geometrical axis of the input PTS -348 cannot be expected to be precisely concentric with the rotational axis of the assembly as defined by the -347 sleeve. This is confirmed by inspection of any -347/-348 assembly, where there are typically signs of heavy bearing in just one angular region (Fig.31). This is to be expected, as it is not likely that the -348 PTS will centre itself.

(b) The lack of alignment of the -348 shaft will result in a centre-of-mass peak eccentricity of half of the clearance, that is, up to 0.0028/2 = 0.0014 ins, which is well in excess of the balance criterion of 0.002 oz in - note that 0.002 oz in is equivalent to centre-of-mass eccentricity of 0.00012 in (the flange end weighs 16 oz). Therefore the side clearance can introduce an unbalance into the assembly of more than ten times the balance tolerance of the -348 shaft.

(c) The side clearance also effectively unbalances the 19E215-1 shaft by a sizeable extent, due to both the transverse displacement and, more particularly, the angular misalignment introduced by the clearance (Fig. 32), as can be seen from the above table. This will introduce a large effective initial unbalance into this shaft assembly, far in excess of production balance tolerances.

It appears that the position that is taken up by the -348 PTS relative to the -347 sleeve appears not to be random chance, or a function of the unbalance in components, but is determined by the alignment of the spline axis of the -347/-348 shafts. Measurements have been undertaken on three assemblies at Lucas Aerospace Sydney. These

measurements demonstrated that when a torque was applied to the PTS shaft -348, when assembled with the -347, that the -348 took up a position that was coincident with the bearing marks on both assemblies. Further, measurements of the side force versus torque showed that a significant force was required to overcome this side movement of the -347 relative to the -348. This does not suggest, however, that correction of spline misalignment will improve matters. There is a tolerance on spline manufacture (pcd centre-line 0.002 ins), which, as a broaching operation is involved, is probably necessary. The accuracy of location of the -348 relative to the -347 can only effectively be determined by the tolerance on the diameters A,B,D and E (Figs. 10 and 29).

Further confirmation of this hypothesis was provided by vibration measurements on two AMAD gearboxes during the initial trials of the RAAF procedure of rotating the 19E215-1 driveshaft relative to the -348 input PTS, to minimise vibration (refer Section 6). During the course of these trials the vibration of the AMAD casing was recorded, as well as the phase of this vibration relative to a tacho signal from reflective tape on the 19E215-1 shaft. When the 19E215-1 shaft was rotated at intervals of 120 deg. relative to the input PTS, it was noted that the phase of the once per revolution vibration remained virtually constant relative to the angular position of the input PTS -348 shaft. This implied that the angular location of unbalance was determined by the -348 shaft, and almost unaffected by the 19E215-1 shaft position. This was despite the sizeable vibration reduction (approximately 40%) due to rotation of the 19E215-1 shaft. This observation, which at the time could not be explained, is consistent with the hypothesis put forward above.

Balancing of the -347/-348 shafts as an assembly is not practicable. As discussed above, significant clearance exists between these items. There is no obvious rationale for centring the -348 relative to the -347. Again, as described above, when in operation the -348 adopts a particular position relative to the -347, which appears (as evidenced by bearing marks) to be consistently in the one position, but it cannot be assumed that this will always be the case. It makes little sense to centre the -348 relative to the -347 for balance purposes, as it does not run at this position. Trim-balancing of this particular assembly, aside from the problem of finding a suitable means of attaching weights, is not desirable where the unbalance is caused by the side clearance in the -347/-348 assembly. Reduction of the clearances A-E and B-D (Fig. 10), to the minimum possible commensurate with allowing relative sliding, will assist in reducing the clearance-induced unbalance of the drive system.

11. Side Mount Wear

Wear of the lower side mounts, particularly the sliding mount (Fig. 7), is a continuing problem. A feature of this that may at times be overlooked is the very high aerodynamic buffet loading on the rear of the fuselage at high angles of attack, caused by bursting of the vortex from the leading edge extensions (LEX's) near the vertical

and horizontal stabilators. This can introduce vertical accelerations as measured at the engine mounts of 2.5g rms and over 5g peak, at 20 deg angle of attack [12]. It is probable that the vibratory environment in the region of the AMAD gearbox attachment points is similar. The AMAD gearbox total weight (with accessories) is in excess of 91 kg (200 lbm), so that the buffet loads, coupled with a constant manoeuvring 'g' load, will create a severe environment for the two lower mounts. In contrast, the vibratory load at the mounts due to driveshaft vibration is likely to be appreciably less. The initial survey on Aircraft A21-116 showed that the AMAD gearbox casing vibration level during ground running was significantly less at the base of the gearbox than at the PTS housing. The considerable weight of the gearbox plus accessories can be expected to minimise transmission of vibration from the driveshaft to the mounts. Conversely, in the presence of an externally introduced vibration such as manoeuvring and buffet loading, this sizeable gearbox mass will act to increase the load on the gearbox mounts. In addition, the frequency content of the buffet loading spectrum is such that the fundamental bending modes of the gearcase, for example the 27 Hz vertical resonance [3], could be excited, thus dynamically magnifying the loading.

12. Conclusions

(a) AMAD gearbox input housing vibration measurements have shown very high vibration levels on some aircraft. The vibration appears largely due to unbalance in the driveshaft assembly.

(b) Measurements of drive-shaft motion have confirmed synchronous forward whirl of the driveshaft which couples the engine to the AMAD gearbox The driveshaft orbits are nearly circular.

(c) The driveshaft system appears to operate below its first critical speed, but the rapid increase in vibration levels at the higher speeds indicates that the first critical speed may not be far above running speed. There is no evidence of significant driveshaft system resonances during the operating speed range of idle to full military power.

(d) The primary cause of unbalance appears to be clearances in the AMAD gearbox input shaft assembly, in particular of the -347/-348 shafts. These clearances will bring about an initial unbalance of the assembly much greater than individual component balance factors.

(e) Rotation of the 19E215-1 driveshaft relative to the input PTS assembly can bring about significant reductions in vibration levels.

13. References

1. Letter to AMRL from RAAF TFLMSQN. AMRL Ref. C2/284 15 Feb 1994

2. Sharp, K., Byrnes, R., Goldsmith, N. T., "Summary of investigations into F/A-18 AMAD Bearing Failures". AMRL AED Defect Assessment and Failure Analysis Investigation No. M91/95, July 1995.

3. Fairchild, M. K., "F-18A Airframe Mounted Auxiliary Drive (SN002) Vibration Test". Report No. NOR 79-313. Feb 1979. Northrop Corporation Hawthorne, Ca.

4. Johnson, H. F., Maresko, W. A., "Critical Speed Testing of the Grumman X-29A Power Take-Off Shaft Subsystem". SAE paper 841603 Oct 1984.

5. Gargiulo, D . J. "Design and Development of a Power Takeoff Shaft" SAE Paper 85-4045 Oct 1985. AIAA/AHS/ASEE Aircraft Design Systems and Operations Meeting, Colorado Springs, CO Oct 14-16 1985.

6. Kershisnik, M., and Harding, E., "An Unstable Subsynchronous Critical Speed Solution", SAE Technical Paper 781055 Nov. 1978.

7. "F-16 PTO Shaft Vibrations". Engineering Report AER 1866. Sundstrand Advanced Technology Operations, Rockford, Illinois. November 1981.

8. Ferguson, H. F., and Stocco, J. A., "Avoiding Destructive Shaft Vibrations", *Machine Design*. June 7 1984 pp 96-98.

9. RAAF TFLM AMAD Vibration Data Base. June 1995.

10. Gatehouse, G., "F/A-18 AMAD Driveshaft Investigation". Ref GRG/BK/ MIL-ENG-0513 23 December 1994.

11. Bendix Test Specification No. U 1778, Rev C, 19E215-1 Power Transmission Shaft.

12. Private communication from Witold Waldman, AMRL (re data from results of ARDU F/A-18 Trial 0174), 1996.

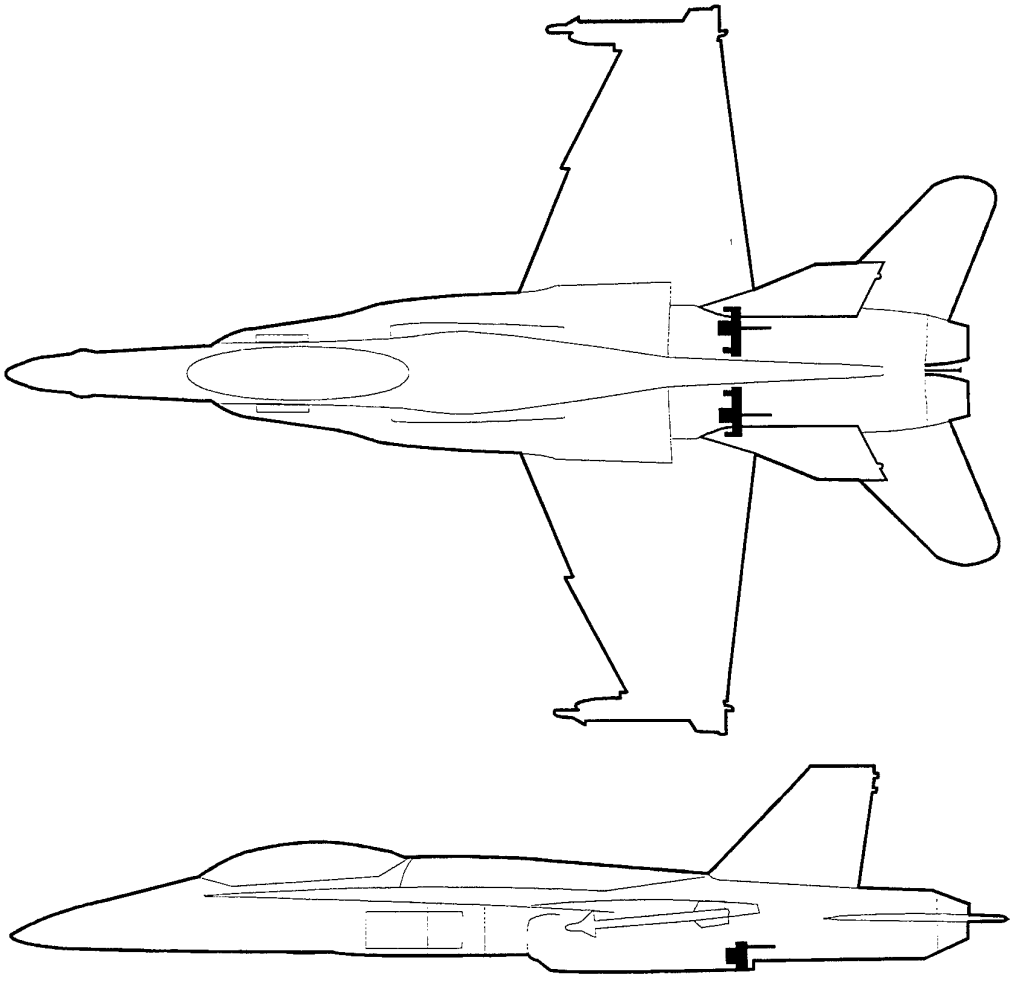

Figure 1 Aircraft location of AMAD

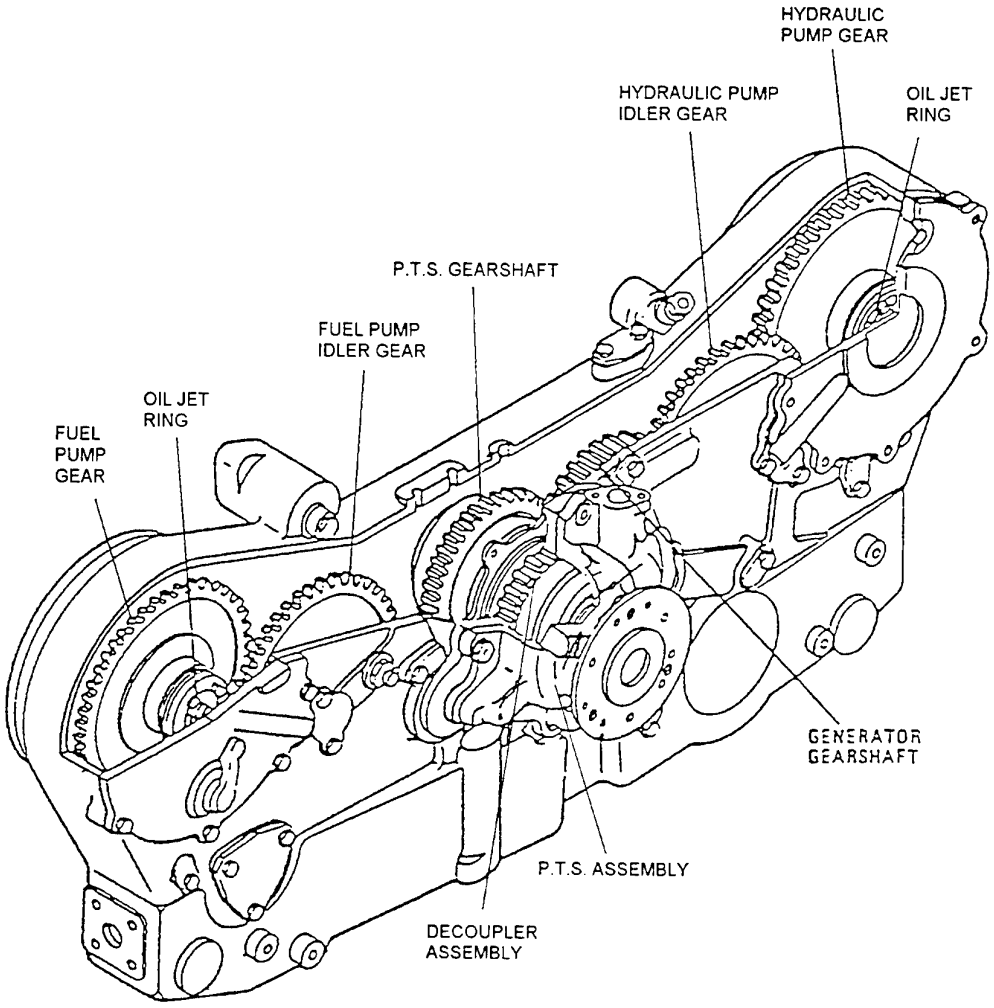

Figure 2 Overall layout of AMAD

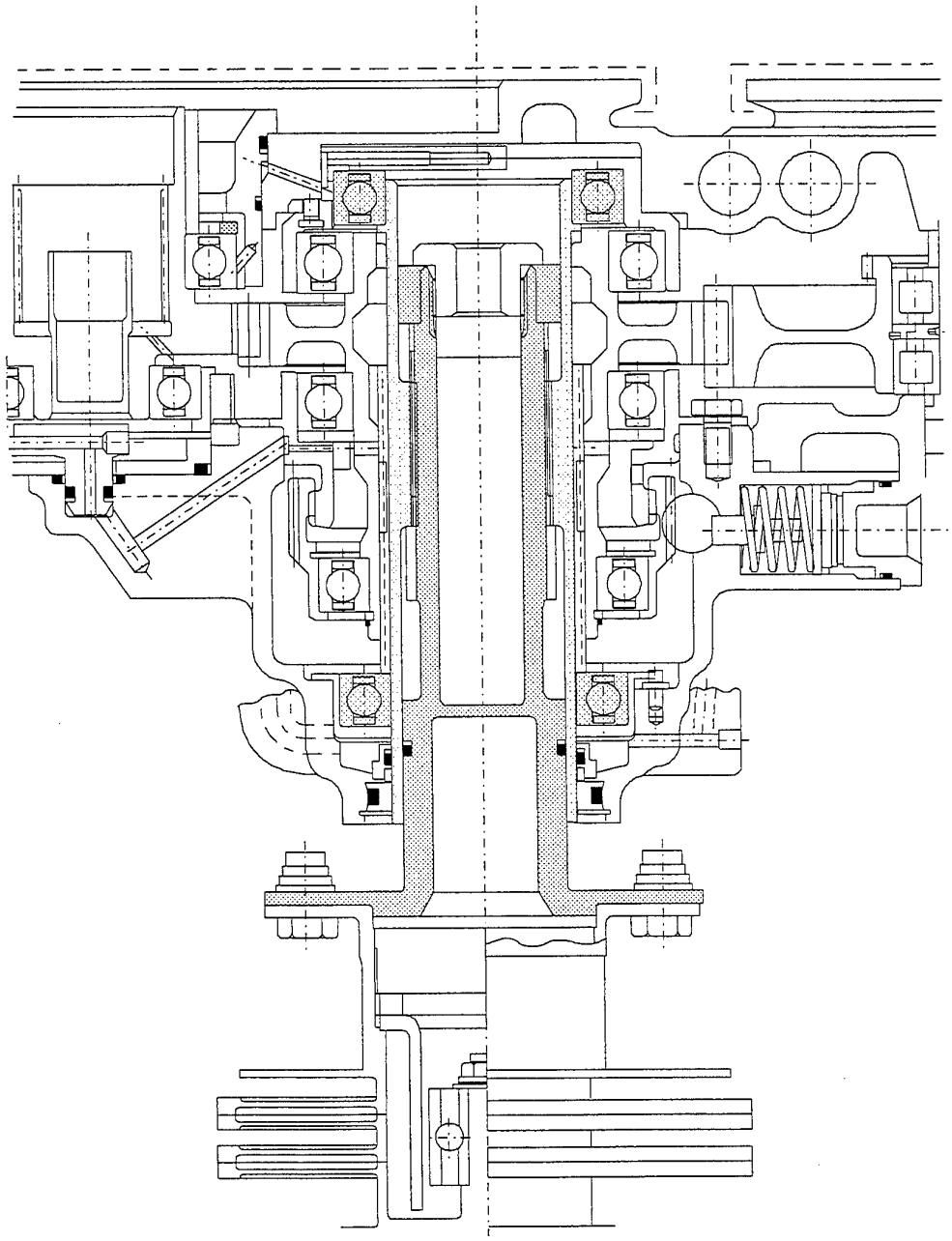

Figure 3 Cross-section through PTS shaft

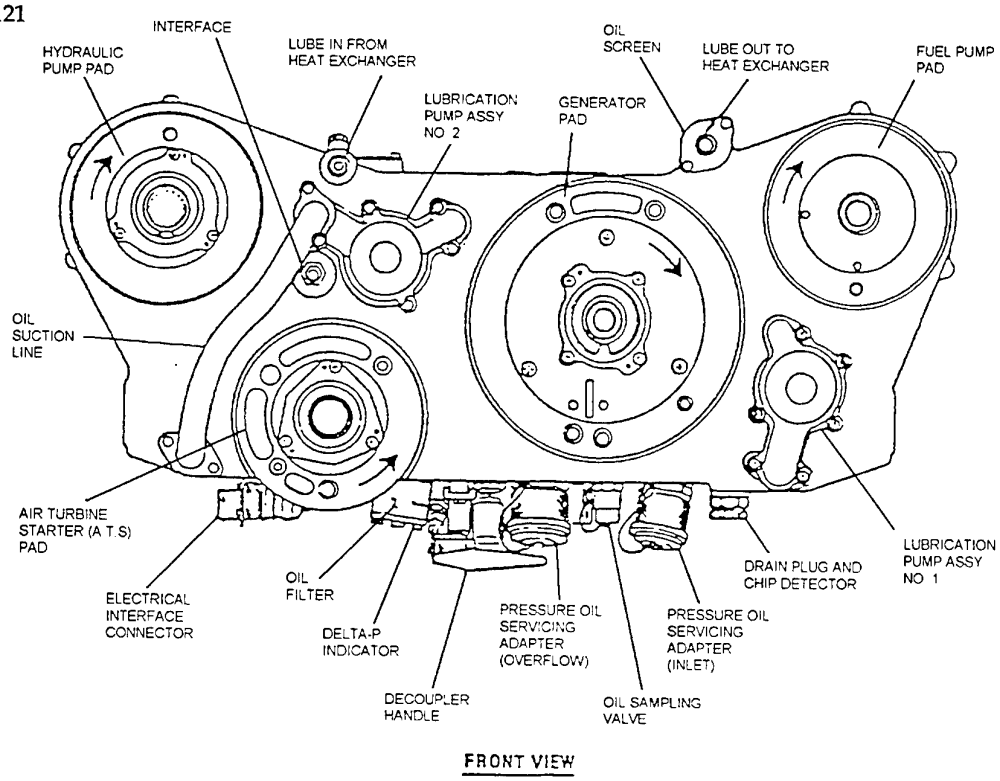

Figure 4 Front view of AMAD

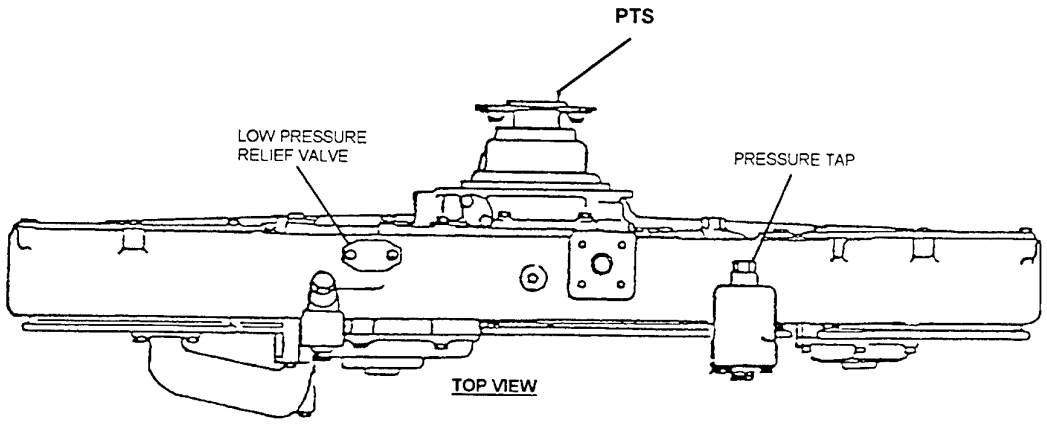

Figure 5 Top view of AMAD

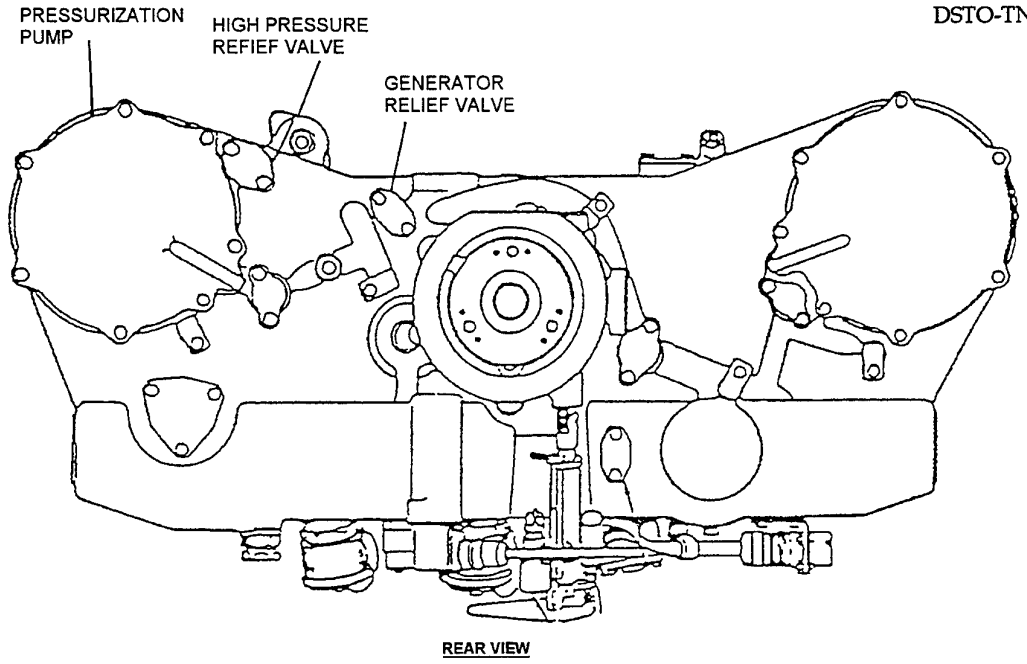

Figure 6 Rear view of AMAD

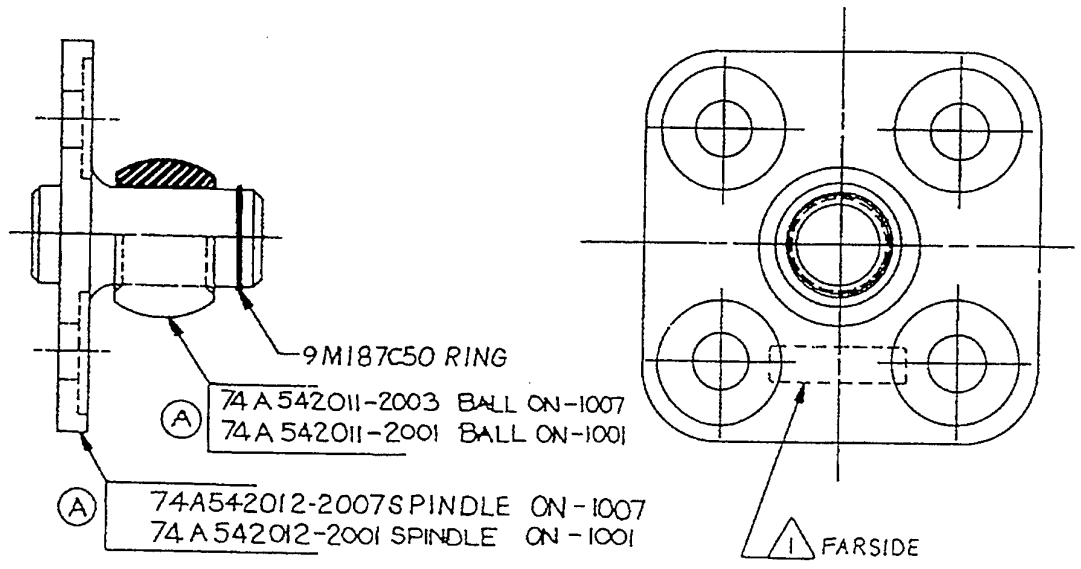

Figure 7 View of AMAD side mount detail

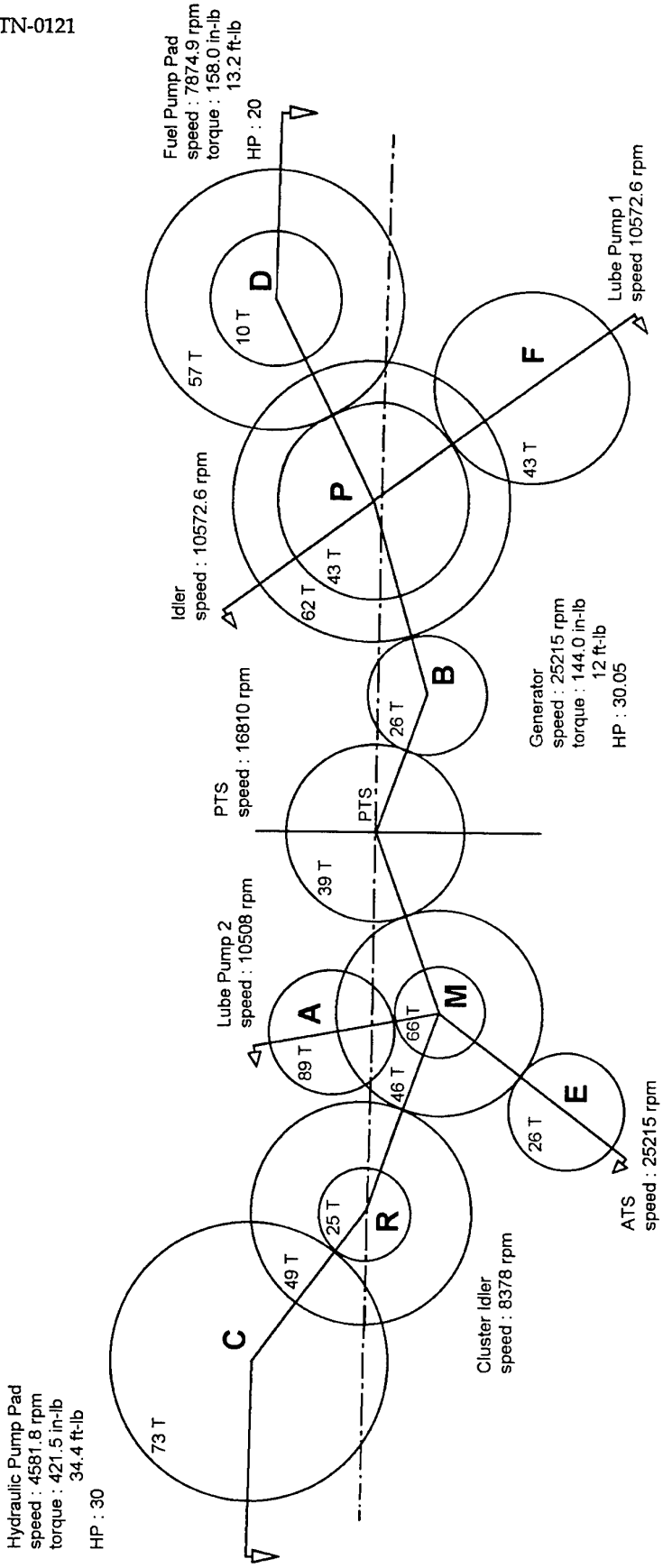

Figure 8 Gear train schematic - ratios, speeds and torques

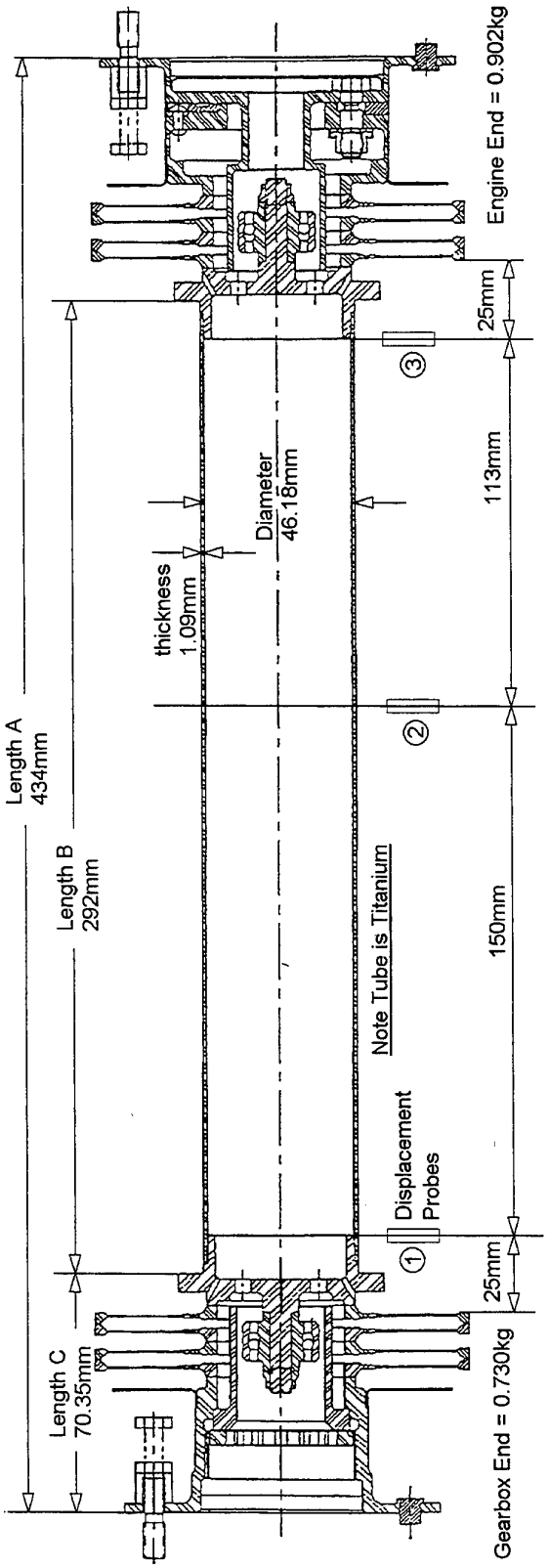

Figure 9 19E215 Lucas Aerospace Power Transmission Company (LAPTC) shaft

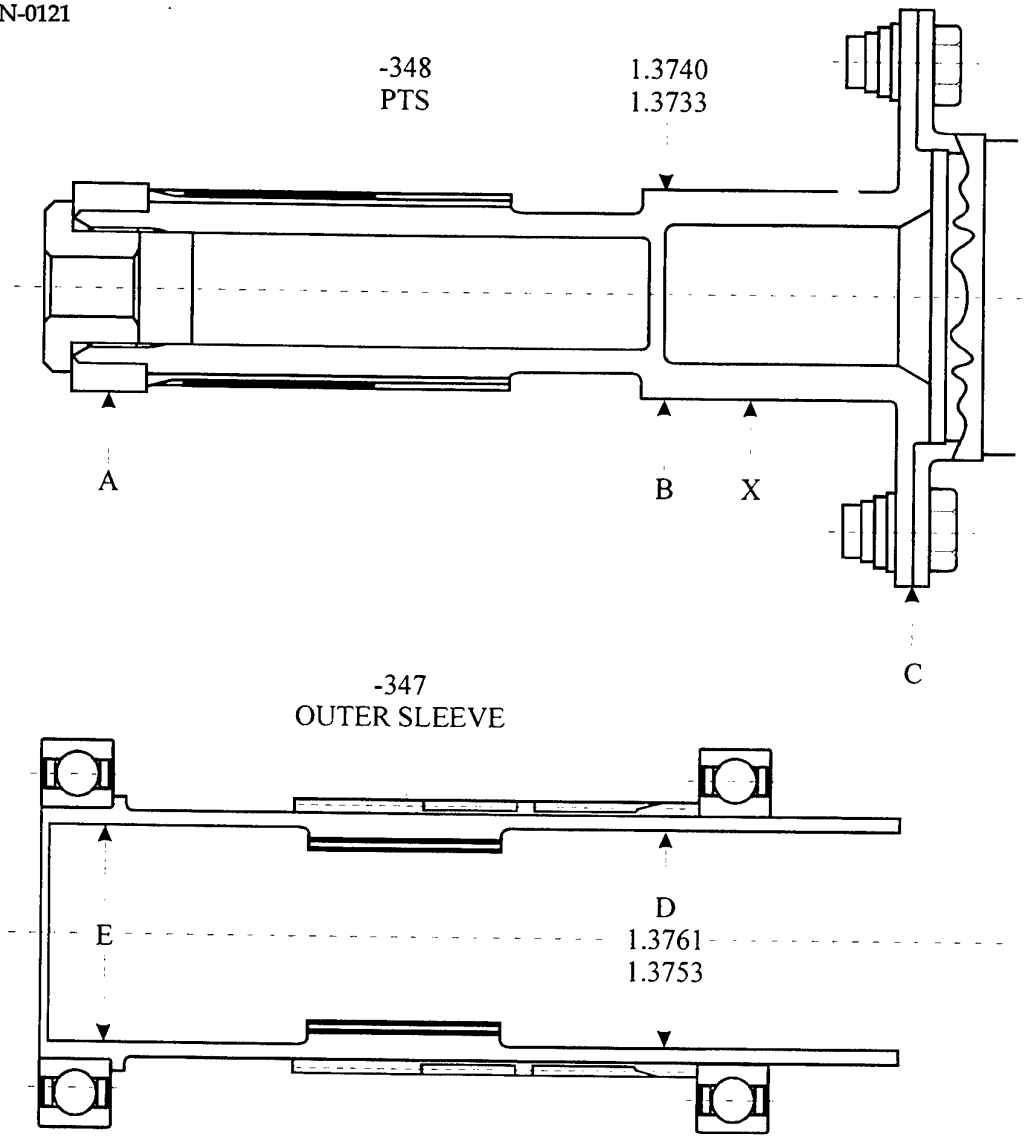

Note: Dimension X is approximately 0.010" smaller than dimension B

Figure 10 Detail of PTS clearance -348/-347

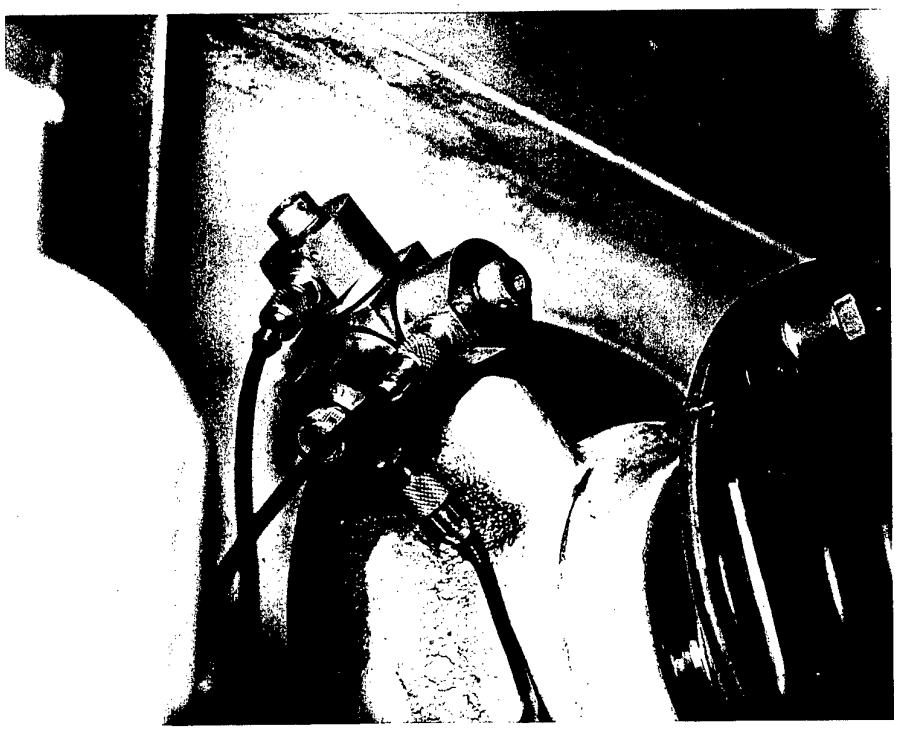

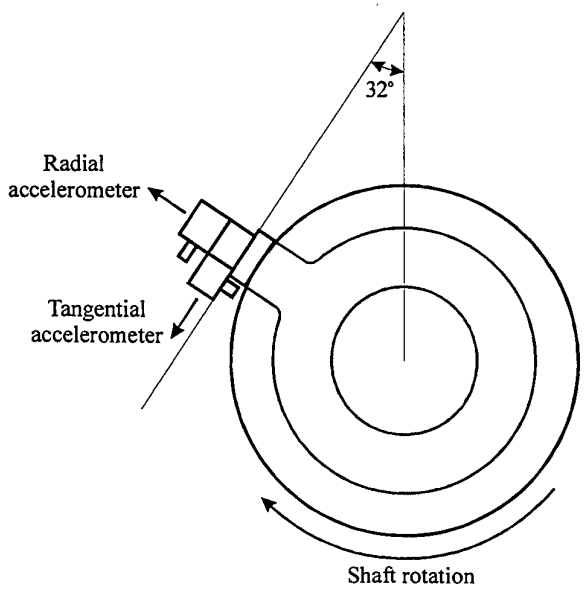

Figure 11 Triaxial accelerometer mount view looking forward

Figure 12 Lower gearcase accelerometer mount

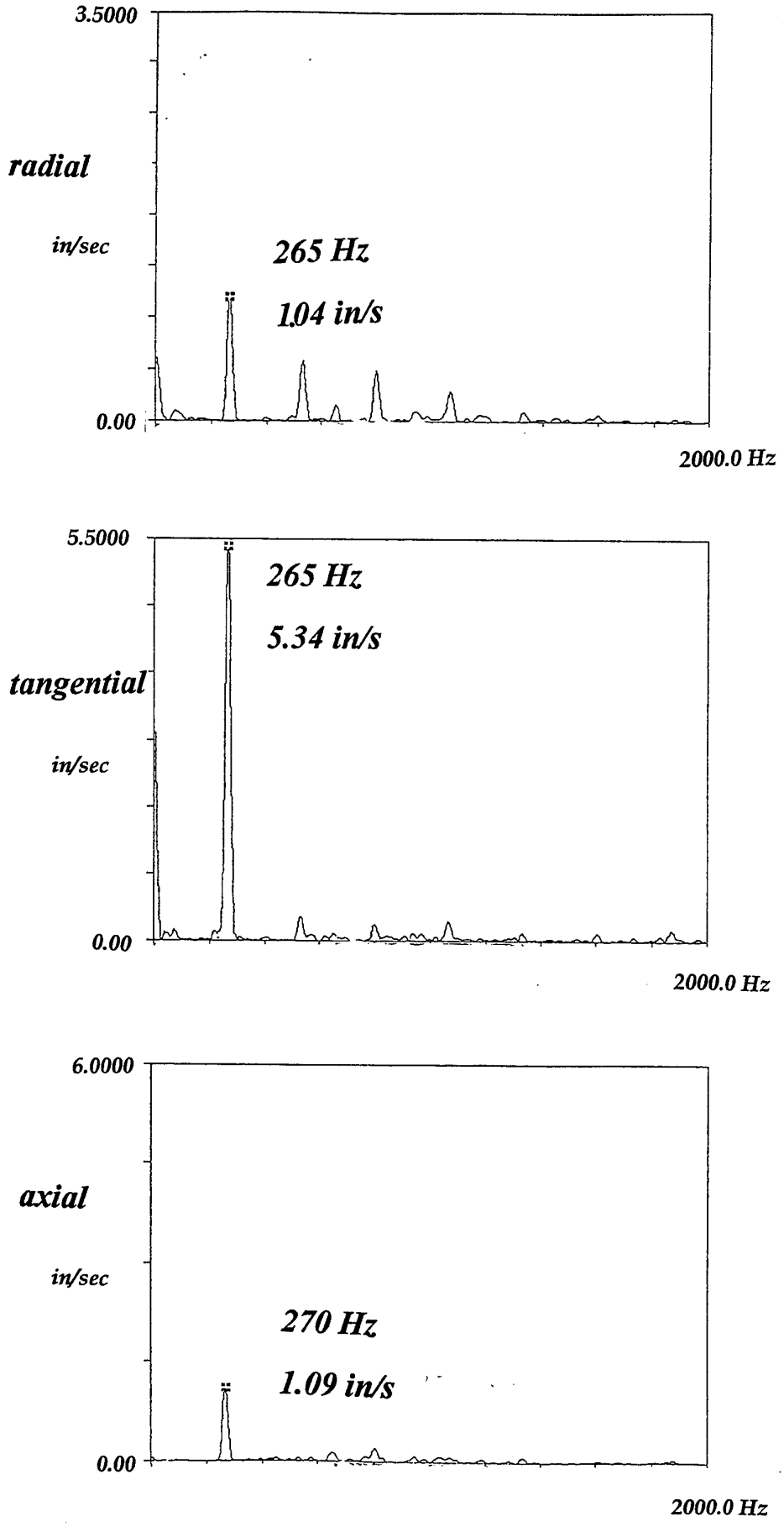

Figure 13 Vibration spectrum A21-116

A/C 116
date 23/2
tape 1

Test 3a - left hand side AMAD

RUN UP

vibration levels at shaft frequency*1

ACC #1 - radial 121.95 g/V

FREQ	RMS(g)	RMS(in/s)
184	0.17	0.06
192	0.23	0.07
216	0.73	0.21
232	0.94	0.25
240	1.62	0.42
256	2.73	0.66
264	5.45	1.27

ACC #2 - circumf 187.8 g/V

FREQ	RMS(g)	RMS(in/s)
184	0.48	0.16
192	1.24	0.40
216	3.40	0.97
232	6.70	1.78
240	8.85	2.27
256	13.82	3.32
264	21.03	4.90

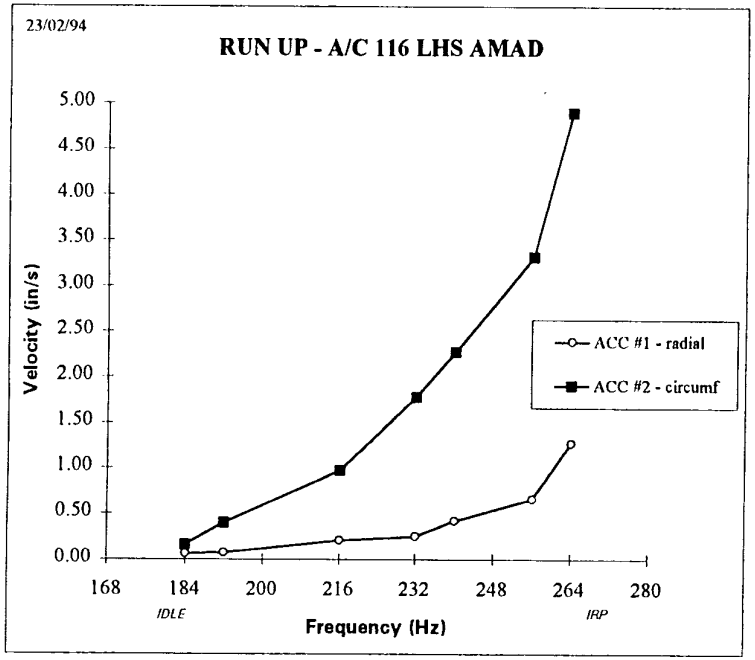

A/C 116
date 23/2
tape 1

Test 3b - left hand side AMAD

RUN DOWN

vibration levels at shaft frequency*1

ACC #1 - radial 121.95 g/V

FREQ	RMS(g)	RMS(in/s)
184	0.30	0.10
200	0.30	0.09
216	1.16	0.33
232	1.05	0.28
240	1.85	0.47
256	3.93	0.94
264	5.45	1.27

ACC #2 - circumf 187.8 g/V

FREQ	RMS(g)	RMS(in/s)
184	0.63	0.21
200	1.74	0.53
216	1.79	0.51
232	7.27	1.93
240	10.52	2.69
256	18.22	4.37
264	21.03	4.90

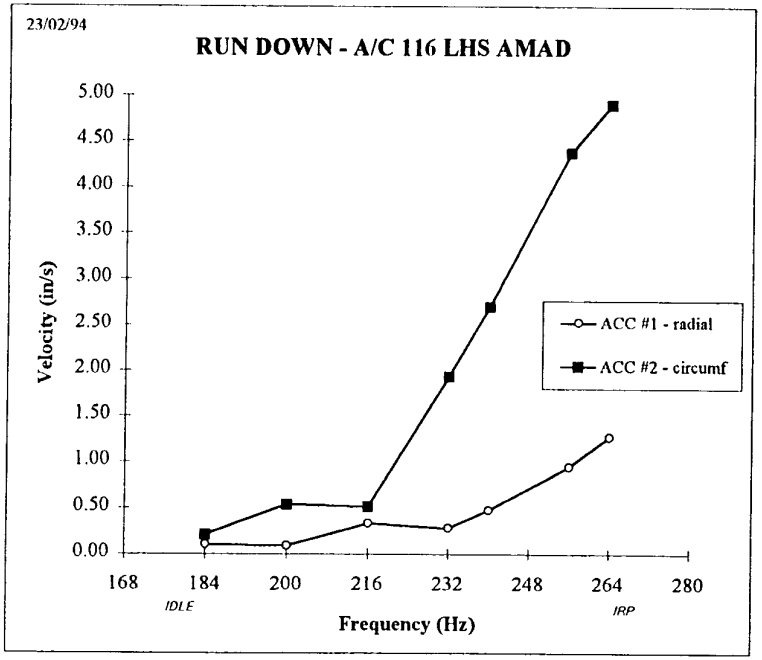

Figure 14(a) Triaxial accelerometer run-up 1X vibration curves A21-116 Left

A/C 116
date 23/2
tape 1

Test 4a - left hand side AMAD

RUN UP

vibration levels at shaft frequency*1

ACC #1 - radial 121.95 g/V

FREQ	RMS(g)	RMS(in/s)
184	0.12	0.04
200	0.32	0.10
216	0.86	0.25
232	0.99	0.26
248	1.26	0.31
256	3.06	0.73
264	5.29	1.23

ACC #3 - axial 164 g/V

FREQ	RMS(g)	RMS(in/s)
184	0.39	0.13
200	0.75	0.23
216	1.38	0.39
232	2.64	0.70
248	3.76	0.93
256	5.36	1.29
264	5.74	1.34

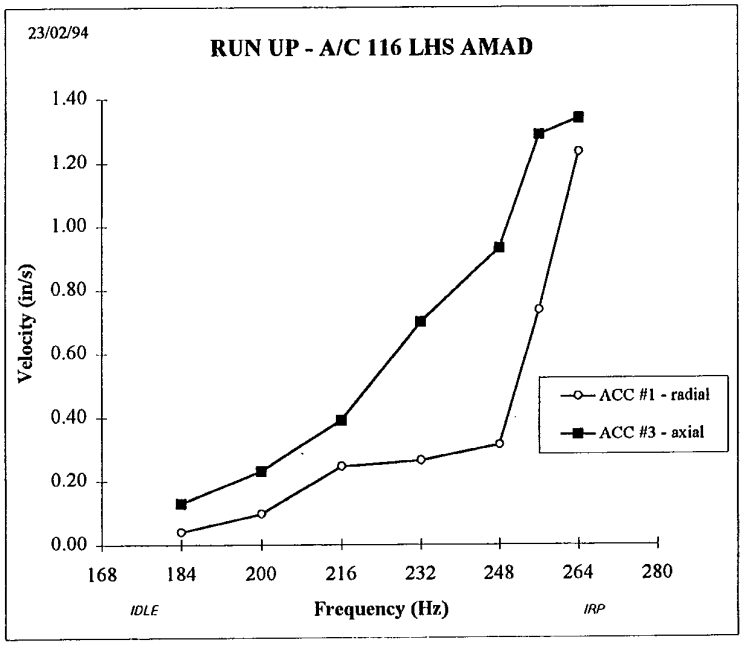

A/C 116
date 23/2
tape 1

Test 4b - left hand side AMAD

RUN DOWN

vibration levels at shaft frequency*1

ACC #1 - radial 121.95 g/V

FREQ	RMS(g)	RMS(in/s)
184	0.20	0.07
200	0.43	0.13
216	1.05	0.30
232	1.15	0.31
240	1.54	0.39
256	2.93	0.70
264	5.29	1.23

ACC #3 - axial 164 g/V

FREQ	RMS(g)	RMS(in/s)
184	0.30	0.10
200	0.90	0.28
216	1.87	0.53
232	3.07	0.81
240	4.20	1.08
256	4.71	1.13
264	5.74	1.34

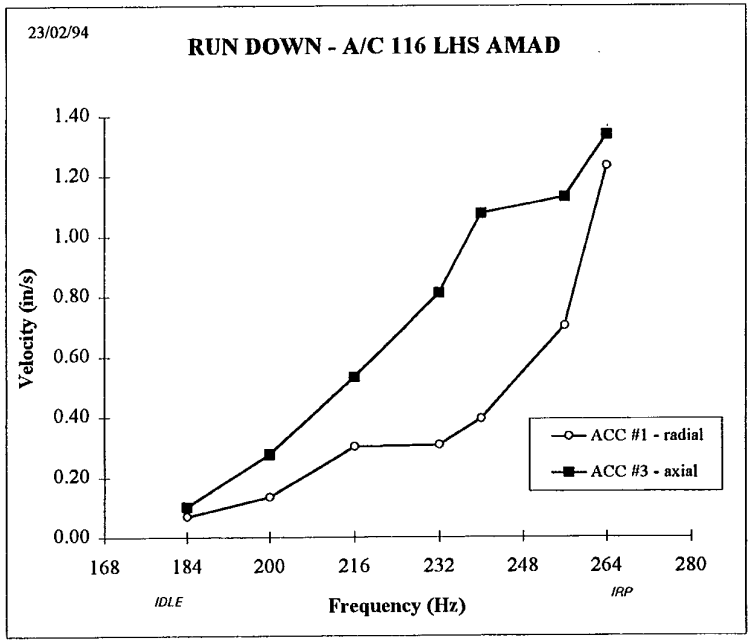

Figure 14(b) Triaxial accelerometer run-up 1X vibration curves A21-116 Left

A/C 116
date 23/2
tape 1

Test 5a - left hand side AMAD

RUN UP

vibration levels at shaft frequency*1

ACC #4 - earth lug 102.4 g/V

FREQ	RMS(g)	RMS(in/s)
208	0.55	0.16
224	0.65	0.18
232	0.29	0.08
240	0.08	0.02
248	0.31	0.08
256	0.46	0.11
264	0.40	0.09

ACC #3 - axial 82 g/V

FREQ	RMS(g)	RMS(in/s)
208	0.82	0.24
224	1.93	0.53
232	2.88	0.76
240	3.75	0.96
248	4.37	1.08
256	5.02	1.20
264	5.50	1.28

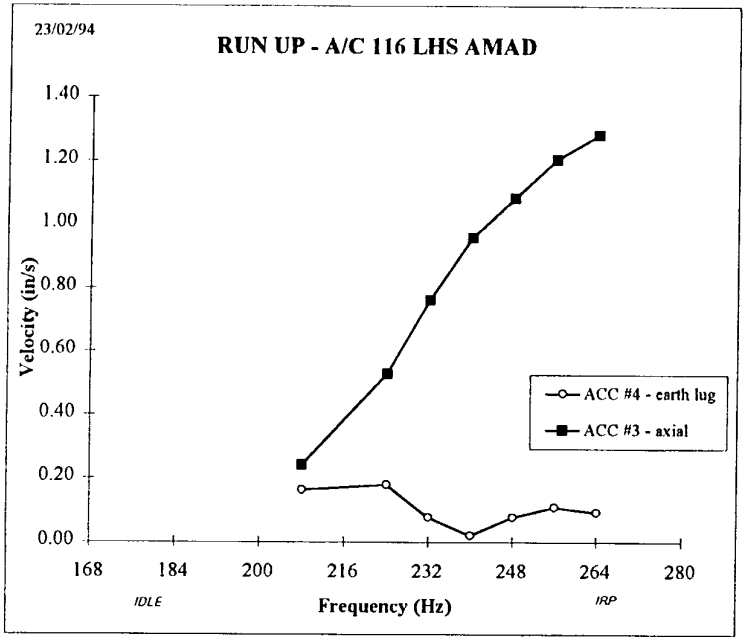

A/C 116
date 23/2
tape 1

Test 6a - left hand side AMAD

RUN UP

vibration levels at shaft frequency*1

ACC #4 - earth lug 102.4 g/V

FREQ	RMS(g)	RMS(in/s)
192	0.27	0.08
200	0.37	0.11
208	0.81	0.24
216	1.78	0.51
224	2.15	0.59
232	2.44	0.65
240	2.33	0.60
248	2.68	0.66
264	3.39	0.79

ACC #2 - circumf 187.8 g/V

FREQ	RMS(g)	RMS(in/s)
192	1.47	0.47
200	1.82	0.56
208	2.70	0.80
216	4.92	1.40
224	6.42	1.76
232	6.87	1.82
240	8.32	2.13
248	11.46	2.84
264	20.28	4.72

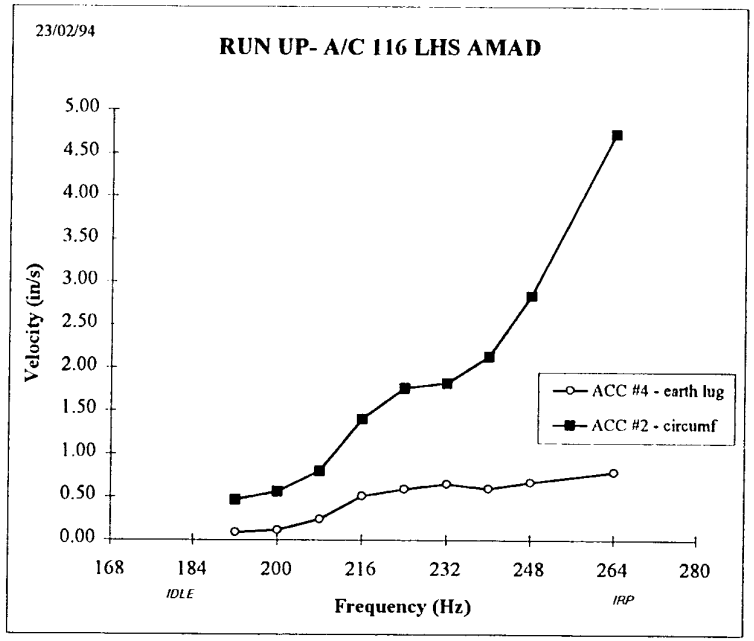

Figure 14(c) Triaxial accelerometer run-up 1X vibration curves A21-116 Left

A/C 116
date 24/2
tape 3

Test 5a - right hand side AMAD

RUN UP

vibration levels at shaft frequency*1

ACC #1 - radial 121.95 g/V

FREQ	RMS(g)	RMS(in/s)
192	0.44	0.14
200	0.73	0.23
208	0.77	0.23
216	1.38	0.39
224	1.77	0.49
232	1.77	0.47
240	2.09	0.53
248	3.20	0.79
256	4.62	1.11
264	6.02	1.40
268	6.98	1.60

ACC #2 - circumf 187.8 g/V

FREQ	RMS(g)	RMS(in/s)
192	0.83	0.27
200	1.34	0.41
208	1.80	0.53
216	2.12	0.60
224	2.78	0.76
232	3.70	0.98
240	4.51	1.15
248	5.71	1.42
256	8.06	1.93
264	10.31	2.40
268	11.68	2.68

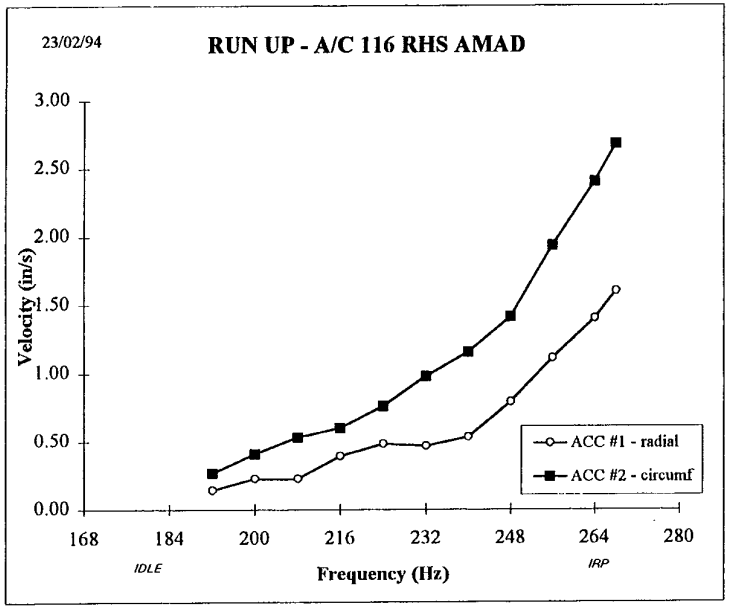

A/C 116
date 24/2/
tape 3

Test 6a - right hand side AMAD

RUN UP

vibration levels at shaft frequency*1

ACC #1 - radial 121.95 g/V

FREQ	RMS(g)	RMS(in/s)
192	0.70	0.22
204	0.70	0.21
216	1.29	0.37
224	1.56	0.43
232	1.59	0.42
240	2.17	0.56
248	3.20	0.79
256	4.80	1.15
264	5.89	1.37
268	7.65	1.75

ACC #3 - axial 164 g/V

FREQ	RMS(g)	RMS(in/s)
192	0.35	0.11
204	0.48	0.14
216	1.12	0.32
224	1.10	0.30
232	1.14	0.30
240	1.44	0.37
248	1.98	0.49
256	2.61	0.63
264	3.21	0.75
268	4.03	0.93

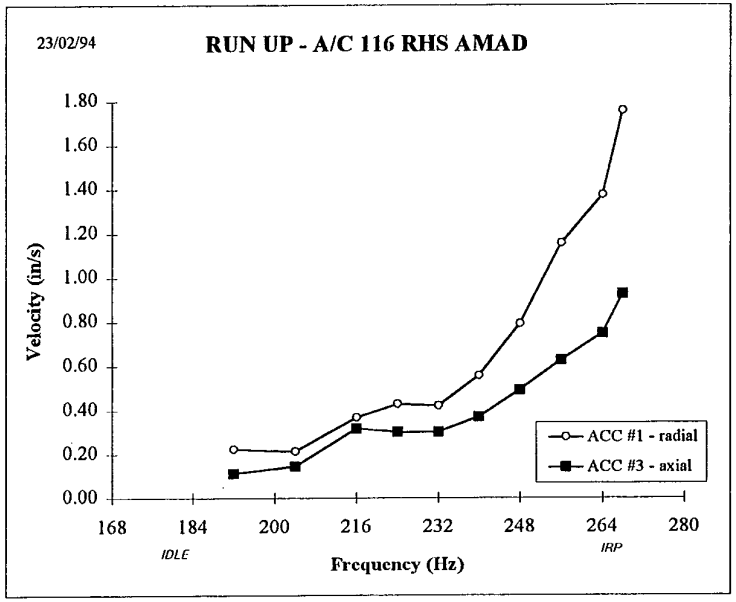

Figure 14(d) Triaxial accelerometer run-up 1X vibration curves A21-116 Right

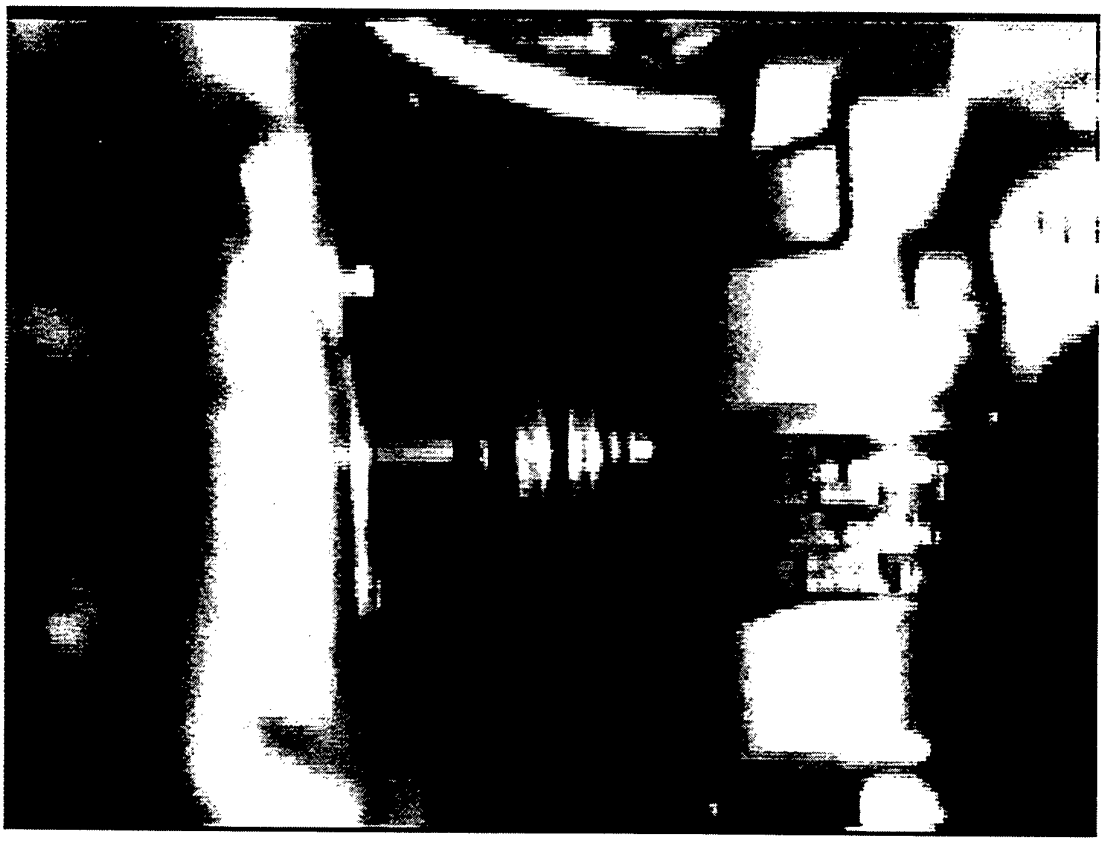

Figure 15 Video image A21-116 LHS shaft

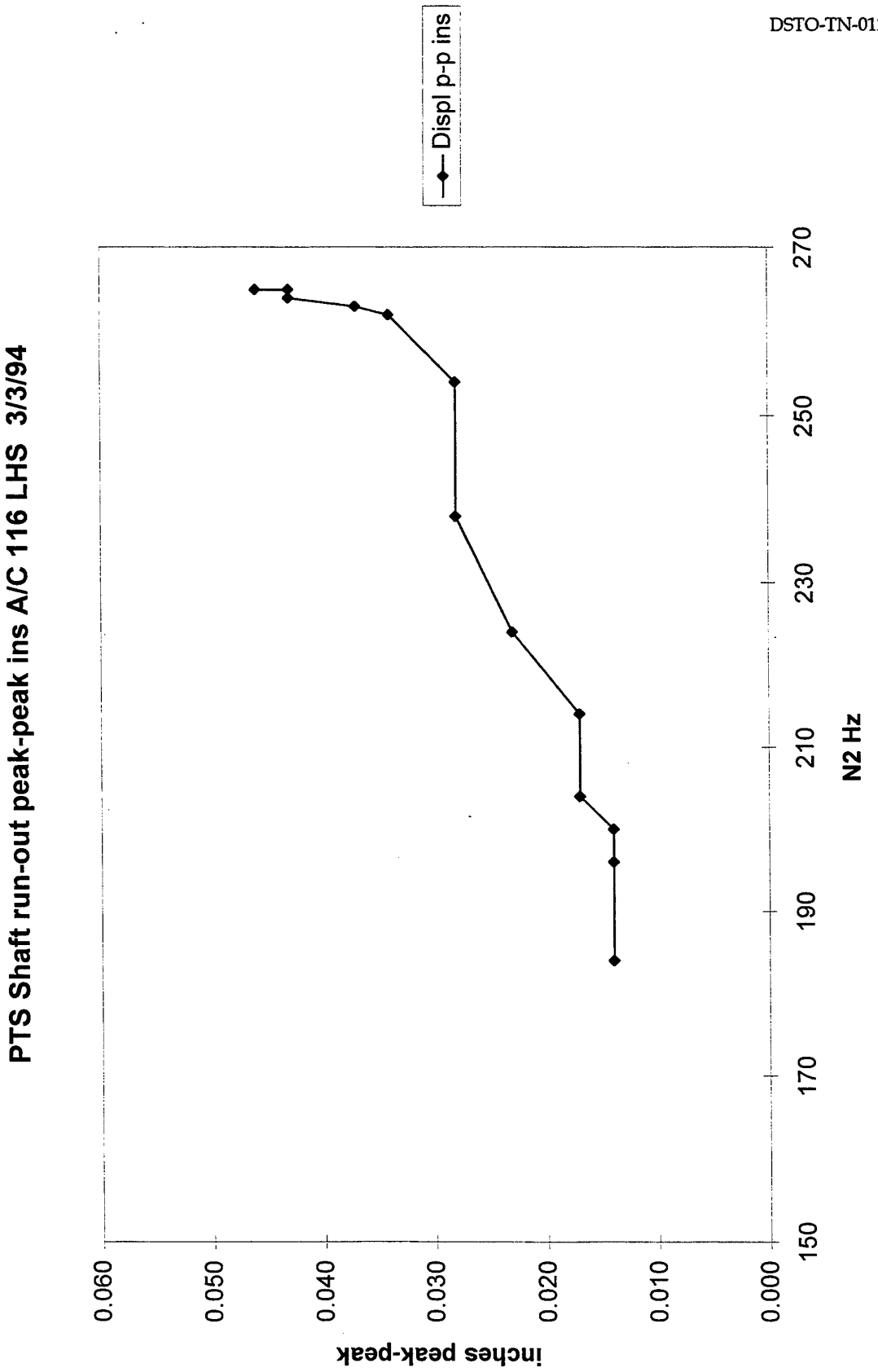

Figure 16 LAPTC shaft dynamic run-out A21-116 LHS

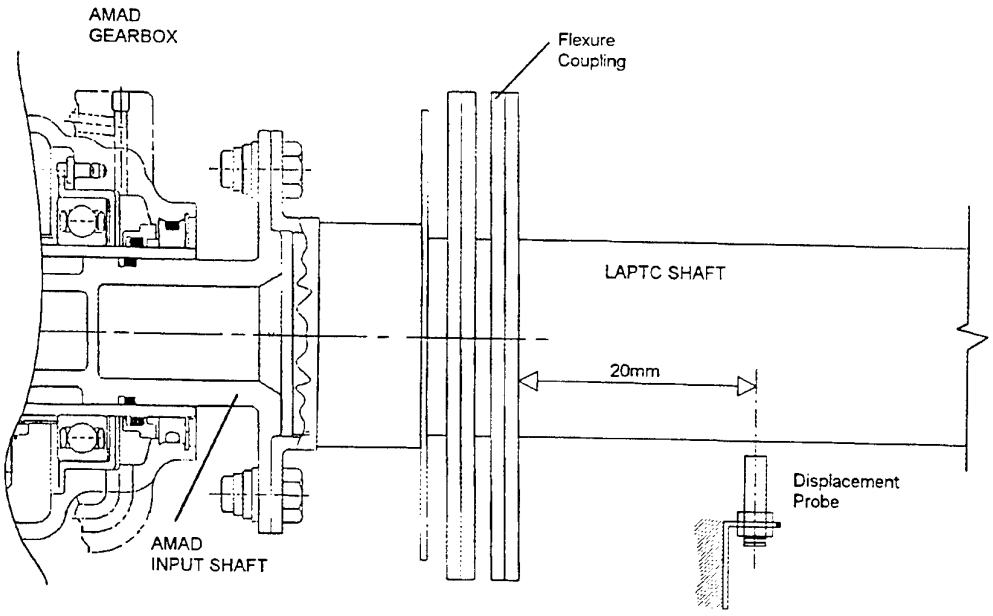

NOTE : An accelerometer (not shown) was attached adjacent to probe to measure probe vibration and compensate if required to provide absolute shaft motion

Figure 17 Schematic of displacement probe location

A/C 4
date24/2
tape 2

Test 2a - left hand side AMAD

RUN UP

vibration levels at shaft frequency*1

ACC #1 - radial 243.9 g/V

FREQ	RMS(g)	RMS(in/s)
184	0.25	0.08
196	0.07	0.02
204	0.05	0.02
208	0.08	0.02
216	0.07	0.02
224	0.15	0.04
232	0.16	0.04
236	0.22	0.06
244	0.45	0.11
256	1.28	0.31
264	1.70	0.40

ACC #2 - circumf 187.8 g/V

FREQ	RMS(g)	RMS(in/s)
184	0.51	0.17
196	0.93	0.29
204	1.34	0.40
208	1.62	0.48
216	2.05	0.58
224	2.55	0.70
232	3.16	0.84
236	3.19	0.83
244	4.38	1.10
256	5.54	1.33
264	6.61	1.54

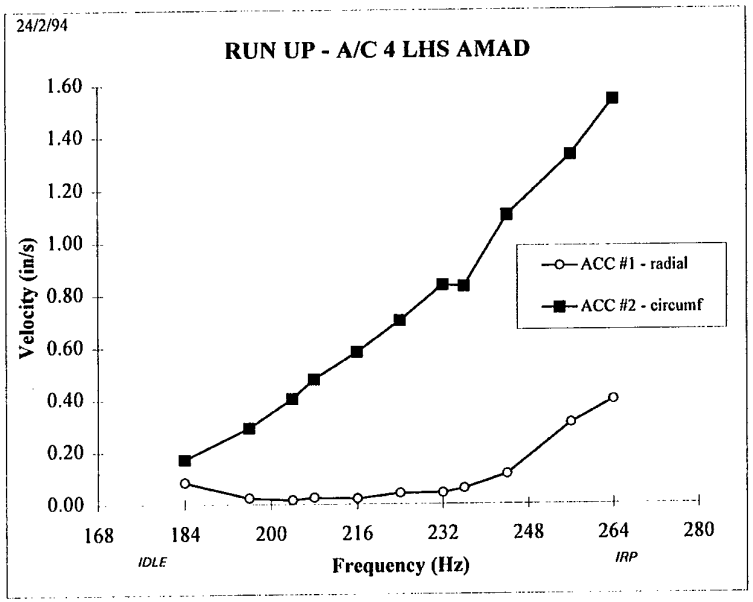

A/C 4
date24/2
tape 2

Test 2b - left hand side AMAD

RUN DOWN

vibration levels at shaft frequency*1

ACC #1 - radial 234.9 g/V

FREQ	RMS(g)	RMS(in/s)
184	0.24	0.08
192	0.16	0.05
204	0.01	0.00
212	0.07	0.02
220	0.17	0.05
232	0.09	0.02
240	0.17	0.04
248	0.55	0.14
256	1.06	0.25
264	1.86	0.43

ACC #2 - circumf 187.8 g/V

FREQ	RMS(g)	RMS(in/s)
184	0.54	0.18
192	0.85	0.27
204	1.27	0.38
212	1.80	0.52
220	2.20	0.61
232	3.12	0.83
240	3.96	1.01
248	4.64	1.15
256	5.39	1.29
264	6.61	1.54

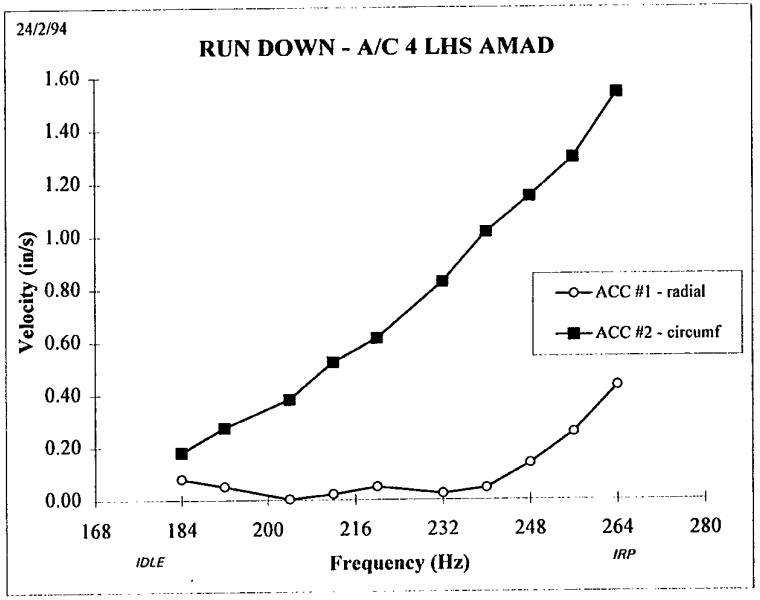

Figure 18(a) Triaxial accelerometer run-up 1X vibration curves A21-04 Left

A/C 4
date24/2
tape 2

Test 3a - left hand side AMAD

RUN UP

vibration levels at shaft frequency*1

ACC #1 - radial 243.9 g/V
121.95

FREQ	RMS(g)	RMS(in/s)
184	0.06	0.02
192	0.09	0.03
200	0.06	0.02
208	0.03	0.01
216	0.09	0.02
224	0.28	0.08
232	0.09	0.02
240	0.41	0.10
248	0.66	0.16
260	1.33	0.31
264	1.66	0.39

ACC #3 - axial 164 g/V

FREQ	RMS(g)	RMS(in/s)
184	0.40	0.13
192	0.55	0.18
200	0.62	0.19
208	0.75	0.22
216	1.17	0.33
224	1.26	0.34
232	1.45	0.38
240	1.75	0.45
248	2.13	0.53
260	2.59	0.61
264	3.12	0.73

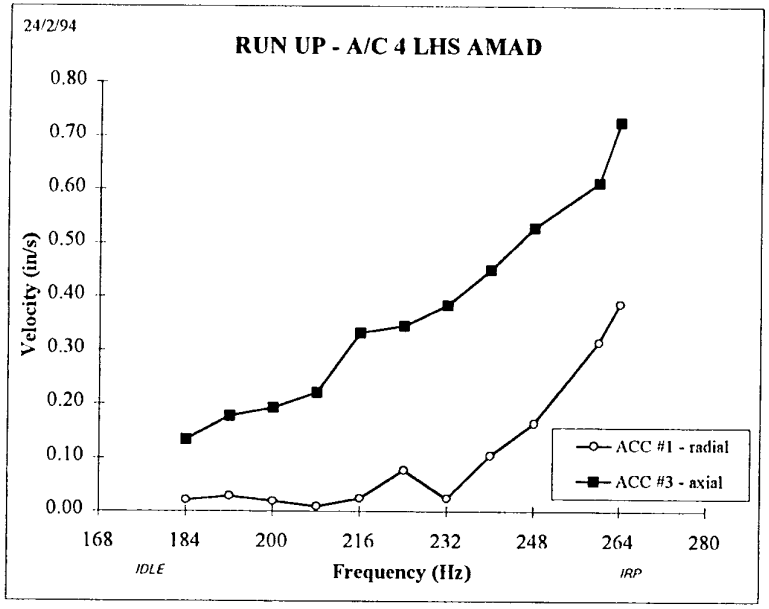

A/C 4
date24/2
tape 2

Test 3b - left hand side AMAD

RUN DOWN

vibration levels at shaft frequency*1

ACC #1 - radial 121.95 g/V

FREQ	RMS(g)	RMS(in/s)
184	0.22	0.07
200	0.08	0.02
208	0.04	0.01
216	0.07	0.02
224	0.21	0.06
232	0.11	0.03
240	0.20	0.05
248	0.50	0.12
256	1.27	0.30
264	1.66	0.39

ACC #3 - axial 164 g/V

FREQ	RMS(g)	RMS(in/s)
184	0.38	0.13
200	0.61	0.19
208	0.78	0.23
216	0.92	0.26
224	1.20	0.33
232	1.58	0.42
240	1.64	0.42
248	1.66	0.41
256	2.56	0.61
264	3.12	0.73

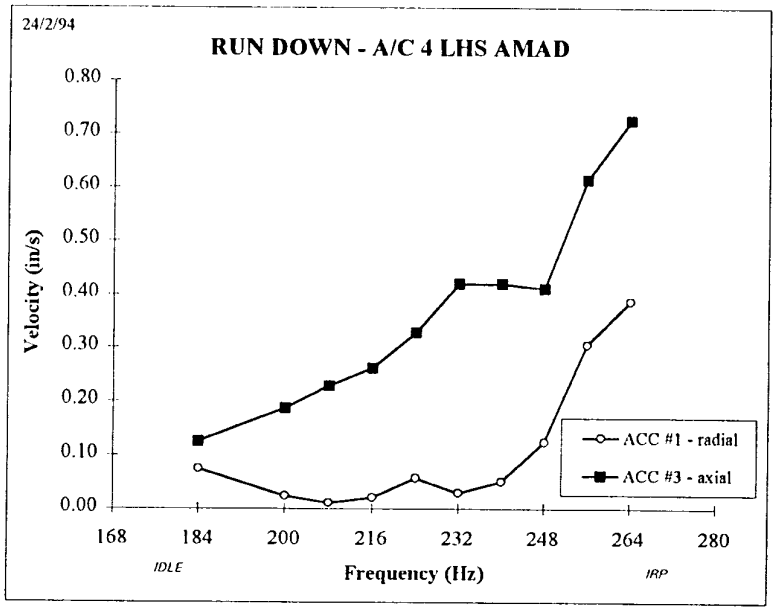

Figure 18(b) Triaxial accelerometer run-up 1X vibration curves

A21-04 Left

A/C 04
date 24/2
tape 2

Test 4a - right hand side AMAD

RUN UP

vibration levels at shaft frequency*1

ACC #1 - radial 121.95 g/V

FREQ	RMS(g)	RMS(in/s)
184	0.13	0.04
192	0.16	0.05
200	0.24	0.07
208	0.11	0.03
216	0.22	0.06
224	0.55	0.15
232	0.76	0.20
240	1.22	0.31
248	1.61	0.40
256	2.27	0.54
264	2.93	0.68

ACC #2 - circumf 187.8 g/V

FREQ	RMS(g)	RMS(in/s)
184	0.66	0.22
192	1.12	0.36
200	1.25	0.39
208	1.54	0.46
216	1.80	0.51
224	2.10	0.58
232	2.65	0.70
240	3.59	0.92
248	4.30	1.07
256	5.56	1.33
264	7.23	1.68

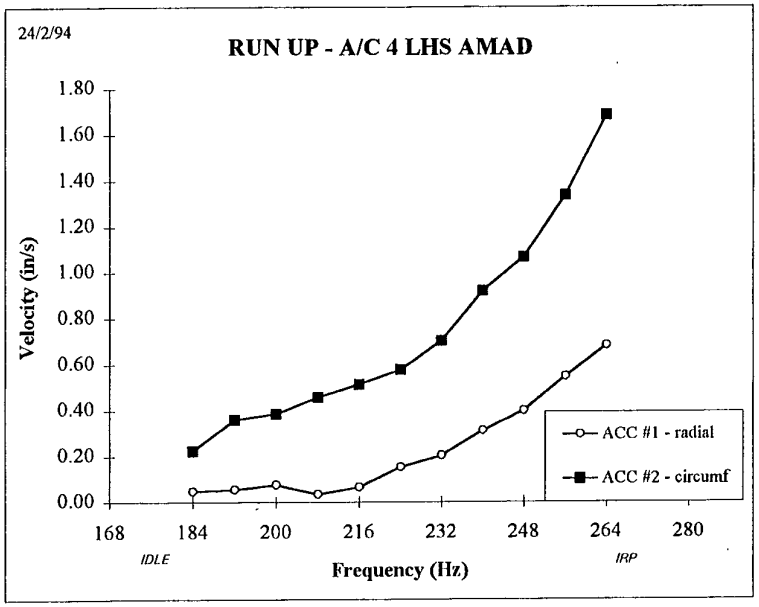

A/C 04
date 24/2
tape 2

Test 4b - right hand side AMAD

RUN DOWN

vibration levels at shaft frequency*1

ACC #1 - radial 121.95 g/V

FREQ	RMS(g)	RMS(in/s)
184	0.11	0.04
188	0.14	0.05
200	0.25	0.08
204	0.17	0.05
216	0.22	0.06
224	0.64	0.18
232	0.83	0.22
240	1.22	0.31
248	1.72	0.43
256	2.37	0.57
264	2.93	0.68

ACC #2 - circumf 187.8 g/V

FREQ	RMS(g)	RMS(in/s)
184	0.79	0.26
188	1.01	0.33
200	1.37	0.42
204	1.55	0.47
216	1.90	0.54
224	2.40	0.66
232	2.84	0.75
240	3.61	0.92
248	4.64	1.15
256	5.78	1.39
264	7.23	1.68

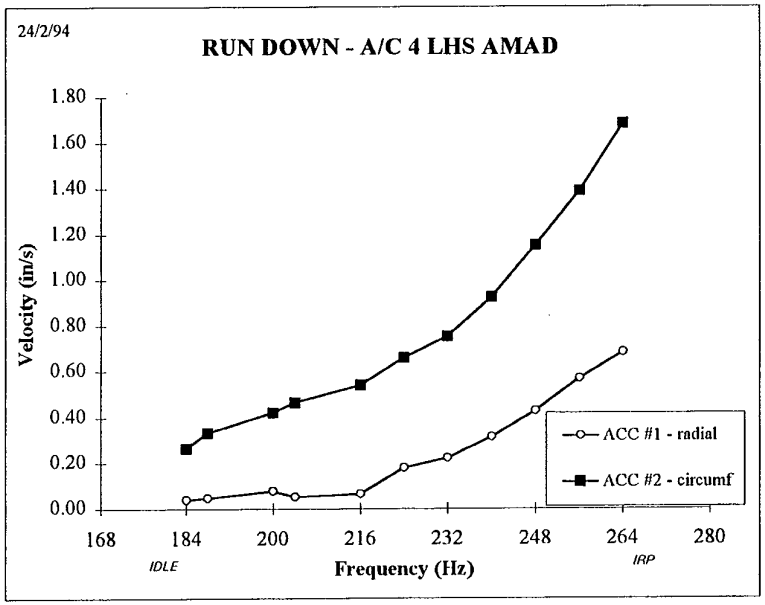

Figure 18(c) Triaxial accelerometer run-up 1X vibration curves A21-04 Right

A/C 04
date 24/2/
tape 2

Test 5a - right hand side AMAD
RUN UP
vibration levels at shaft frequency*1

ACC #1 - radial 121.95 g/V

FREQ	RMS(g)	RMS(in/s)
184	0.11	0.04
192	0.12	0.04
200	0.27	0.08
208	0.08	0.02
216	0.26	0.07
224	0.55	0.15
232	0.89	0.24
240	1.16	0.30
248	1.66	0.41
256	2.40	0.58
264	3.07	0.72
268	3.29	0.76

ACC #3 - axial 164 g/V

FREQ	RMS(g)	RMS(in/s)
184	0.44	0.15
192	0.43	0.14
200	0.75	0.23
208	0.68	0.20
216	0.95	0.27
224	1.30	0.36
232	1.74	0.46
240	2.10	0.54
248	2.76	0.68
256	3.71	0.89
264	4.41	1.03
268	4.76	1.09

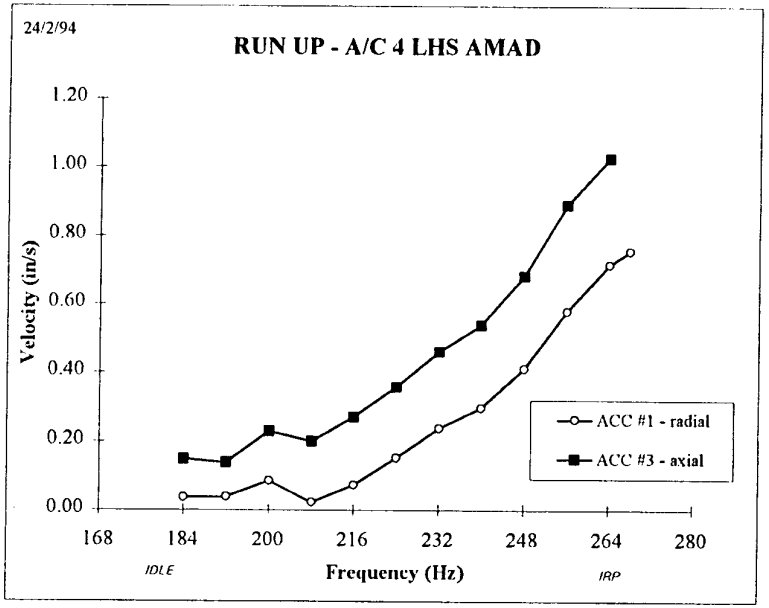

A/C 04
date 24/2/
tape 2

Test 5b - right hand side AMAD
RUN DOWN
vibration levels at shaft frequency*1

ACC #1 - radial 121.95 g/V

FREQ	RMS(g)	RMS(in/s)
184	0.11	0.04
192	0.14	0.05
200	0.27	0.08
216	0.73	0.21
224	0.64	0.17
232	0.87	0.23
240	1.30	0.33
248	1.76	0.44
256	2.17	0.52
268	3.29	0.76

ACC #3 - axial 164 g/V

FREQ	RMS(g)	RMS(in/s)
184	0.44	0.15
192	0.45	0.14
200	0.80	0.24
216	0.93	0.26
224	1.47	0.40
232	1.74	0.46
240	2.31	0.59
248	2.98	0.74
256	3.58	0.86
268	4.76	1.09

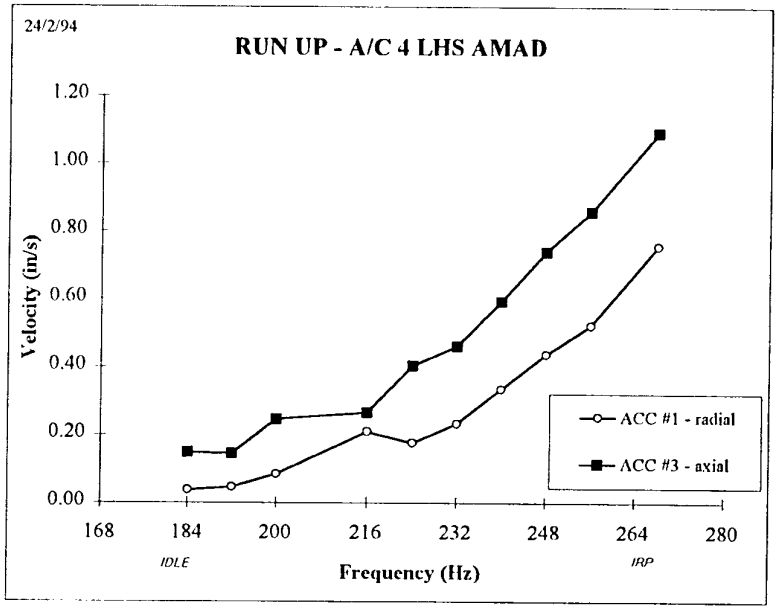

Figure 18(d) Triaxial accelerometer run-up 1X vibration curves A21-04 Right

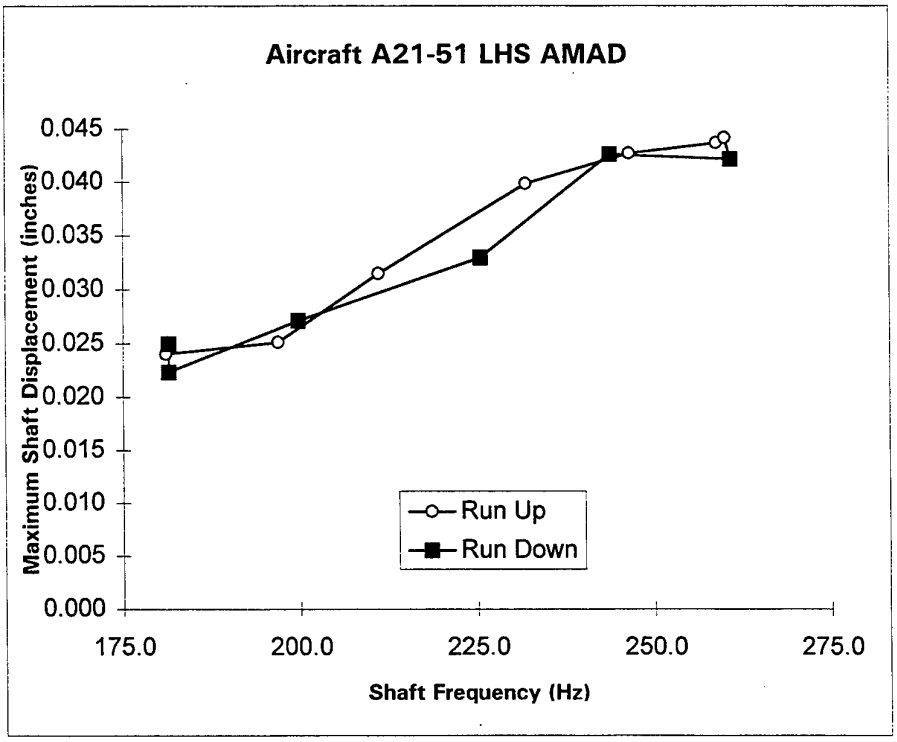

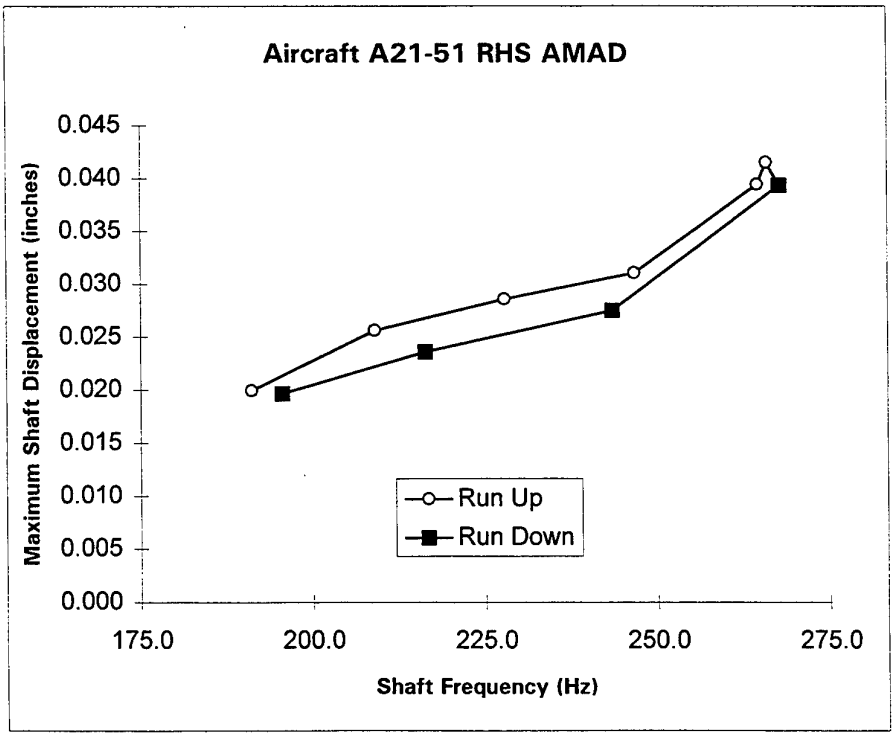

Figure 19(a) Shaft dynamic displacements A21-51

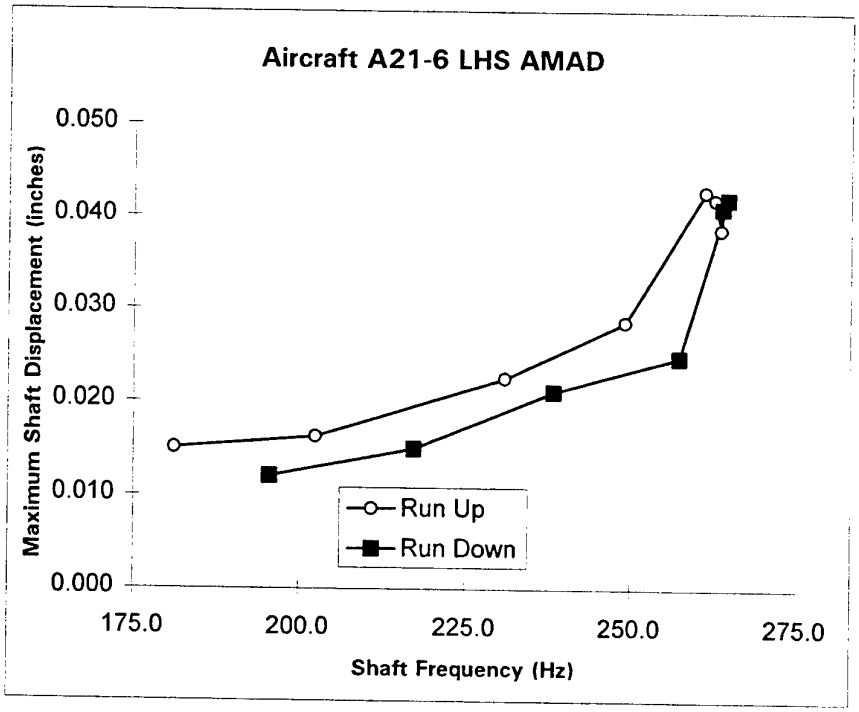

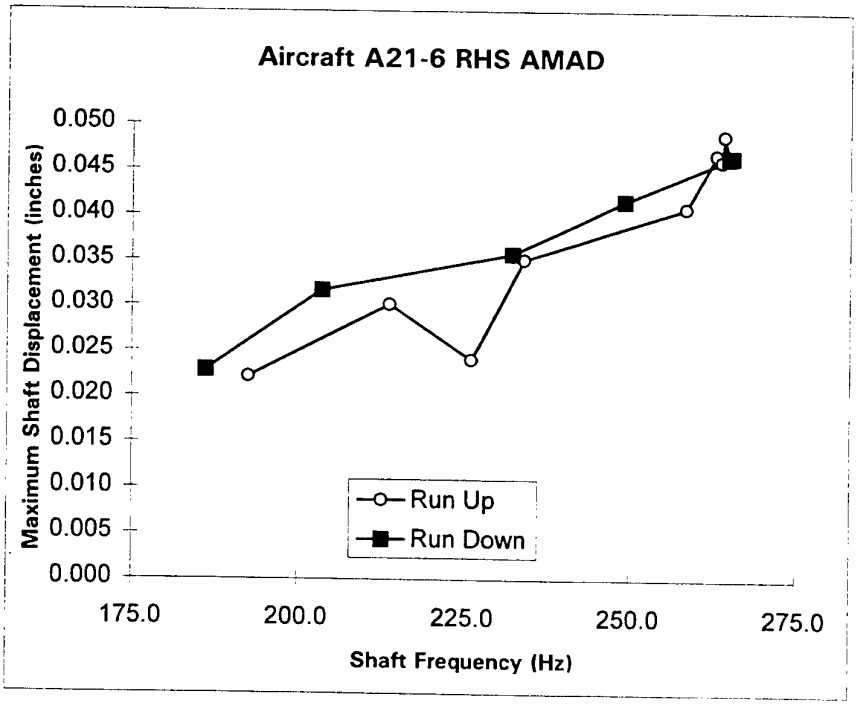

Figure 19(b) Shaft dynamic displacements A21-06

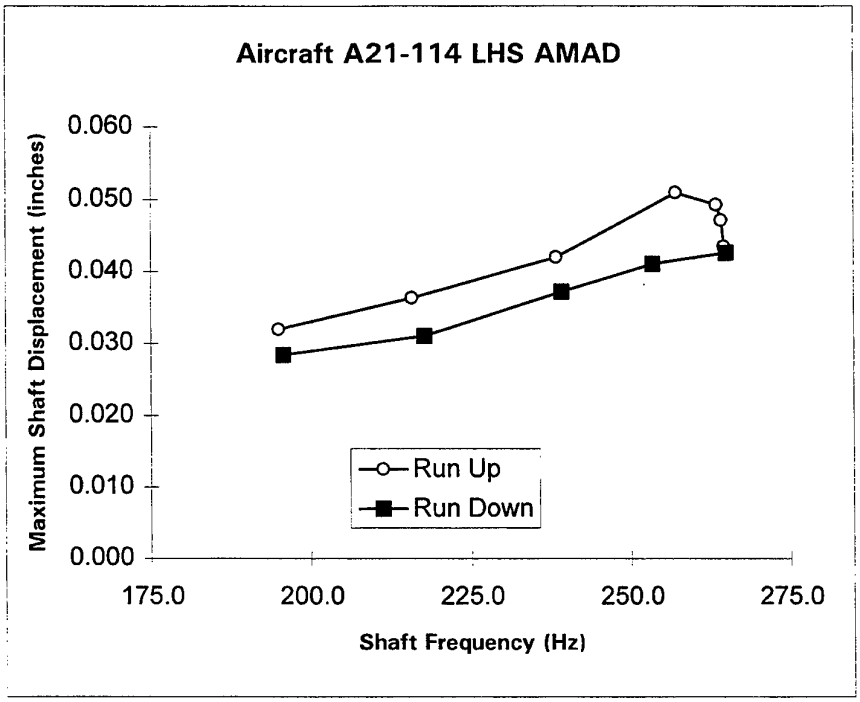

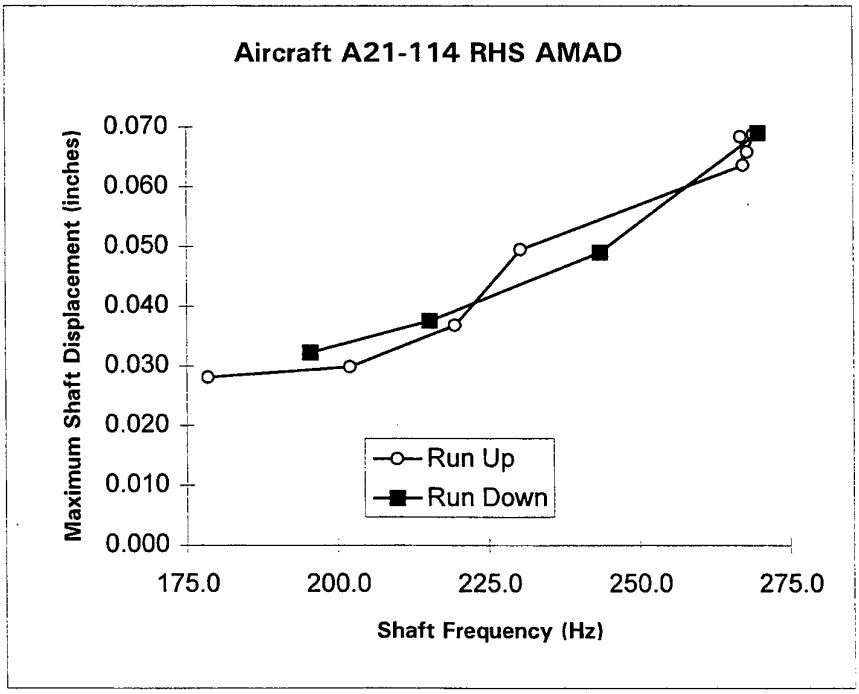

Figure 19(c) Shaft dynamic displacements A21-114

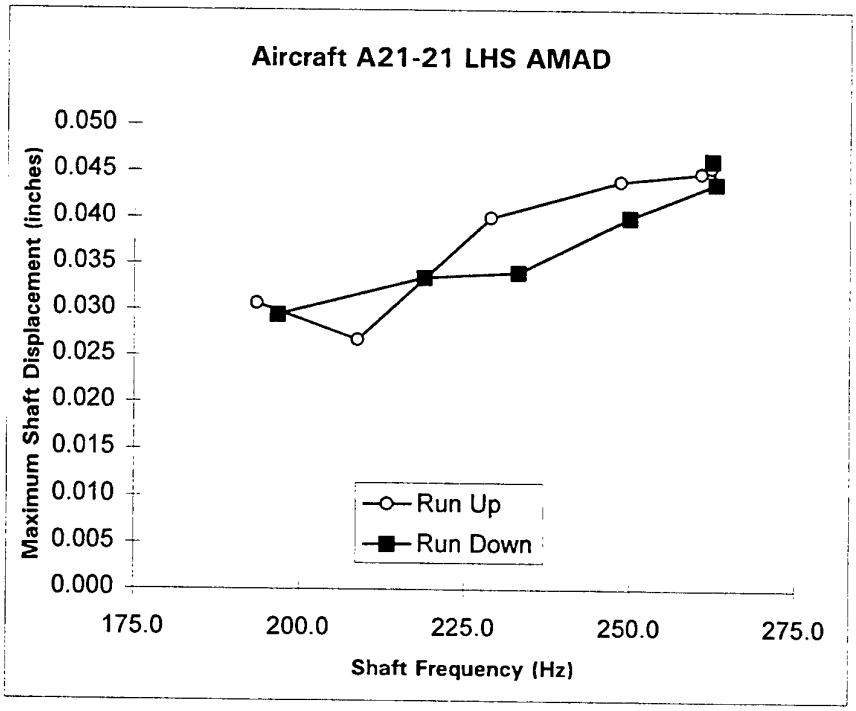

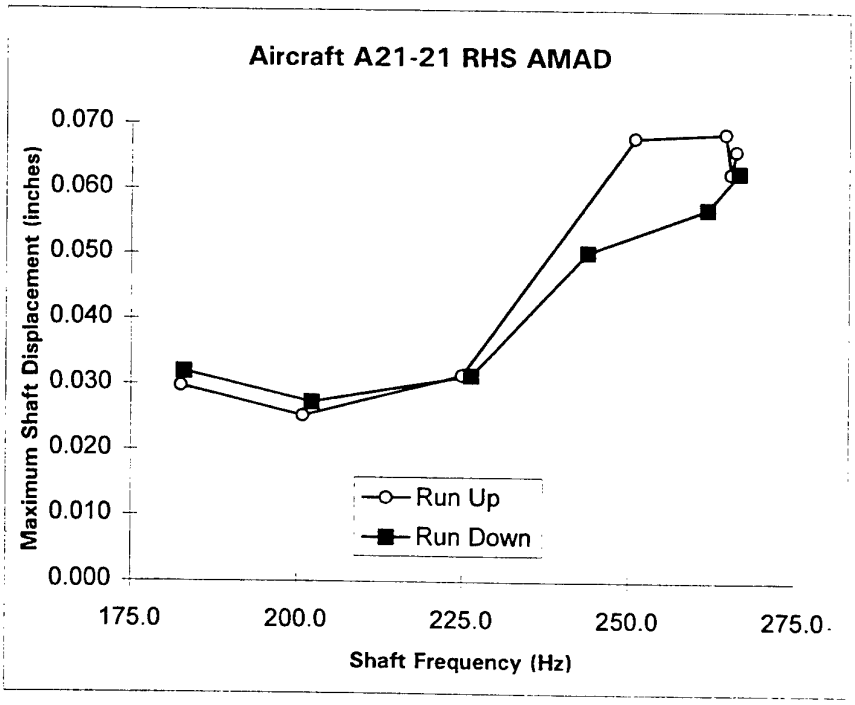

Figure 19(d) Shaft dynamic displacements A21-21

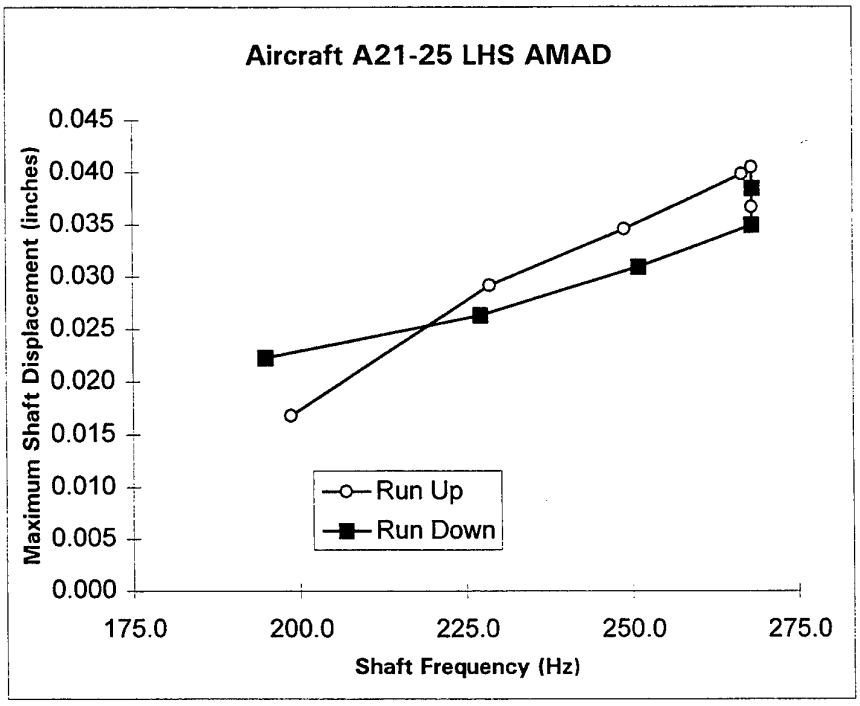

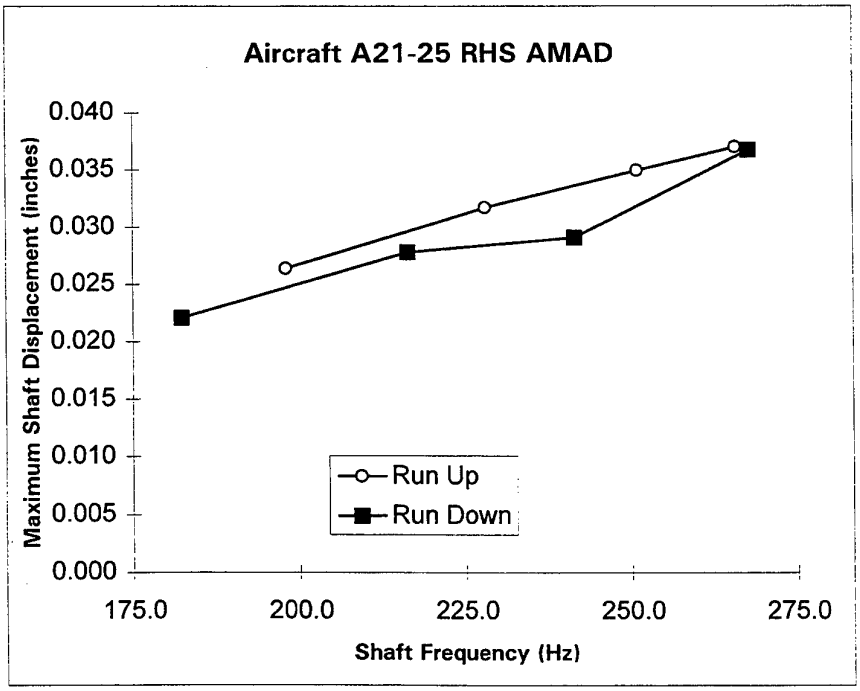

Figure 19(e) Shaft dynamic displacements A21-25

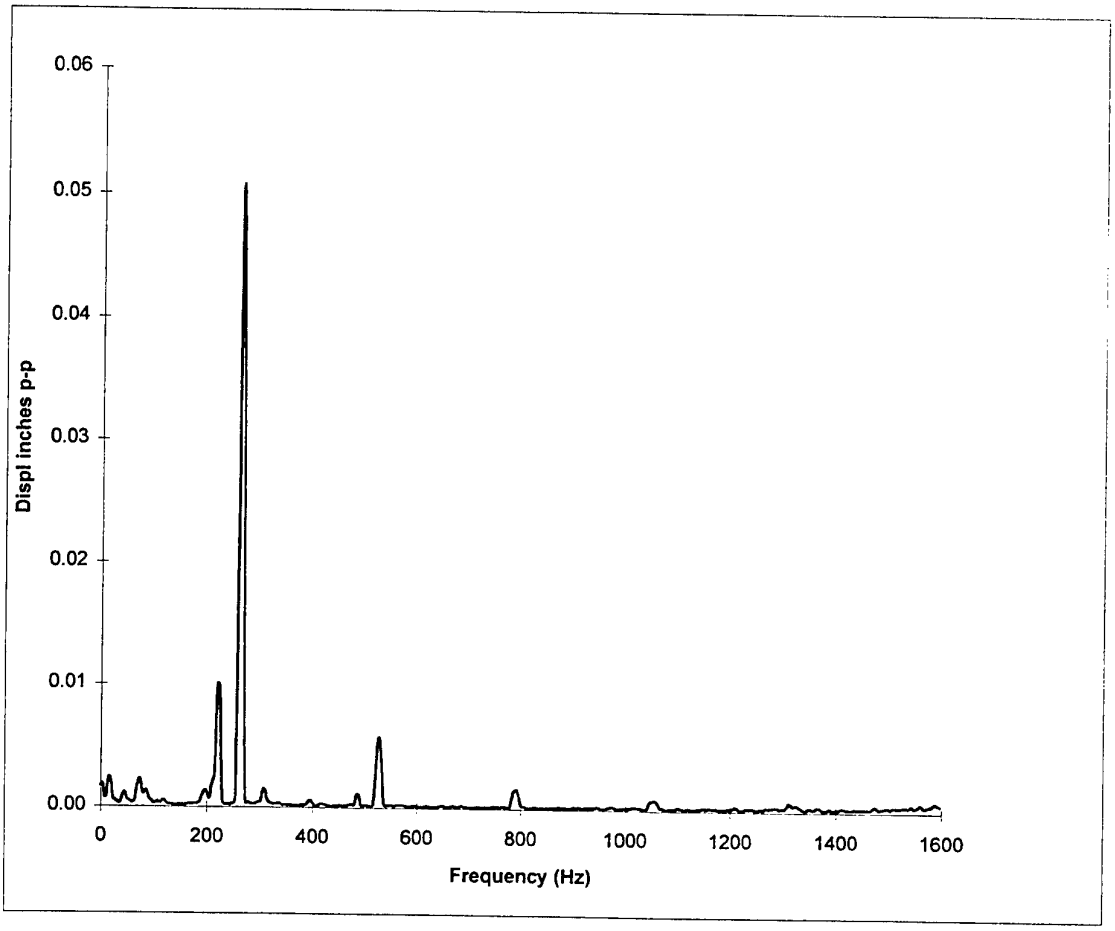

Figure 20 Shaft vibration frequency spectrum A21-06 RHS

AIRCRAFT 35 LHS AMAD GEARBOX

RUN 2

RUN UP

Time *h.mm.ss*	Frequency *Hz*	Velocity *in/s peak*
0.15.08	191.30	0.24
0.15.14	193.13	0.27
0.15.20	197.77	0.27
0.15.27	204.06	0.35
0.15.33	209.52	0.42
0.15.39	214.99	0.57
0.15.45	220.46	0.63
0.15.51	227.74	0.79
0.15.58	233.21	0.80
0.16.04	238.67	0.82
0.16.10	242.32	0.85
0.16.16	245.96	0.88
0.16.22	251.43	1.00
0.16.27	258.72	1.17
0.16.33	260.54	1.29
0.16.39	262.36	1.34
0.16.45	260.54	1.33
0.16.51	262.36	1.34
0.17.05	262.36	1.34
0.17.18	262.36	1.39
0.17.32	262.36	1.42
0.17.45	264.18	1.45
0.18.04	264.18	1.45

RUN DOWN

Time *h.mm.ss*	Frequency *Hz*	Velocity *in/s peak*
0.18.11	264.18	1.46
0.18.17	264.18	1.38
0.18.24	264.18	1.50
0.18.30	255.07	1.18
0.18.36	247.78	1.01
0.18.42	242.32	0.92
0.18.48	233.21	0.85
0.18.53	225.92	0.90
0.19.00	216.81	0.53
0.19.05	207.70	0.48
0.19.11	198.59	0.34
0.19.17	194.95	0.29
0.19.23	191.30	0.24
0.19.28	182.19	0.21
0.19.34	178.55	0.20

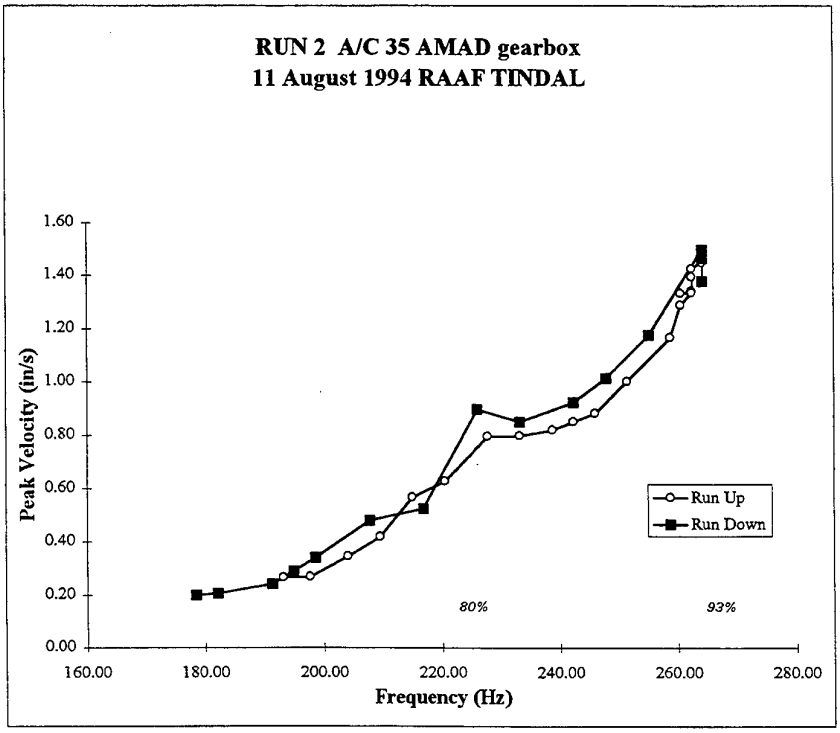

Figure 21 Aircraft A21-35 Left AMAD Vibration

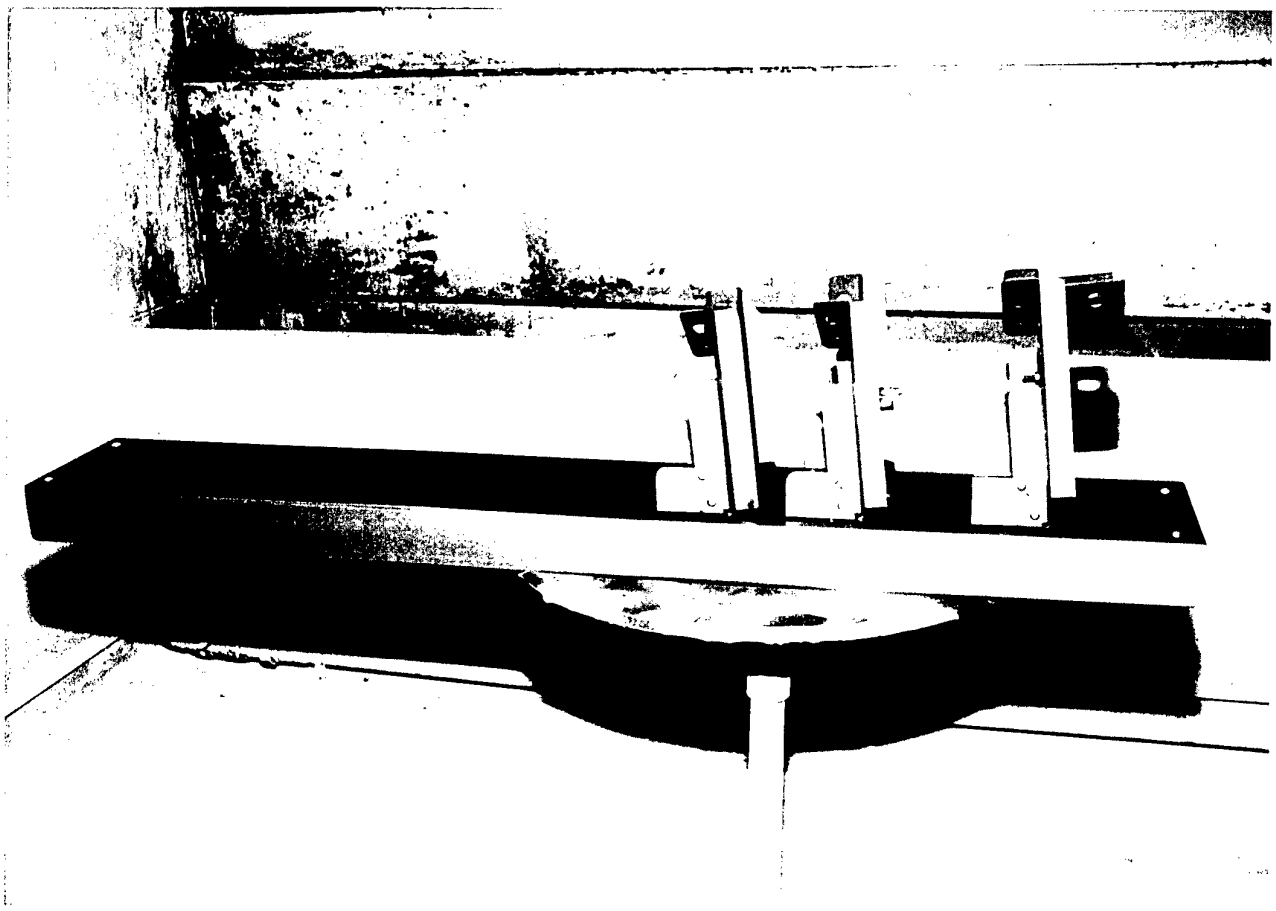

Figure 22 Proximity-probe mounting frame

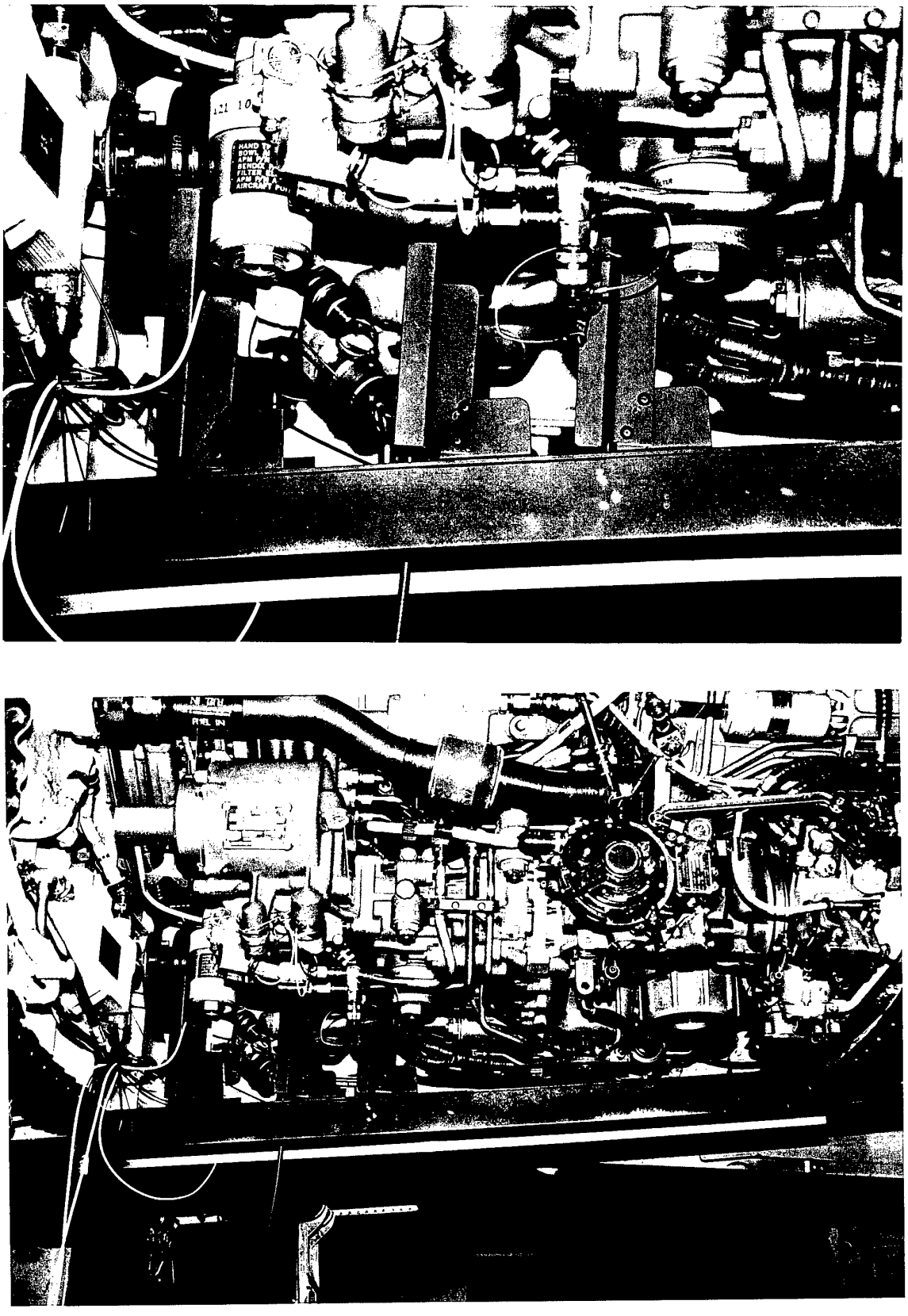

Figure 23 (a) - (b) Airframe installation of proximity-probe mounts

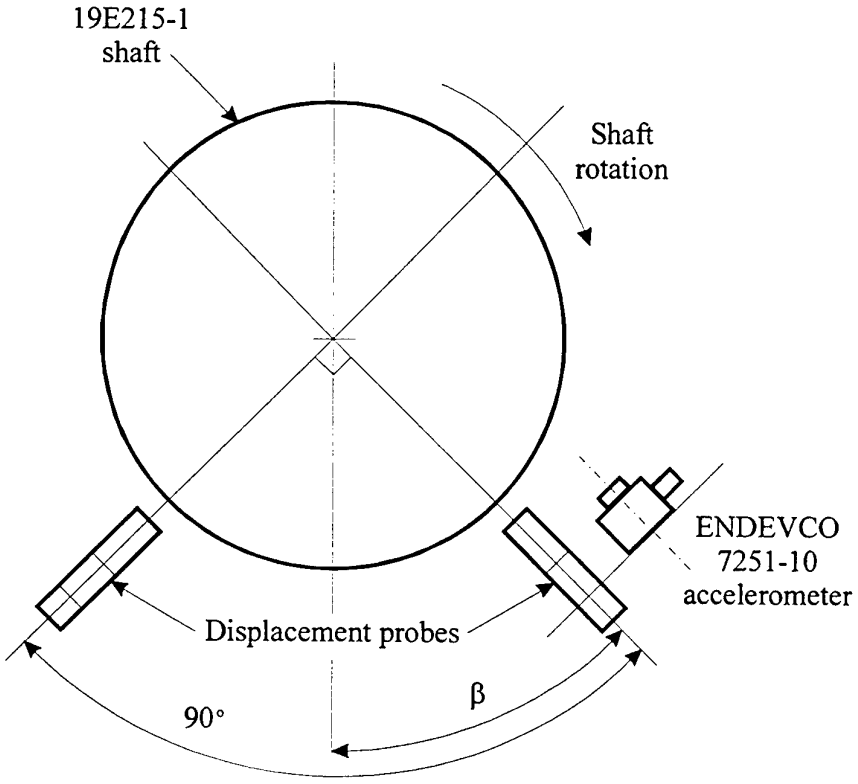

β = 45° for middle and rear probe sets

β = 53° for front probe set

In both cases included angle is 90° as shown

Figure 24 View of probe set-up looking forward

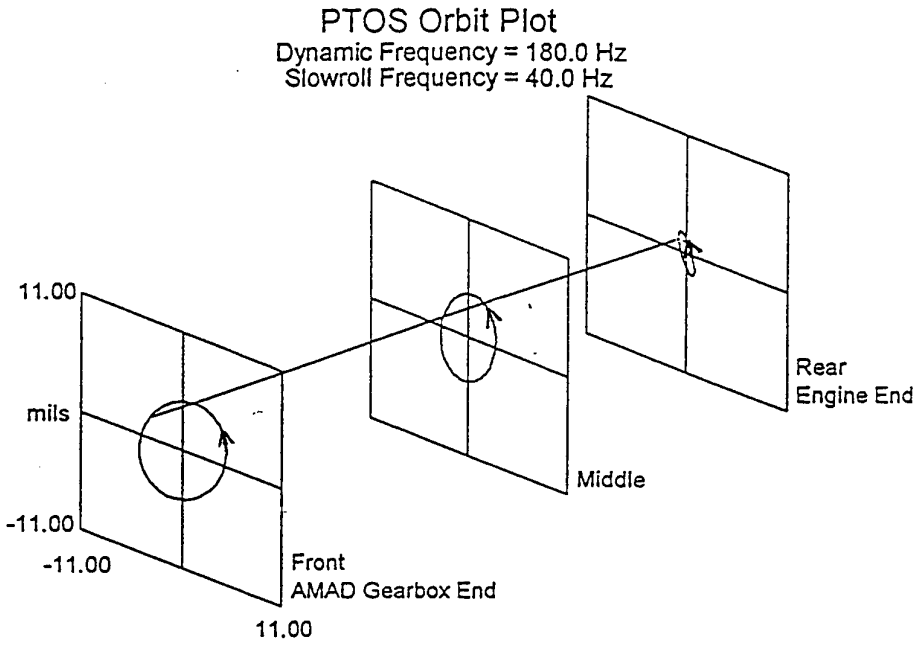

Figure 25(a) LAPTC shaft dynamic plot

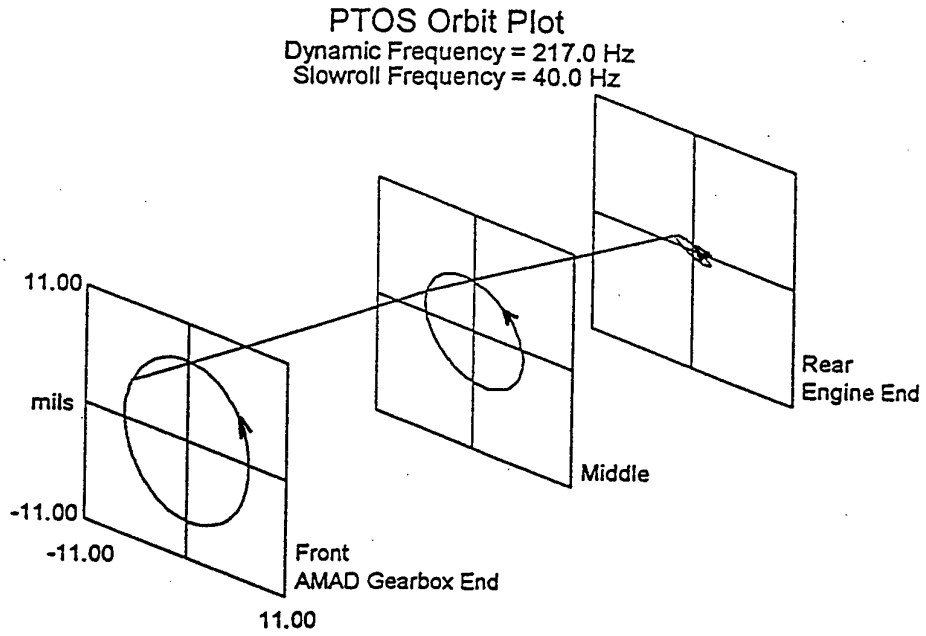

Figure 25(b) LAPTC shaft dynamic plot

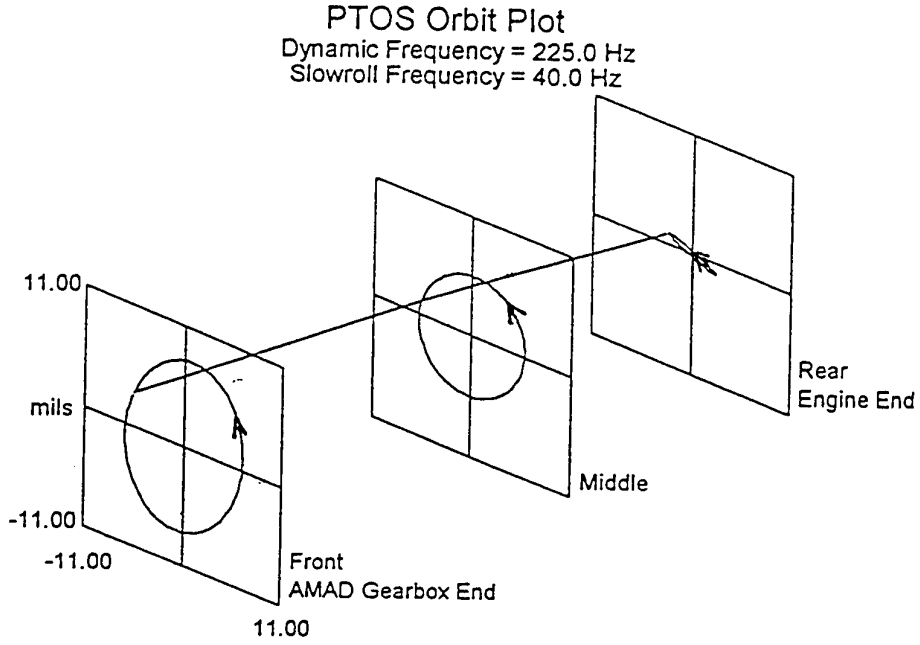

Figure 25(c) LAPTC shaft dynamic plot

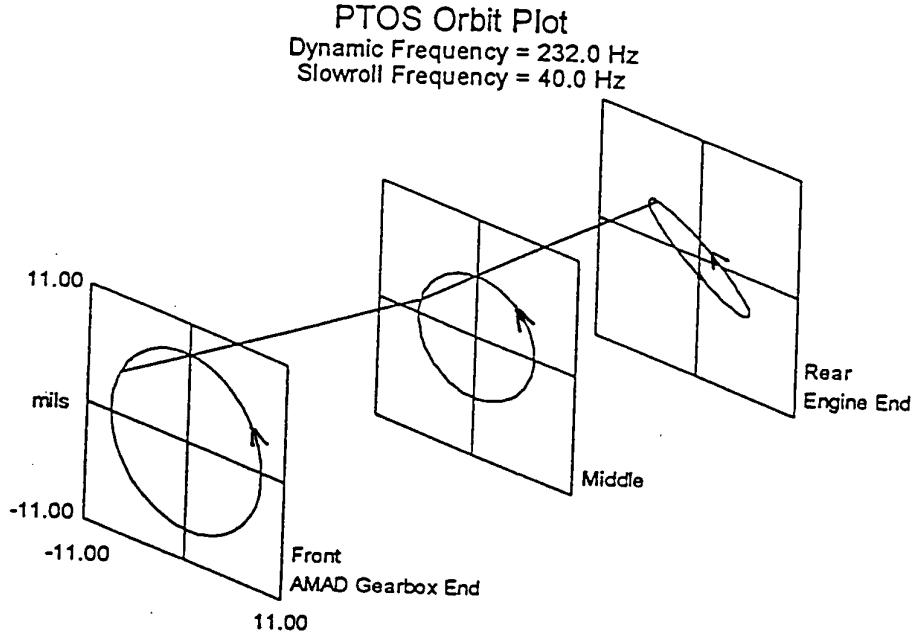

Figure 25(d) LAPTC shaft dynamic plot

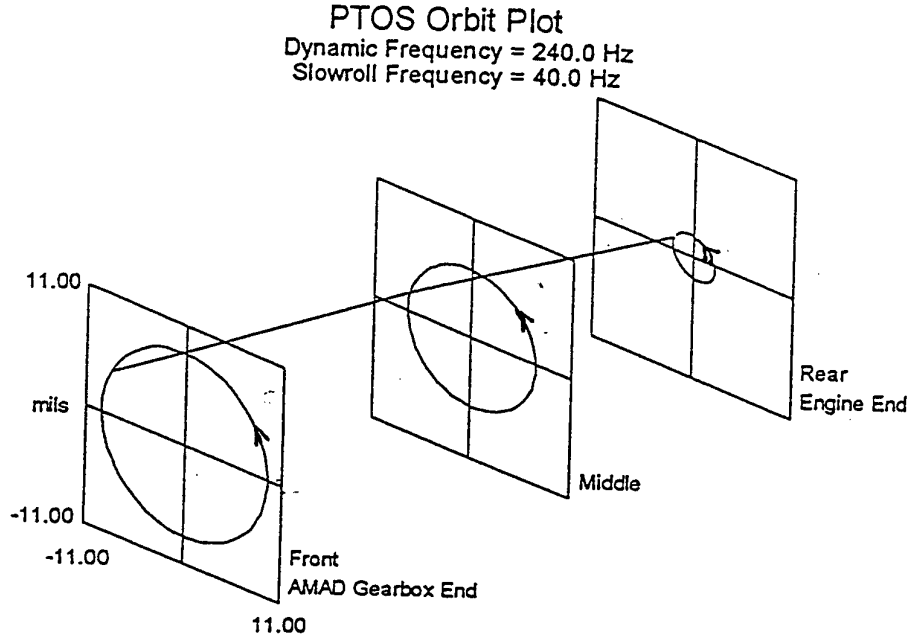

Figure 25(e) LAPTC shaft dynamic plot

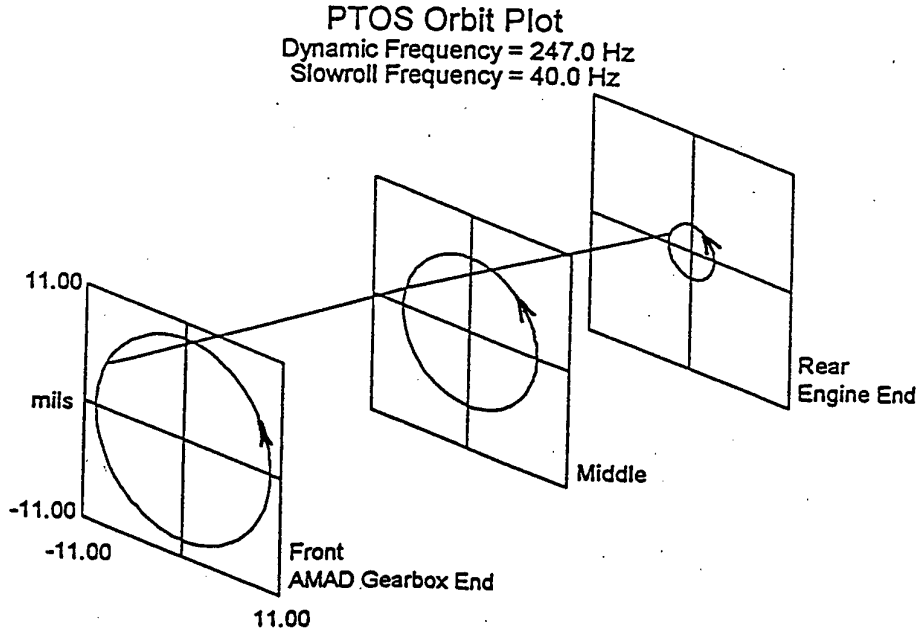

Figure 25(f) LAPTC shaft dynamic plot

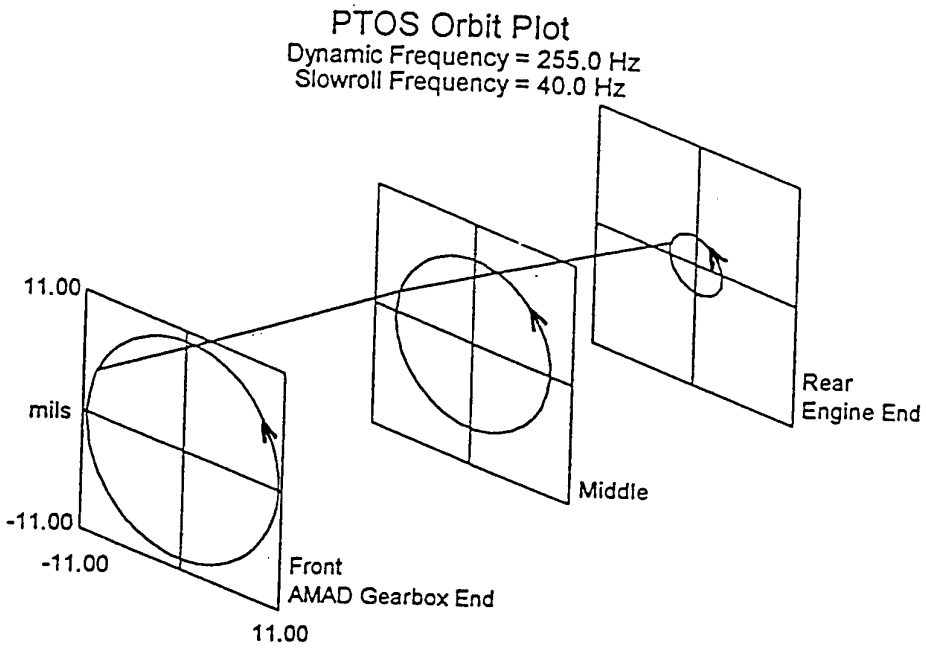

Figure 25(g) LAPTC shaft dynamic plot

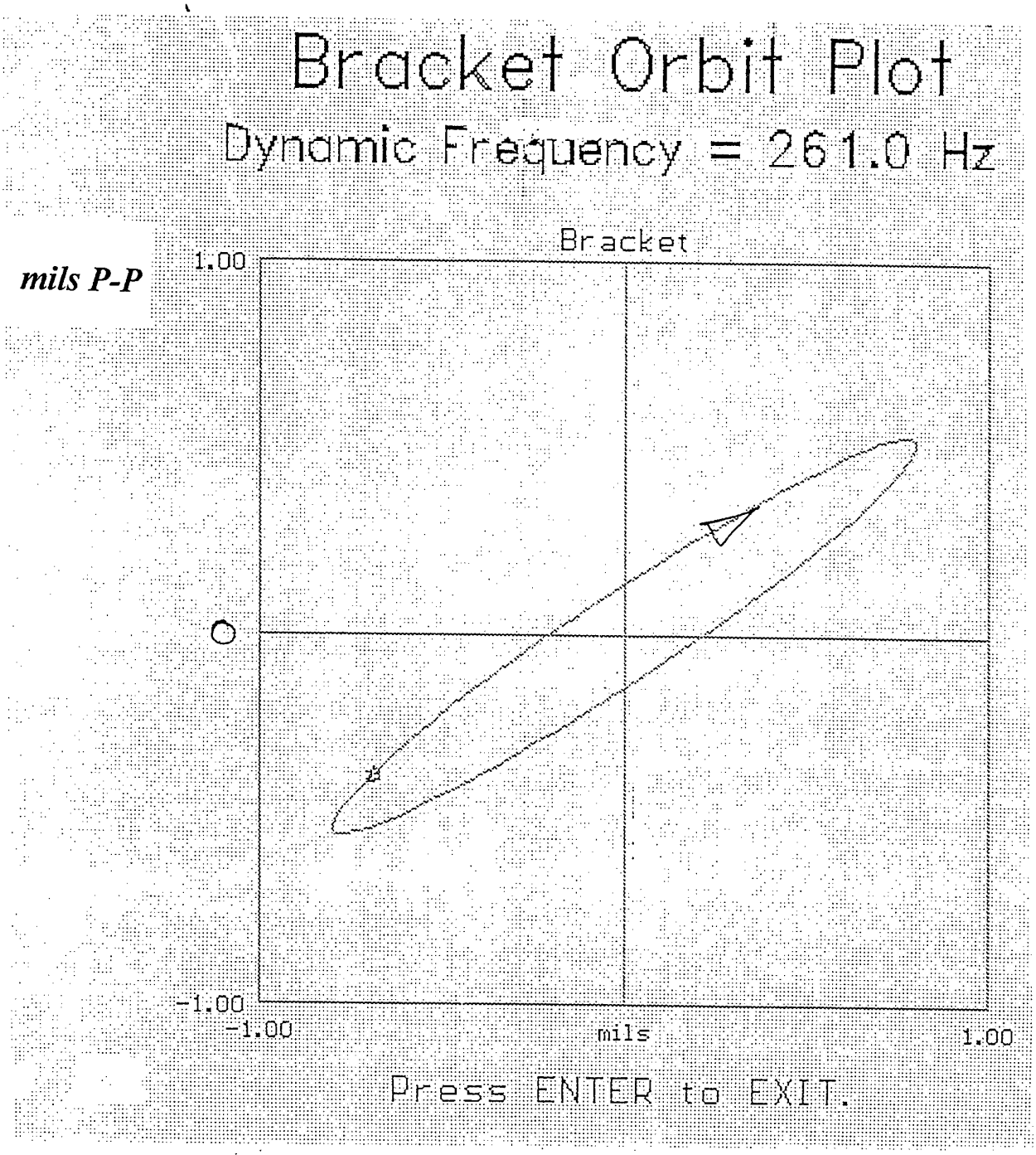

Figure 26 Casing orbit (261Hz)

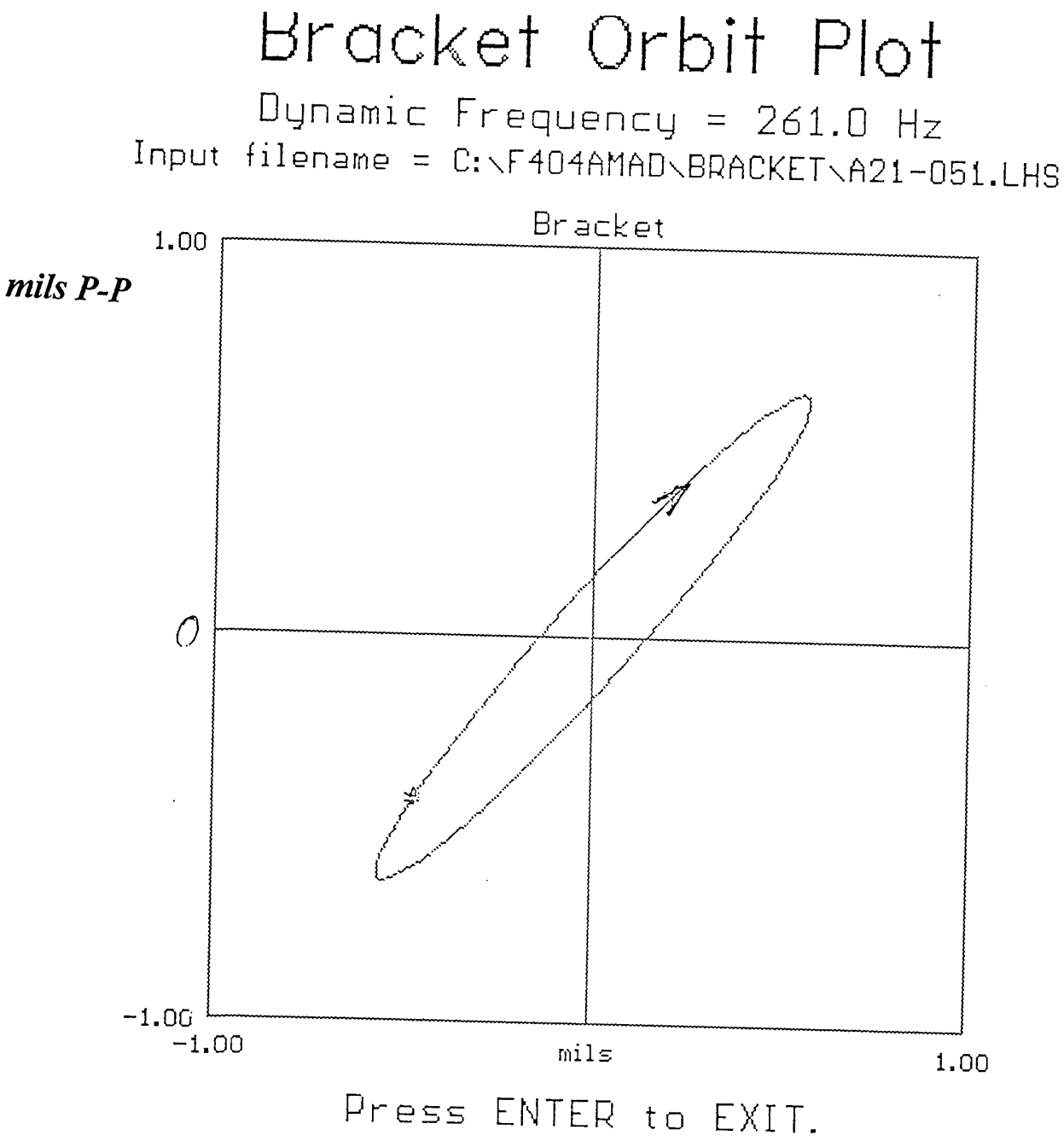

Figure 27(a) Casing orbit A21-51 LHS

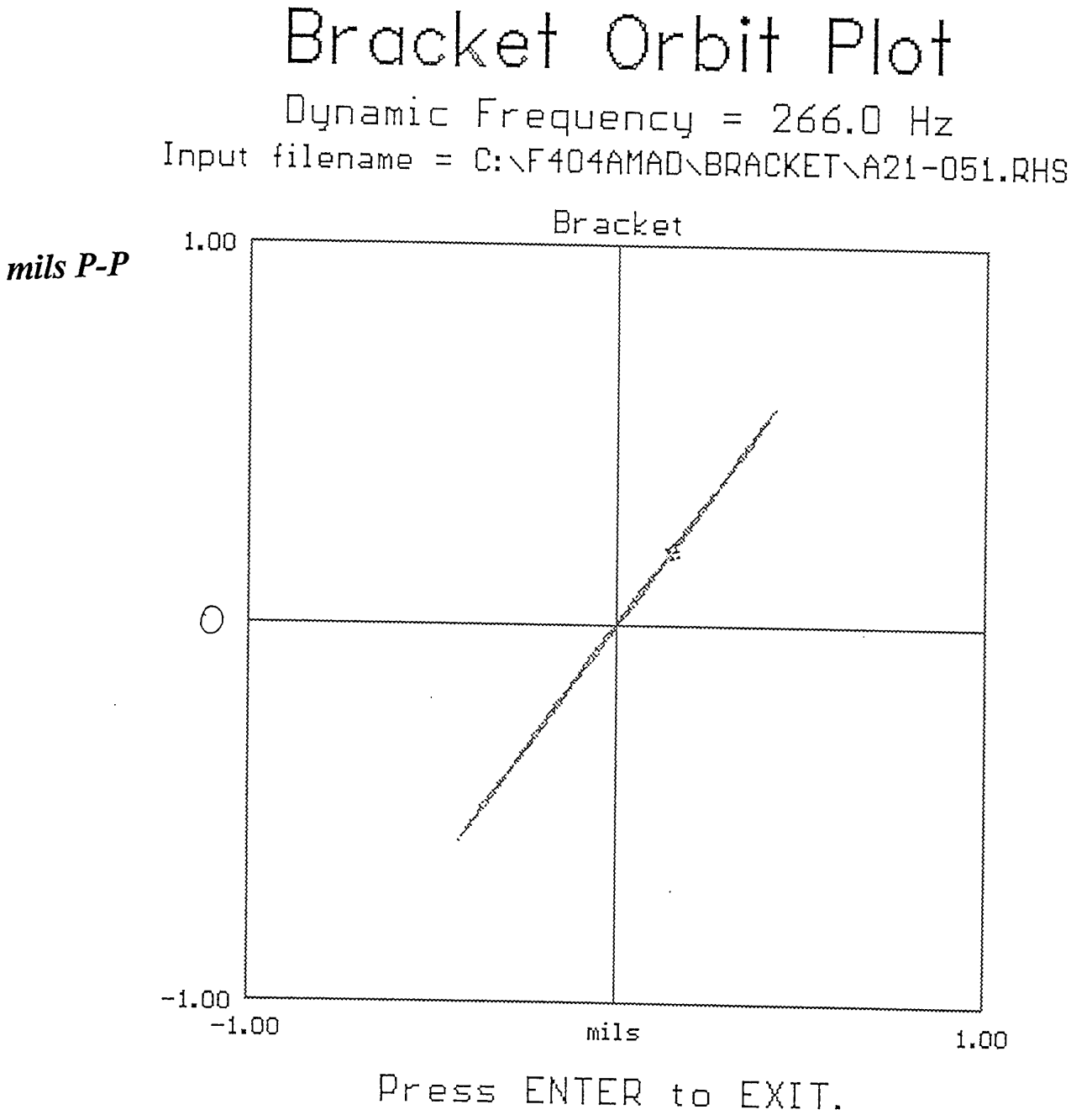

Figure 27(b) Casing orbit A21-51 RHS

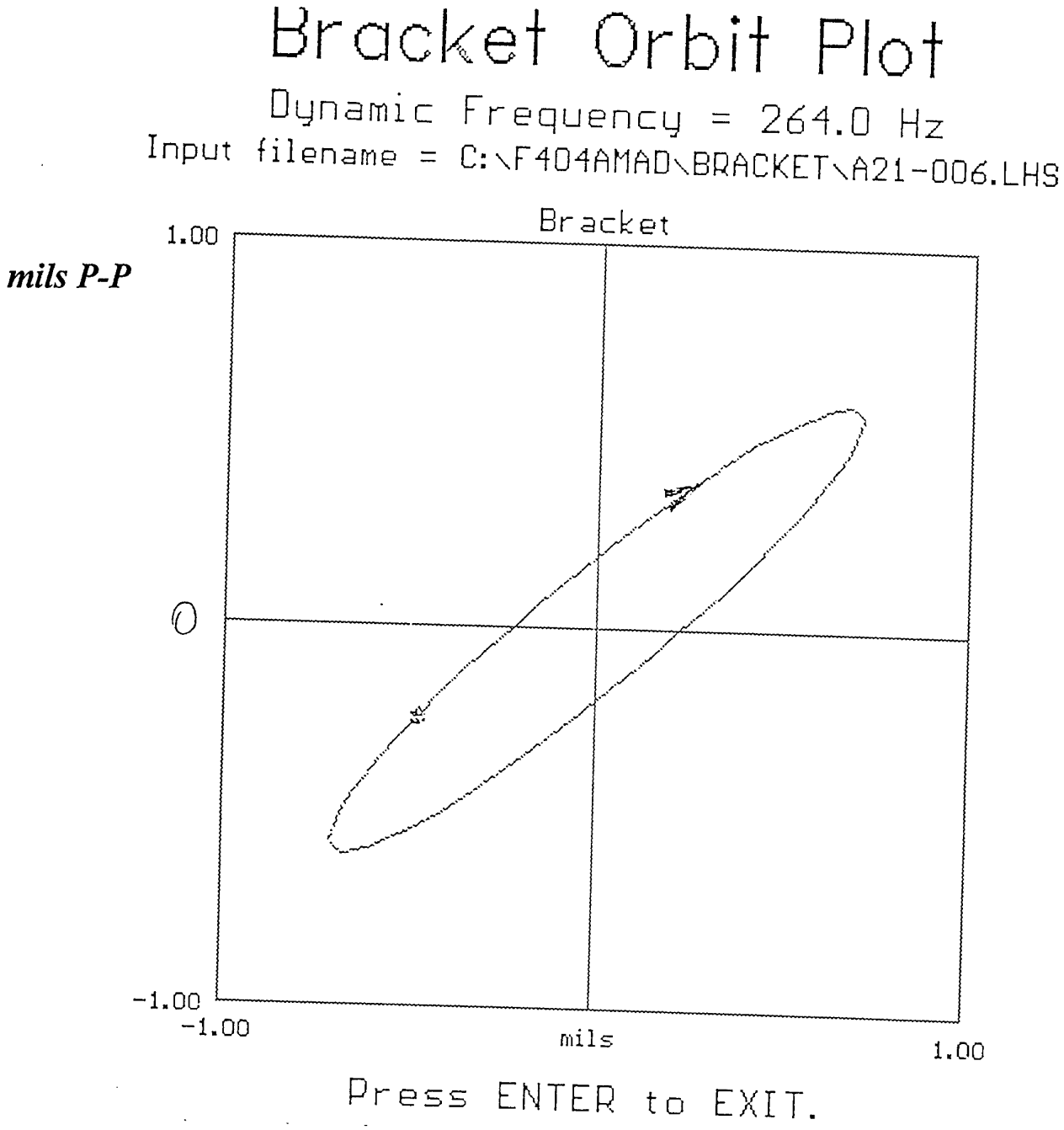

Figure 27(c) Casing orbit A21-06 LHS

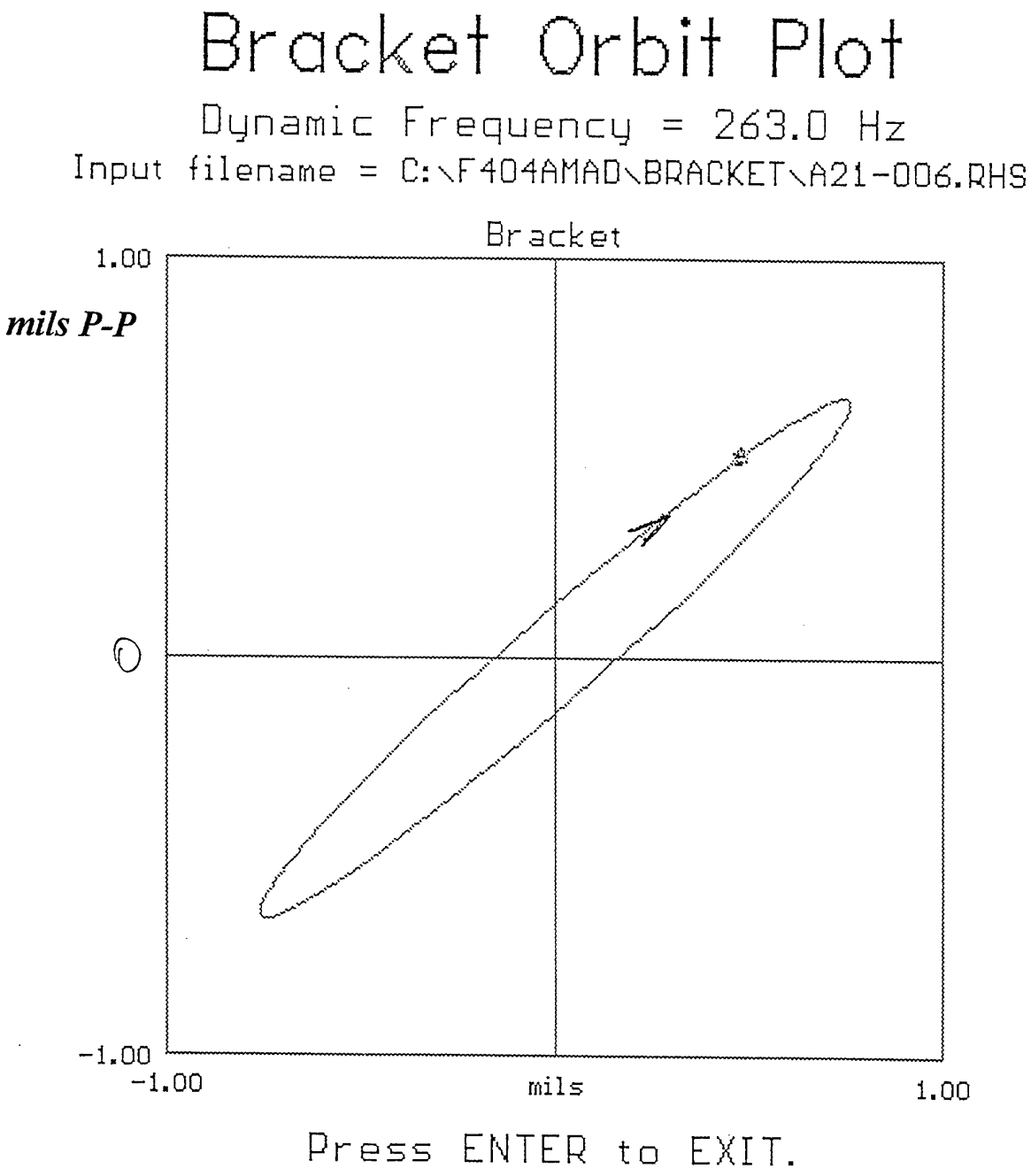

Figure 27(d) Casing orbit A21-06 RHS

Nyquist Plots Amplitude Vs Phase LAPTC Shaft

Lucas Test Rig 25/11/94 LAPTC Shaft from A21-49 and "old" PTS Housing

Shaft freq *Hz*	Ampl P-P *mils*	Phase *Degrees*	x-coord *mils*	y-coord *mils*
27	11	4.3	0.00	0.00
116	13	17.7	1.42	3.13
131	14	19	2.27	3.73
146	16.7	26	4.04	6.50
165	18.4	29.1	5.11	8.12
180	20.1	31	6.26	9.53
198	22	29	8.27	9.84
216	25.1	29	10.98	11.35
260	32	27	17.54	13.70
280	41	28	25.23	18.43
290	47	25	31.63	19.04
302	58	23	42.42	21.84

corrected for slow-roll run-out

Shaft rotated 120 deg relative to initial position

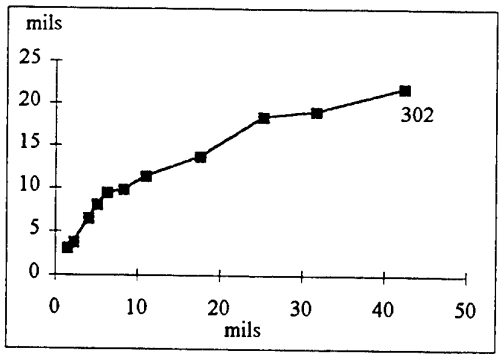

Shaft freq *Hz*	Ampl P-P *mils*	Phase *Degrees*	x-coord *mils*	y-coord *mils*
20	10.5	21	0.00	0.00
55	11.1	29	-0.09	1.62
80	11.2	34	-0.52	2.50
102	12.2	39	-0.32	3.92
127	13.4	44	-0.16	5.55
152	14.1	46	-0.01	6.38
175	15	49	0.04	7.56
195	19	53	1.63	11.41
225	21.7	47	5.00	12.11
262	29.1	39	12.81	14.55
282	38	28	23.75	14.08
305	49	14	37.74	8.09

corrected for slow-roll run-out

Shaft rotated 240 deg relative to initial position

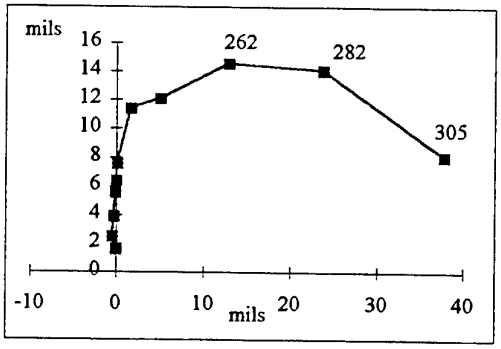

Shaft freq *Hz*	Ampl P-P *mils*	Phase *Degrees*	x-coord *mils*	y-coord *mils*
	low freq. data not available			
177	7.7	37	6.15	4.63
187	7.4	36	5.99	4.35
205	9	42	6.69	6.02
217	10.3	43	7.53	7.03
247	16.8	-22	15.58	-6.29
255	18.7	-21	17.46	-6.70
272	24	-24	21.92	-9.76
282	29	-24	26.49	-11.80
290	31	-29	27.11	-15.03
295	33.7	-36	27.26	-19.81
290	31	-29	27.11	-15.03
302	32.7	-47	25.37	-27.21

not corrected for slow-roll run-out

Shaft at initial position

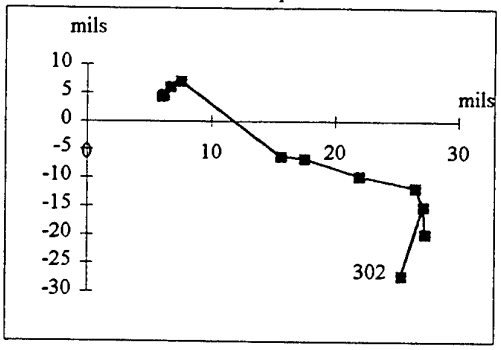

Figure 28 Shaft Nyquist plots Lucas Test Rig

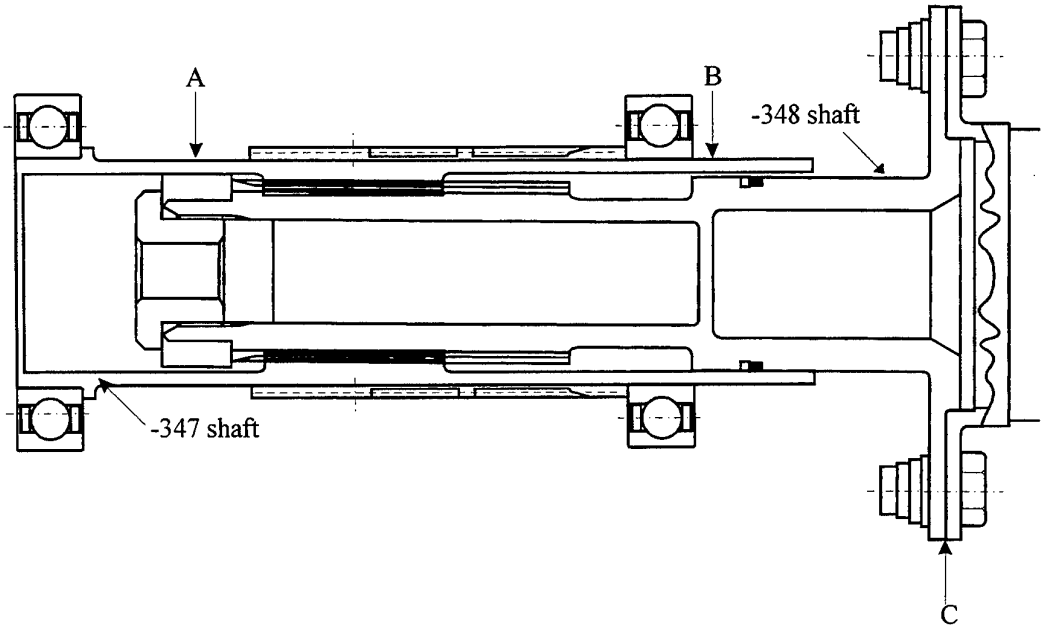

Figure 29 PTS drive assembly

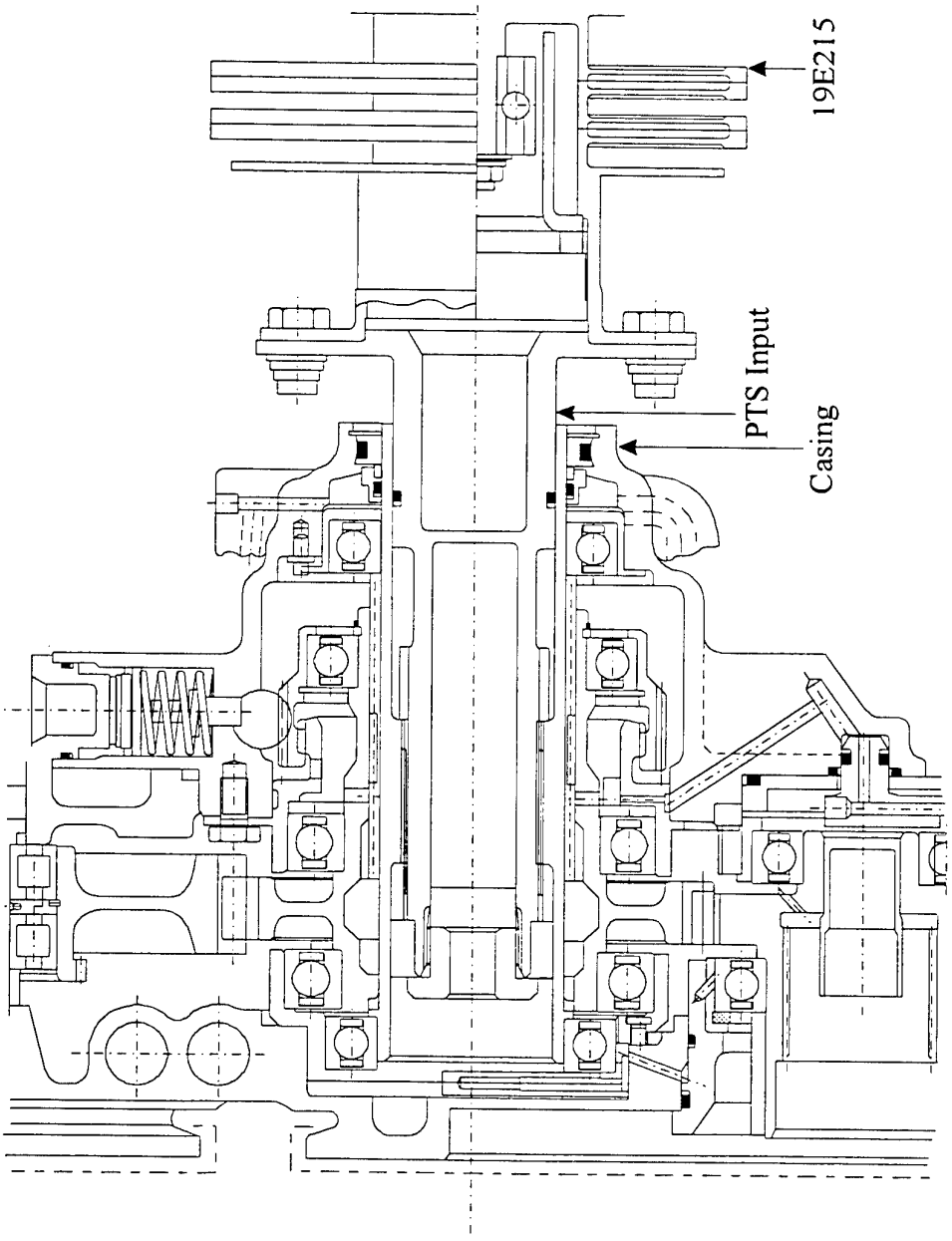

Figure 30 Measurement locations of PTS assembly clearance

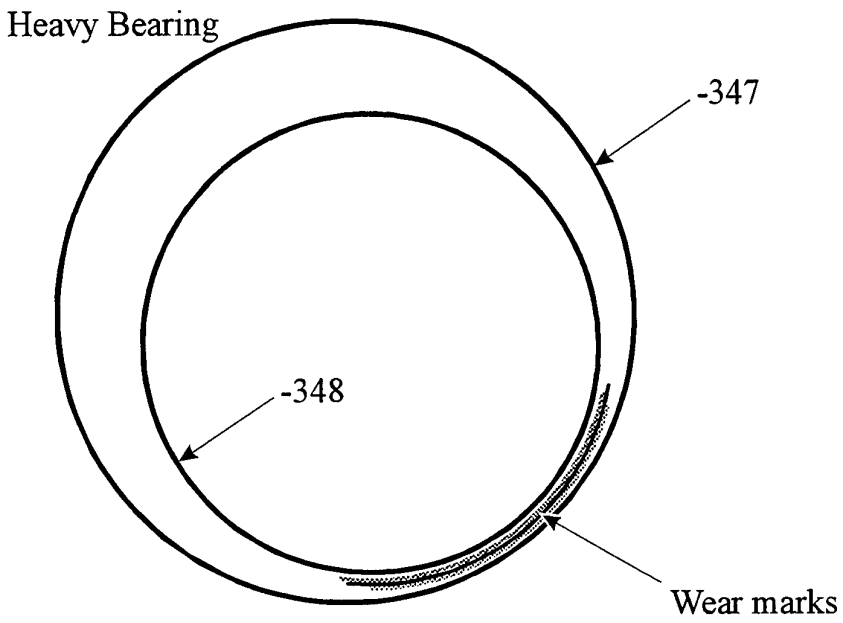

Section through (B) (Fig. 29)

Figure 31 Bearing wear on -347/-348 assembly

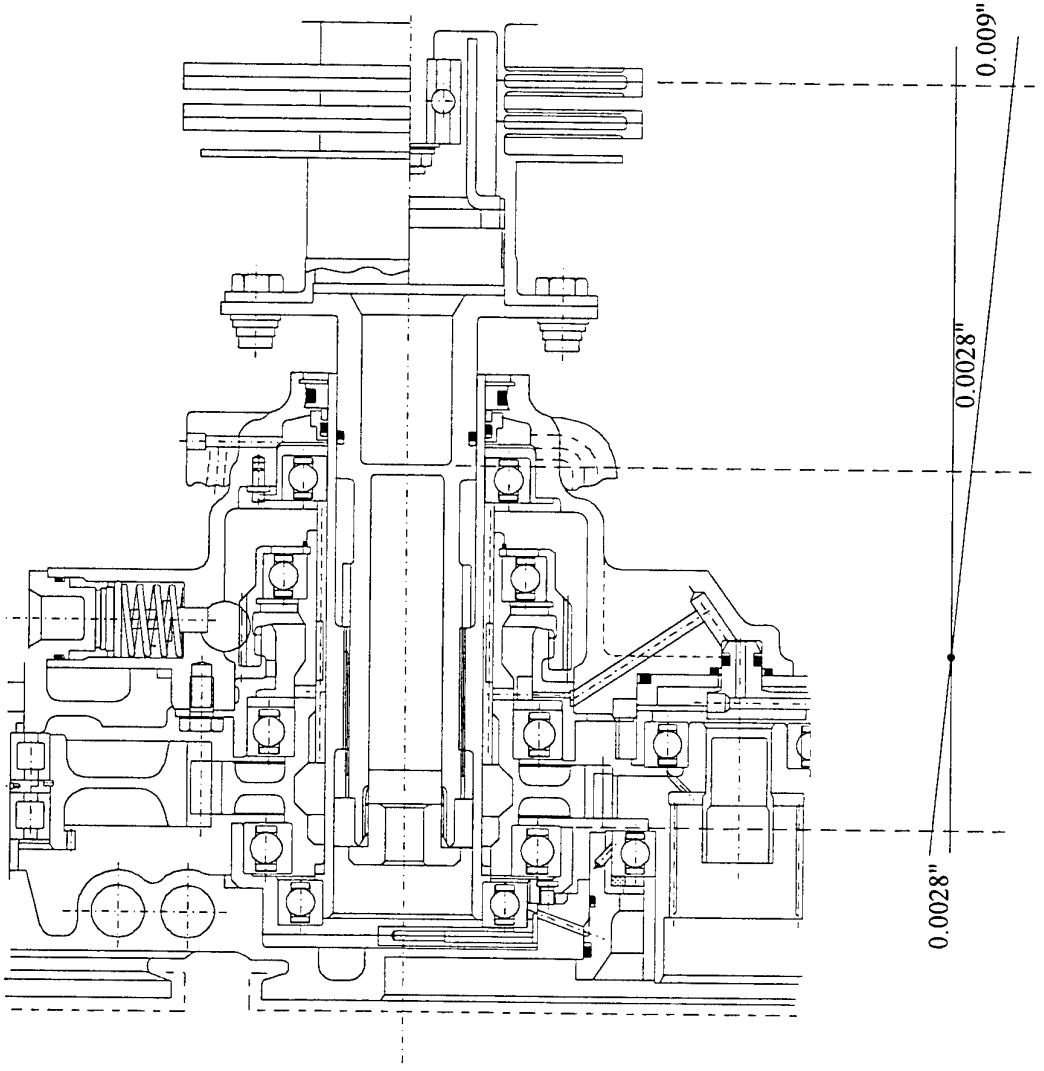

Figure 32 Clearance of 19E215 shaft due to transverse displacement and angular misalignment

HORNET AMAD GEARBOX SPEED RATIOS

ITEM		*RATIO*	*TEETH*
INPUT SHAFT		1.0000	39
ATS CLUSTER GEAR	(M)	0.8478	46/66
No. 2 OIL PUMP	(A)	0.6287	89
ATS GEAR	(E)	1.5000	26
HYDRAULIC PUMP IDLER	(R)	0.7959	49/25
HYDRAULIC PUMP	(C)	0.2726	73
GENERATING GEAR	(B)	1.5000	26
FUEL PUMP IDLER GEAR	(P)	0.6290	62/43
No. 1 OIL PUMP	(F)	0.6290	43
FUEL PUMP	(D)	0.4745	57

AMAD INPUT BEARING DETAILS:

Number of balls :	13
Diameter of balls :	0.240"
Distance from bearing centre to centre of balls :	0.975"

Fault Frequencies :

Fault Type	**Ratio**	**fault frequency at 80% military speed (13500Hz)**
Outer race fault	5.700	1277.5 Hz
Inner race fault	7.300	1636.2 Hz
Ball fault	4.001	896.8 Hz
Cage fault	0.4385	0.0983 Hz

Table 1 Gearbox Ratios

Left-Hand Engine AMAD

Circumferential Accelerometer

Run-Up

Frequency Hz	*g rms*	*vel in/s rms*
196	2.08	0.65
204	2.61	0.79
208	3.47	1.02
218	5.11	1.44
226	6.21	1.69
236	8.77	2.28
248	12.2	3.02
262	18.1	4.24
263	19	4.44
264	20.1	4.68
265	21.2	4.91
266	21.7	5.01
267	22	5.06

Run-Down

Frequency Hz	*g rms*	*vel in/s rms*
260	17.3	4.09
254	15.3	3.7
248	12.5	3.1
238	9.73	2.51
228	6.71	1.81
216	5.43	1.54
206	3.38	1.01
188	1.61	0.53
182	1.29	0.44

Radial Accelerometer

Run-Up

Frequency Hz	*g rms*	*vel in/s rms*
196	0.44	0.14
204	0.7	0.21
228	1.73	0.47
244	2.11	0.53
260	4.81	1.14
264	5.82	1.35
268	6.2	1.42

Axial Accelerometer

Run-Up

Frequency Hz	*g rms*	*vel in/s rms*
196	0.6	0.19
216	1.56	0.44
226	2.24	0.61
234	2.89	0.76
242	3.9	0.99
254	4.7	1.14
266	5.33	1.23

Right-Hand Engine AMAD

Run-Up

	Frequency Hz	*g rms*	*vel in/s rms*
Radial Accelerometer	264	6.53	1.52
Circumferential Accelerometer	264	11.1	2.58
Axial Accelerometer	266	4	0.92

Table 2 Summary of vibration levels A21-116

Aircraft 116 Left-Hand Engine AMAD 3/3/94

N2	Frequency	Circumferential Acceleration		Velocity rms	Phase	Displacement	PTS shaft Displacement	Shaft Phase
Rpm	*Hz*	*mV*	*g rms*	*in/s*		*V*	*in p-p*	
11040	184	10	2	0.67	-93	0.58	0.014	-81
11760	196	16.5	3.3	1.03	-102	0.58	0.014	-74
12000	200	19.9	3.98	1.22	-103	0.58	0.014	-69
12240	204	24.6	4.92	1.48	-105	0.57	0.017	-70
12840	214	34.3	6.86	1.97	-117	0.57	0.017	-81
13440	224	39	7.8	2.14	-123	0.55	0.023	-62
14280	238	54.9	10.98	2.83	-130	0.53	0.028	-74
15240	254	81.4	16.28	3.94	-148	0.53	0.028	-88
15720	262	102	20.4	4.78	-157	0.51	0.034	-97
15780	263	104	20.8	4.86	-158	0.5	0.037	-98
15840	264	107	21.4	4.98	-160	0.48	0.043	-99
15900	265	108	21.6	5.01	-163	0.48	0.043	-101
15900	265	101	20.2	4.68	-157	0.47	0.046	-102
14880	248	64.1	12.82	3.18	-142	0.5	0.037	-85
14220	237	44	8.8	2.28	-134	0.52	0.031	-79
13440	224	37	7.4	2.03	-131	0.55	0.023	-66
12960	216	25.1	5.02	1.43	-109	0.56	0.020	-75
11880	198	15.5	3.1	0.96	-102	0.57	0.017	-78
10920	182	9.8	1.96	0.66	-95	0.58	0.014	-78
10920	182	9.4	1.88	0.63	-95	0.58	0.014	-79

NOTE: Phase angles are relative to shaft once/rev tacho pulse.

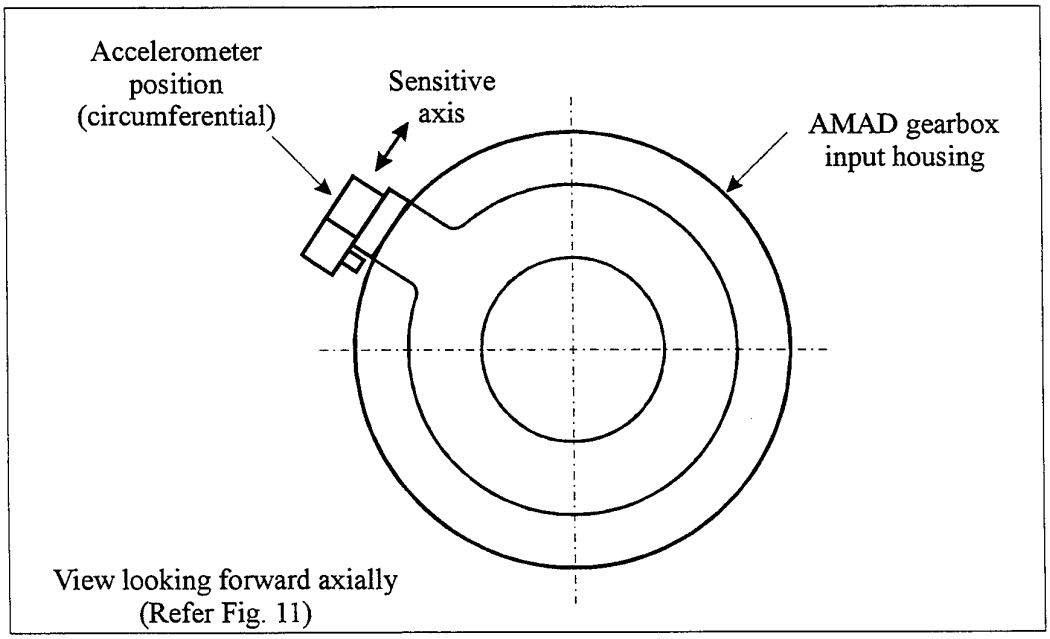

Table 3 LAPTC shaft dynamic run-out A21-116

Aircraft ID	Shaft speed (% Throttle/Hz)	Maximum displacement (peak-peak mils)	1*Tangential acceleration (in/s rms) *
A21-051 LHS	93% / 260	44	0.96
A21-051 RHS	95% / 266	41	0.98
A21-006 LHS	93% / 261	43	1.25
A21-006 RHS	94% / 264	49	1.25
A21-114 LHS	92% / 257	51	1.15
A21-114 RHS	96% / 270	69	
A21-021 LHS	94% / 262	46	1.29
A21-021 RHS	94% / 265	69	1.25
A21-025 LHS	96% / 268	40	1.25
A21-025 RHS	96% / 268	37	1.72

* The highest vibration levels were recorded on the tangential accelerometer

Table 4 Summary of results from A21-51, 06, 114, 21 and 25

A21-51 LHS AMAD

Frequency (Hz)	*Max Disp.* (inches)*	*Avg Disp.* (inches)*
181.1	0.024	0.020
196.9	0.025	0.019
211.1	0.031	0.023
231.9	0.040	0.031
246.5	0.043	0.033
258.8	0.044	0.037
260.0	0.044	0.037
260.8	0.042	0.035
243.8	0.043	0.034
225.5	0.033	0.026
199.8	0.027	0.022
181.5	0.022	0.018
181.5	0.025	0.020

A21-51 RHS AMAD

Frequency (Hz)	*Max Disp. (inches)*	*Avg Disp. (inches)*
191.1	0.020	0.015
209.0	0.026	0.019
227.8	0.029	0.022
246.6	0.031	0.024
264.5	0.039	0.031
265.8	0.041	0.032
267.7	0.039	0.030
243.4	0.027	0.022
216.3	0.024	0.018
195.6	0.020	0.015

A21-6 LHS AMAD

Frequency (Hz)	*Max Disp. (inches)*	*Avg Disp. (inches)*
181.2	0.015	0.012
202.5	0.016	0.012
231.0	0.023	0.016
249.2	0.029	0.021
261.2	0.043	0.033
262.7	0.042	0.031
263.6	0.039	0.030
263.8	0.041	0.030
264.6	0.042	0.033
257.4	0.025	0.020
238.3	0.021	0.017
217.3	0.015	0.011
195.6	0.012	0.009

A21-6 RHS AMAD

Frequency (Hz)	*Max Disp. (inches)*	*Avg Disp. (inches)*
192.6	0.022	0.017
213.7	0.030	0.023
226.1	0.024	0.018
234.0	0.035	0.029
258.5	0.041	0.036
263.0	0.047	0.038
263.8	0.046	0.036
264.2	0.049	0.038
264.9	0.046	0.034
265.4	0.047	0.038
249.2	0.042	0.310
232.2	0.036	0.029
203.6	0.032	0.026
186.1	0.023	0.018

* All displacements are peak-peak inches

Table 5(a) Shaft vibration run-up/down

A21-114 LHS AMAD

Frequency (Hz)	*Max Disp. (inches)*	*Avg Disp. (inches)*
195.0	0.032	0.025
215.8	0.036	0.033
283.3	0.042	0.038
257.1	0.051	0.043
263.4	0.049	0.045
264.2	0.047	0.042
264.6	0.043	0.041
264.9	0.043	0.040
253.4	0.041	0.036
239.1	0.037	0.034
217.7	0.031	0.028
195.7	0.028	0.023

A21-114 RHS AMAD

Frequency (Hz)	*Max Disp. (inches)*	*Avg Disp. (inches)*
178.6	0.028	0.023
202.1	0.030	0.024
219.4	0.037	0.030
230.4	0.050	0.044
267.3	0.064	0.056
266.9	0.068	0.056
268.0	0.066	0.054
269.0	0.069	0.058
269.8	0.069	0.057
243.5	0.049	0.045
215.3	0.038	0.032
195.6	0.032	0.025

A21-21 LHS AMAD

Frequency (Hz)	*Max Disp. (inches)*	*Avg Disp. (inches)*
193.5	0.031	0.026
208.9	0.027	0.021
228.9	0.040	0.034
248.5	0.044	0.035
260.8	0.045	0.039
262.3	0.046	0.039
262.4	0.046	0.039
263.0	0.044	0.039
249.9	0.040	0.034
233.1	0.034	0.030
218.9	0.033	0.027
196.7	0.029	0.025

A21-21 RHS AMAD

Frequency (Hz)	*Max Disp. (inches)*	*Avg Disp. (inches)*
182.6	0.030	0.023
200.9	0.025	0.019
224.9	0.031	0.025
250.9	0.068	0.052
264.6	0.069	0.056
265.4	0.063	0.053
266.2	0.066	0.053
266.6	0.063	0.051
261.9	0.057	0.051
243.8	0.050	0.042
226.3	0.031	0.025
202.2	0.027	0.021
183.0	0.032	0.024

Table 5(b) Shaft vibration run-up/down

A21-25 LHS AMAD

Frequency (Hz)	*Max Disp. (inches)*	*Avg Disp. (inches)*
198.7	0.017	0.013
228.7	0.029	0.024
248.9	0.035	0.027
266.6	0.040	0.033
268.1	0.040	0.036
268.1	0.037	0.031
268.2	0.038	0.033
268.1	0.035	0.031
251.0	0.031	0.027
227.3	0.026	0.021
194.9	0.022	0.017

A21-25 RHS AMAD

Frequency (Hz)	*Max Disp. (inches)*	*Avg Disp. (inches)*
198.0	0.026	0.020
228.1	0.032	0.025
250.9	0.035	0.029
265.7	0.037	0.032
267.7	0.037	0.029
267.7	0.037	0.031
241.5	0.029	0.023
216.3	0.028	0.020
182.4	0.022	0.017

Table 5(c) Shaft vibration run-up/down

Tape *h:mm:ss*	Order	Freq *Hz*	Amp *mV rms*	Accel *in/s^2*	Accel phase *deg*	Disp *mils P-P*	Disp phase *deg*
A21 - 051 LHS - 16/3/94 Tape #1: Tacho in B&K Ch#A, Vib in B&K Ch#B							
Radial Accelerometer							
0:10:00	1	261	8.75	336.34	174.4	0.35	-5.6
	2	522	19.40	745.71	14.2	0.20	-165.8
	3	783	6.56	252.16	58.2	0.03	-121.8
Tangential Accelerometer							
0:10:00	1	261	41.40	1591.36	136.5	1.67	-43.5
	2	522	2.28	87.64	170.1	0.02	-9.9
	3	783	21.70	834.12	129.2	0.10	-50.8
Axial Accelerometer							
0:10:00	1	261	21.20	814.90	-62.5	0.86	-242.5
	2	522	7.20	276.76	-49.2	0.07	-229.2
	3	783	14.10	541.98	-86.3	0.06	-266.3
A21 - 051 RHS - 16/3/94 Tape #1: Tacho in B&K Ch#A, Vib in B&K Ch#B							
Radial Accelerometer							
0:40:00	1	266	3.03	116.47	66.8	0.12	-113.2
	2	531	17.70	680.36	-168.7	0.17	-348.7
Tangential Accelerometer							
0:40:00	1	266	36.60	1406.85	69.6	1.42	-110.4
	2	531	7.24	278.30	0.2	0.07	-179.8
Axial Accelerometer							
0:40:00	1	266	10.30	395.92	-133.8	0.40	-313.8
	2	531	4.31	165.67	-60.2	0.04	-240.2
A21 - 0006 LHS - 16/3/94 Tape #1: Tacho in B&K Ch#A, Vib in B&K Ch#B							
Radial Accelerometer							
1:09:00	1	263	15.80	607.33	-64.2	0.63	-244.2
	2	527	39.90	1533.70	-23.6	0.40	-203.6
	3	790	8.06	30.82	-174.6	0.04	-354.6
Tangential Accelerometer							
1:09:00	1	263	48.10	1848.90	-43.9	1.92	-223.9
	2	527	24.10	926.37	-123.7	0.24	-303.7
	3	790	28.80	1107.03	-101.2	0.13	-281.2
Axial Accelerometer							
1:09:00	1	263	17.30	664.99	106.0	0.69	-74.0
	2	527	10.10	388.23	155.9	0.10	-24.1
	3	790	11.70	449.73	63.8	0.05	-116.2
A21 - 006 RHS - 16/3/94 Tape #1: Tacho in B&K Ch#A, Vib in B&K Ch#B							
Radial Accelerometer							
1:37:00	1	264	15.90	611.17	-151.3	0.63	-331.3
	2	527	29.70	1141.63	-169.1	0.29	-349.1
	3	791	4.46	171.44	-106.3	0.02	-286.3
Tangential Accelerometer							
1:37:00	1	264	43.90	1687.45	-121.7	1.73	-301.7
	2	527	14.30	549.67	75.4	0.14	-104.6
	3	791	14.40	553.52	56.2	0.06	-123.8
Axial Accelerometer							
1:37:00	1	264	18.90	726.49	26.8	0.75	-150.2
	2	527	8.11	311.74	17.4	0.08	-162.2
	3	791	7.79	299.44	175.2	0.03	-4.8

NOTE : Phase is for acceleration signal relative to tacho.
180° to be added to correct for displacement.

Table 6 Casing vibration data A21-51 RHS, LHS, -06 RHS, LHS

Vibration levels in 'in/s' at both 80% (225Hz) and 94% (264Hz)

Aircraft	ACC #1 (radial) 80% 225Hz	ACC #1 (radial) 93% 264 Hz	ACC #2 (tangential) 80% 225Hz	ACC #2 (tangential) 93% 264 Hz	ACC #3 (axial) 80% 225Hz	ACC #3 (axial) 93% 264 Hz
	Left hand side AMAD Gearbox					
4	0.08	0.39	0.6	1.59	0.34	0.73
6	0.07	0.36	0.43	1.07	0.15	0.41
21	0.11	0.42	0.64	1.12	0.35	0.59
25	0.06	0.32	0.6	1.11	0.27	0.44
51	0.02	0.19	0.41	0.9	0.13	0.24
114	0.26	0.77	0.65	1.36	0.26	0.76
116	0.48	1.18	1.62	4.55		
	Right hand side AMAD Gearbox					
4	0.15	0.68	0.57	1.68	0.36	1.03
6	0.1	0.33	0.51	1.06	0.25	0.38
21	0.16	0.4	0.38	1.07	0.3	0.49
25	0.07	0.37	0.42	1.48	0.28	0.37
51	0.03	0.07	0.23	0.8	0.13	0.25
114	0.23	0.74	0.6	1.53	0.41	0.84
116	0.48	1.4	0.76	2.4		

Comparison between aircraft and accelerometer position

Ratio of Aircraft	radial to tangential 80% 225Hz	radial to tangential 93% 264 Hz	axial to tangential 80% 225Hz	axial to tangential 93% 264 Hz
	Left hand side AMAD Gearbox			
4	0.13	0.25	0.58	0.46
6	0.16	0.34	0.34	0.39
21	0.18	0.38	0.55	0.53
25	0.09	0.28	0.45	0.4
51	0.04	0.21	0.32	0.27
114	0.41	0.57	0.4	0.56
116	0.3	0.26		
MEAN	*0.17*	*0.34*	*0.44*	*0.43*
	Right hand side AMAD Gearbox			
4	0.26	0.41	0.62	0.61
6	0.2	0.31	0.48	0.46
21	0.4	0.38	0.78	0.25
25	0.18	0.25	0.67	0.25
51	0.14	0.08	0.57	0.32
114	0.39	0.48	0.69	0.55
116	0.64	0.58		
MEAN	*0.26*	*0.32*	*0.63*	*0.43*

Table 7(a) Comparison data for different accelerometer location and power settings

Table 7(b) Comparison data for different accelerometer location and power settings

Comparison between vibration levels at differing shaft speeds

Ratio of 94% (264Hz) to 80% (225Hz)

Aircraft	ACC #1 (radial)		ACC #2 (tangential)		ACC #3 (axial)	
	LHS	RHS	LHS	RHS	LHS	RHS
4	0.20	0.22	0.38	0.34	0.47	0.29
6	0.18	0.31	0.40	0.49	0.35	0.55
21	0.27	0.38	0.57	0.36	0.59	0.52
25	0.18	0.20	0.54	0.29	0.61	0.65
51	0.09	0.47	0.46	0.29	0.55	0.44
114	0.34	0.32	0.48	0.39	0.35	0.42
116	0.41	0.34	0.36	0.32		
MEAN	*0.21*	*0.32*	*0.47*	*0.36*	*0.49*	*0.48*

Comparison between vibration levels at differing shaft speeds

Ratio of RHS to LHS

Aircraft	ACC #1 (radial)			ACC #2 (tangential)			ACC #3 (axial)		
	80%	94%	*MEAN*	80%	94%	*MEAN*	80%	94%	*MEAN*
4	1.90	1.74	*1.82*	0.96	1.06	*1.01*	1.03	1.41	*1.22*
6	1.56	0.91	*1.23*	1.21	0.99	*1.10*	1.71	0.93	*1.32*
21	1.36	0.96	*1.16*	0.61	0.95	*0.78*	0.86	0.84	*0.85*
25	1.32	1.17	*1.24*	0.71	1.34	*1.02*	1.06	0.85	*0.95*
51	1.75	0.35	*1.05*	0.56	0.89	*0.73*	1.00	1.07	*1.03*
114	0.88	0.96	*0.92*	0.92	1.12	*1.02*	1.58	1.11	*1.34*
116	1.00	1.19	*1.09*	0.47	0.53	*0.50*			
MEAN	*1.46*	*1.01*	*1.24*	*0.83*	*1.06*	*0.94*	*1.20*	*1.03*	*1.12*

Ch #1 - Tangential

Tape (h:mm:ss)	Order	Frequency (Hz)	Amplitude (mV rms)	Acceleration (in/s^2)	Acc. Phase (deg)	Displacement (mils P-P)	Disp. Phase (deg)
0:00:10	1	188	5.99	230.25	-161.6	0.47	-341.6
	2	376	1.43	54.97	66.5	0.03	-113.5
	3	567	6.11	234.86	57.2	0.05	-122.8
0:00:03	1	194	8.15	313.27	-165.4	0.60	-345.4
	2	388	2.11	81.11	62.6	0.04	-117.4
	3	582	10.40	399.76	31.2	0.08	-148.8
0:01:40	1	200	8.21	315.58	-160.8	0.57	-340.8
	2	401	1.17	44.97	71.2	0.02	-108.8
	3	601	19.10	734.18	-39.2	0.15	-219.2
0:01:50	1	204	8.45	324.81	-164.6	0.56	-344.6
	2	409	1.89	72.65	99.7	0.03	-80.3
	3	612	11.10	426.67	-131.0	0.08	-311.0
0:02:10	1	210	10.30	395.92	-155.7	0.64	-335.7
	2	420	2.78	106.86	87.2	0.04	-92.8
	3	630	5.78	222.18	137.7	0.04	-42.3
0:02:30	1	218	11.90	457.42	-149.2	0.69	-329.2
	2	435	4.93	189.50	155.9	0.07	-24.1
	3	653	12.10	465.11	92.9	0.08	-87.1
0:02:50	1	225	18.20	699.58	-147.6	0.99	-327.6
	2	450	6.08	233.71	78.5	0.08	-101.5
	3	675	20.10	772.62	47.8	0.12	-132.2
0:03:10	1	232	16.70	641.92	-153.5	0.85	-333.5
	2	464	5.11	196.42	71.9	0.07	-108.1
	3	696	6.81	261.77	85.9	0.04	-94.1
0:03:30	1	238	22.00	845.65	-153.9	1.07	-333.9
	2	476	7.69	295.59	70.6	0.09	-109.4
	3	713	9.97	383.23	72.2	0.05	-107.8
0:03:50	1	243	25.20	968.65	-148.9	1.18	-328.9
	2	489	9.06	348.25	68.4	0.10	-111.6
	3	729	11.90	457.42	67.3	0.06	-112.7
0:04:10	1	251	32.60	1253.10	-144.5	1.43	-324.5
	2	502	11.40	438.20	64.9	0.12	-115.1
	3	753	13.60	522.76	68.5	0.07	-111.5
0:04:30	1	258	38.70	1487.57	-142.1	1.60	-322.1
	2	516	13.10	503.55	60.5	0.14	-119.5
	3	773	13.70	526.61	51.0	0.06	-129.0
0:05:50	1	261	44.30	1702.83	-142.0	1.79	-322.0
	2	522	18.60	714.96	56.2	0.19	-123.8
	3	783	18.50	711.11	42.0	0.08	-138.0

NOTE: Phase is as-measured acceleration input relative to tacho.
For correct displacement phase add 180 deg to above figures.
Also note accelerometer orientation on casing
For Sinusoidal input, max displacement in
y direction will have negative output

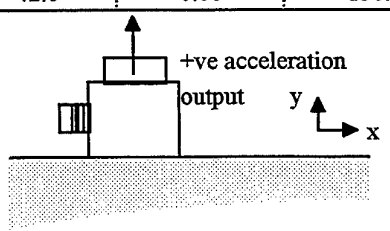

Table 8(a) Casing Vibration data A21-102 LH AMAD

Ch #2 - Radial

Tape (h:mm:ss)	Order	Frequency (Hz)	Amplitude (mV rms)	Acceleration (in/s^2)	Acc. Phase (deg)	Displacement (mils P-P)	Disp. Phase (deg)
0:00:10	1	188	2.13	81.87	-35.8	0.17	-215.8
	2	376	4.07	156.45	150.1	0.08	-29.9
	3	567	1.91	73.42	4.2	0.02	-175.8
0:00:03	1	194	2.95	113.39	-58.2	0.22	-238.2
	2	388	6.23	239.47	151.0	0.11	-29.0
	3	582	3.33	128.00	-34.1	0.03	-214.1
0:01:40	1	200	2.71	104.17	-102.2	0.19	-282.2
	2	401	6.93	266.38	164.8	0.12	-15.2
	3	601	9.31	357.86	-96.7	0.07	-276.7
0:01:50	1	204	0.79	30.37	-101.9	0.05	-281.9
	2	409	8.11	311.74	163.7	0.13	-16.3
	3	612	9.52	365.94	174.2	0.07	-5.8
0:02:10	1	210	1.91	73.42	-89.8	0.12	-269.8
	2	420	10.20	392.07	154.3	0.16	-25.7
	3	630	5.28	202.96	110.5	0.04	-69.5
0:02:30	1	218	2.74	105.32	-105.1	0.16	-285.1
	2	435	12.00	461.26	163.7	0.17	-16.3
	3	653	4.28	164.54	59.0	0.03	-121.0
0:02:50	1	225	4.33	166.44	-118.6	0.24	-298.6
	2	450	16.00	615.02	146.7	0.22	-33.3
	3	675	5.10	196.04	5.5	0.03	-174.5
0:03:10	1	232	4.24	162.98	-143.9	0.22	-323.9
	2	464	12.90	495.86	147.0	0.17	-33.0
	3	696	3.96	152.22	93.9	0.02	-86.1
0:03:30	1	238	6.01	231.02	-145.8	0.29	-325.8
	2	476	18.90	726.49	144.1	0.23	-35.9
	3	713	4.26	163.75	78.5	0.02	-101.5
0:03:50	1	243	7.70	295.98	-145.8	0.36	-325.8
	2	489	22.60	868.71	144.8	0.26	-35.2
	3	729	5.97	229.48	69.9	0.03	-110.1
0:04:10	1	251	11.30	434.36	-153.5	0.49	-333.5
	2	502	28.80	1107.03	144.9	0.31	-35.1
	3	753	7.11	273.30	67.1	0.03	-112.9
0:04:30	1	258	14.10	541.98	-157.5	0.58	-337.5
	2	516	26.20	1007.09	144.7	0.27	-35.3
	3	773	5.67	217.95	52.4	0.03	-127.6
0:05:50	1	261	18.10	695.74	-161.9	0.73	-341.9
	2	522	39.00	1499.11	144.1	0.39	-35.9
	3	783	7.29	280.22	43.1	0.03	-136.9

Table 8(b) Casing Vibration data A21-102 LH AMAD

Aircraft A21-102 LH AMAD 19-23 September 1994

Probe position 1 (25mm aft of leading flex coupling), LH probe

Freq Hz	1X mils P-P	1X phase	2X mils P-P	2X phase	3X mils P-P	3X phase
180.1	13.6	70	2.2	-162	0.7	-111
187	14.1	68	2.2	-163	0.7	-105
195.1	16.7	63.5	2.2	-165	0.7	-93
210	12.25	54.5	2	-165	0.8	-102
217	16.6	65.1	2.1	-165	0.78	-101
225	17.8	67.4	2.2	-168	0.7	-95
232	19.1	61.1	2.1	-171	0.8	-100
240	20.8	59.4	2.2	-172	0.8	-100
243	20.7	60.2	2.2	-174	0.8	-100
247	22.1	60	2.2	-173	0.7	-97
255	23.8	58.6	2.2	-177	1	-117
258	25.1	57	2.3	179	1.3	-91

Table 9 Displacement data A21-102, including 2X, 3X displacements and phase

	Rotate shaft 120 degrees	Shaft Displacement *mils P-P* [3]		Housing Vibration circumferential *in/s rms*	
		80%	100%	80%	100% [4]
Silver Shaft [1] **Old Housing**		9.1	9.8	0.32	0.86
Silver Shaft New Housing		6.0	7.3	0.26	0.63
			8.9		0.94
			9.1		1.04
Silver Shaft Old Housing		9.1	9.8	0.32	0.86
New Shaft [2] **Old Housing**		22.9	39.6	0.75	1.83
A21-049 Shaft Old Housing	Start	12.5	29.0	0.57	1.60
	yes	25.0	41.0	0.66	1.76
	yes	21.7	38.0	0.46	1.44
A21-049 Shaft New Housing		19.3	29.0	0.47	1.14
	yes	22.4	38.0	0.49	1.50
	yes	19.7	37.9	0.21	1.60

1 - The 'Silver Shaft' is the standard Kamatic Test-Rig shaft
2 - This is a LAPTC 19E215 shaft from serviceable stock
3 - These values have not been corrected for slow-roll run-out
4 - 80% and 100% refer to 0.8 and 1.0 times 16810 rpm

Table 10 Vibration and shaft displacement AMAD 1396 Lucas Aerospace Test Rig

Appendix 1

AMAD gearbox PTS ball bearing 42312-366 data

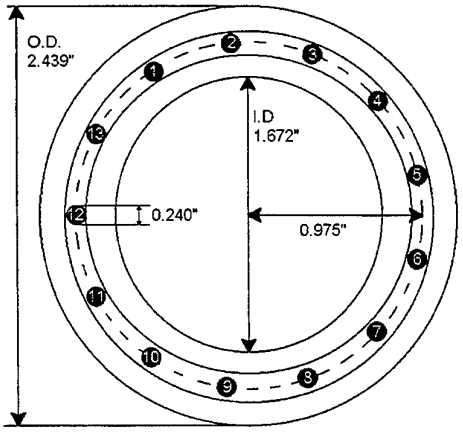

13 Balls

Calculation of characteristic frequencies:

Ball passing frequency relative to stationary outer race - $$f_o = \frac{1}{2} f_s n \left[1 - \left(\frac{r}{R} \right) \cos\alpha \right]$$

Ball passing frequency relative to rotating inner race - $$f_i = \frac{1}{2} f_s n \left[1 + \left(\frac{r}{R} \right) \cos\alpha \right]$$

Ball passing frequency for cage relative to stationary outer race - $$f_c = \frac{1}{2} f_s \left[1 - \left(\frac{r}{R} \right) \cos\alpha \right]$$

Rotation frequency for balls relative to stationary outer race - $$f_r = f_s \frac{R}{2r} \left[1 - \left(\frac{r}{R} \right)^2 \cos^2\alpha \right]$$

f_s - frequency of revolution
n - number of balls
r - radius of balls
R - distance from center of bearing to center of balls
α - contact angle

for contact angle = 0°
f_o - $5.701 f_s$
f_i - $7.300 f_s$
f_c - $0.4385 f_s$
f_r - $4.001 f_s$

Appendix 2

19E215-1 driveshaft characteristics

Table A2.1 load vs deflection for coupling in transverse shear measured at the engine end shaft coupling

Load lbs	*0 deg mils*	*120 deg mils*	*240 deg mils*
0	0	0	0
20	1.2	1.1	1.2
40	2.3	2.25	2.4
60	3.4	3.4	3.6
80	4.6	4.5	4.8
90	5.1	5	5.4

NOTE : Due to the way in which load was applied, the force across the coupling has to be factored by 303/325, so that:

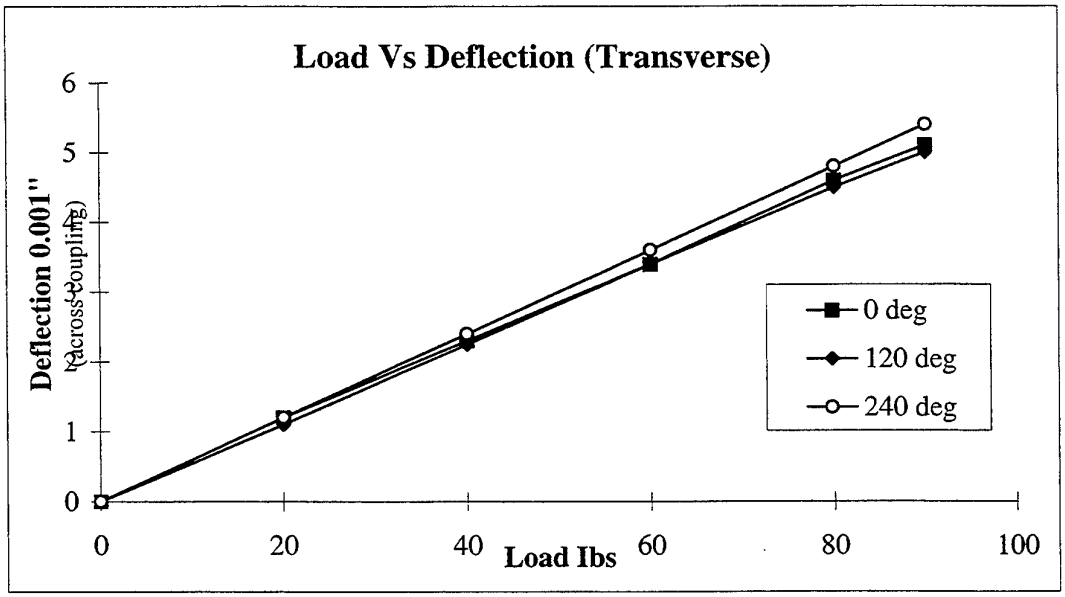

Figure A2.1 load vs deflection for coupling in transverse shear

$$\text{stiffness (lbs/in)}_{\text{(transverse)}} = \frac{90 \text{ lbs} * 303/325}{0.005\text{"(approx)}} = 16{,}781 \text{ lb/in}$$

Appendix 2 (cont.)
19E215-1 driveshaft characteristics

LAPTC (19E215-1) Shaft Dimensions
Tube Thickness 1.09 mm (measured) -Titanium
Central Tube OD 46.18 mm, length 292 mm (measured) - Titanium

Overall weight	1.632 kg	(3.59 lbm)
Gearbox end	0.730 kg	
Engine end	0.902 kg	
Overall length	435.0 mm	(17.125 in)

Angular Stiffness of Coupling

Force N	*Deflection mm*
0	0
1.92	2.54
2.09	2.74
5.09	6.52

NOTE : force applied 310 mm from centre of coupling
deflection measured 382 mm from centre of coupling

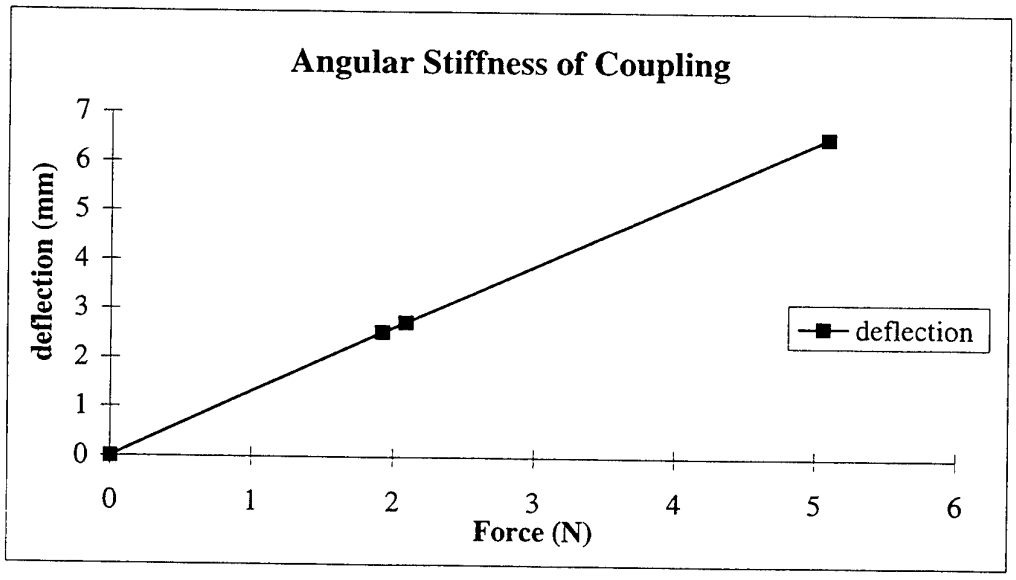

Appendix 3

Vibration data sheet

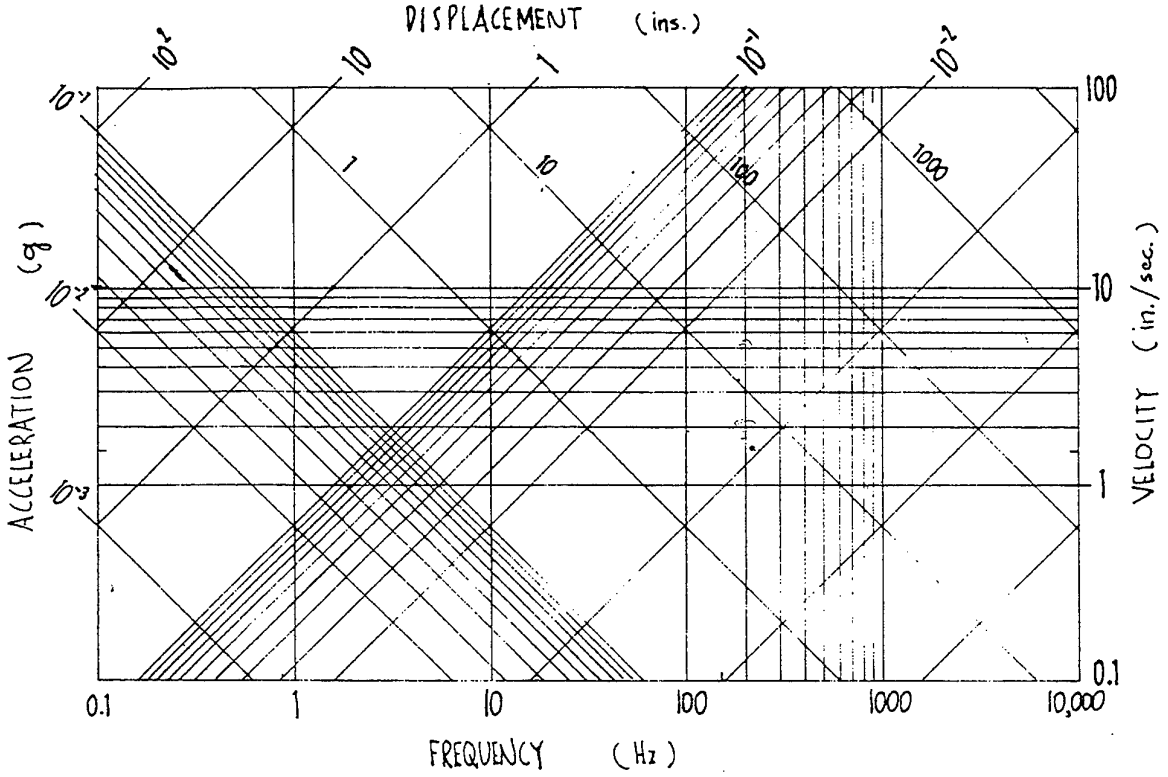

KINEMATIC RELATIONS IN HARMONIC VIBRATION

showing maximum amplitudes of displacement, velocity, acceleration

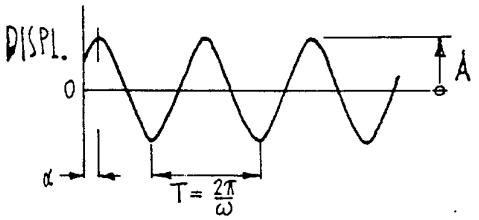

Displacement

$x = A \cos(\omega t + \alpha)$, $|x_{max}| = A$

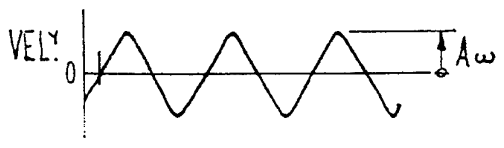

Velocity

$\dot{x} = -A\omega \sin(\omega t + \alpha)$, $|\dot{x}_{max}| = A\omega$

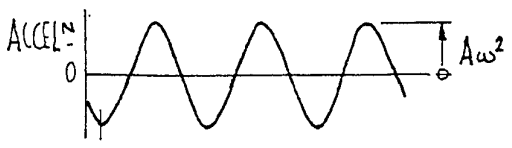

Acceleration

$\ddot{x} = -A\omega^2 \cos(\omega t + \alpha)$, $|\ddot{x}_{max}| = A\omega^2$

A3.1

Appendix 4

A21-039 and A21-052 Chadwick Helmuth 192A comparison and shaft rotation

Aircraft A21-039

Casing vibration

	Endevco in/s peak 1X	**192A** in/s peak 1X	**Phase** Deg
Rotate Left Side AMAD / Power 80% (226 Hz)			
Start	1.2	1.25	152
120 deg CW	0.89		68.8
240 deg CW	0.69		-94
360 deg CW	1.12		147
Right Side AMAD / Power 80%			
Start	0.55		-61
120 deg CW	0.85		
240 deg CW	0.97		167
360 deg CW	0.78		23.3

Aircraft A21-052

Casing vibration

	Endevco in/s peak 1X	**192A** in/s peak 1X
Left Side AMAD	0.97	0.8-0.85
Right Side AMAD	0.61	0.6

Appendix 5

Vibration level comparison summary

Vibration level comparison between accelerometer position, engine speed and the side of measurement on the F/A - 18 AMAD gearbox

1. A relationship has been found that relates the level of vibration[1] at 80% to 94% of maximum shaft speed, where maximum shaft speed is 16810 rpm (280Hz) and 80 % is 13500 rpm (225Hz) and 94% 15633 Hz (264Hz) rated as full military power.

This relationship can be summarised as follows :

RATIO OF 225 Hz (80%) to 264 Hz (94%)

	Right hand side	Left hand side
Radial velocity (in/s)	30 %	20 %
Tangential velocity (in/s)	35 %	48 %
Axial velocity (in/s)	48 %	50 %

2. The relationship between the side of measurement ie; left hand or right hand side can be summarised as follows :

Radial vibration : Right hand side > left hand side
Tangential vibration : Right hand side < left hand side
Axial vibration : Right hand side > left hand side

3. The relationship between the direction acceleration measurement, ie radial, tangential and axial can be summarised as follows :

	Right hand side		Left hand side	
	225 Hz (80%)	264 Hz (94%)	225 Hz (80%)	264 Hz (94%)
Ratio of radial vibration to tangential	0.26	0.32	0.17	0.35
Ratio of axial vibration to tangential	0.63	0.43	0.45	0.45

[1] All vibration measurements refer to once/rev frequency component only.

Appendix 6

Shaft displacement (mils peak-peak) versus speed for shaft orbits A21-102 LH AMAD

Position		amplitude (.001" p-p)	phase						
axial	circumf	40 Hz		50 Hz		70 Hz		100 Hz	
1	A	2.90	76.00	2.90	78.00	3.90	87.00	5.90	70.00
1	B	2.80	165.00	2.40	162.00	2.90	153.00	4.20	158.00
2	A	3.00	129.00	3.00	129.00	3.10	128.00	4.50	105.00
2	B	2.80	-133.00	2.80	-133.00	3.30	-131.00	3.50	-140.00
3	A	1.50	-125.00	1.70	-121.00	1.90	-92.00	1.70	-131.00
3	B	2.02	-30.00	1.50	-30.00	2.26	-19.00	1.24	-11.00

		180 Hz		195 Hz		210 Hz		217 Hz	
1	A	13.60	70.00	16.70	63.50	12.25	54.50	16.60	65.10
1	B	11.00	154.00	11.04	155.00	18.10	158.00	17.60	151.00
2	A	9.90	86.00	12.60	75.10	8.30	73.00	10.70	74.00
2	B	7.50	166.00	7.10	-173.00	11.80	170.00	12.70	169.00
3	A	1.30	146.00	2.50	84.00	1.10	-65.00	0.70	-19.00
3	B	1.70	124.00	0.97	61.00	2.40	178.00	2.30	-156.00

		225 Hz		232 Hz		240 Hz		247 Hz	
1	A	17.80	67.40	19.10	61.10	20.80	59.40	22.10	60.00
1	B	16.90	146.00	19.50	153.00	20.40	154.00	21.80	151.00
2	A	13.20	71.00	13.50	68.00	14.30	68.00	15.90	68.00
2	B	12.10	166.00	13.20	166.00	14.70	165.00	15.40	162.00
3	A	1.50	-26.00	5.10	-83.00	2.30	78.00	3.50	72.00
3	B	3.66	-164.00	10.90	157.00	3.00	180.00	3.10	163.00

		255 Hz	
1	A	23.80	58.60
1	B	22.80	150.00
2	A	17.80	67.00
2	B	17.00	163.00
3	A	3.50	65.00
3	B	3.85	161.00

NOTE
All displacements mils p-p
Indikom probes have a negative sensitivity
ie -100 mV/mil
Phase is as-measured
Displacement output relative to tacho

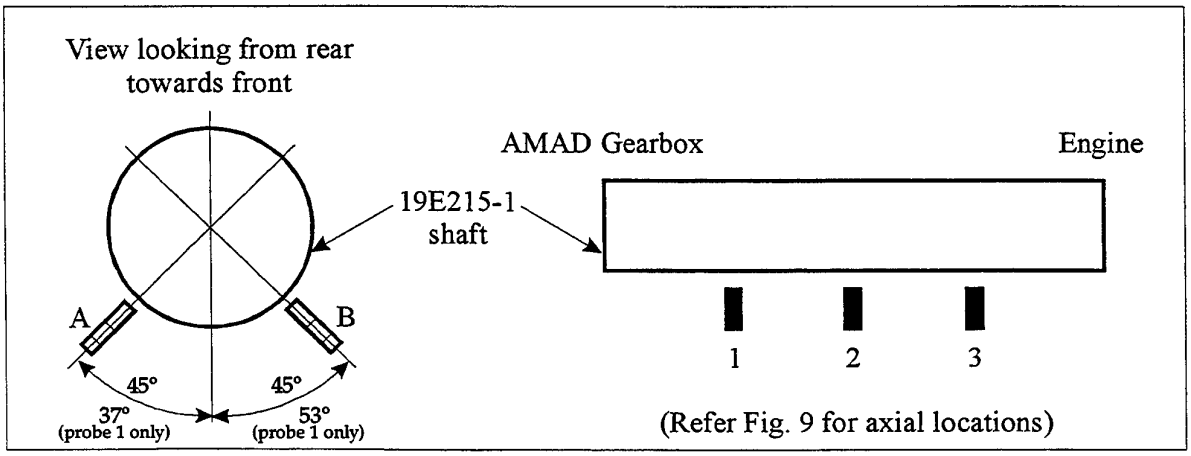

DISTRIBUTION LIST

An Investigation of F/A-18 AMAD Gearbox Driveshaft Vibration

Brian Rebbechi, Madeleine Burchill, Gareth Coco

AUSTRALIA

DEFENCE ORGANISATION

Task Sponsor DTA-LC

S&T Program

Chief Defence Scientist
FAS Science Policy
AS Science Corporate Management
} shared copy

Director General Science Policy Development
Counsellor Defence Science, London (Doc Data Sheet)
Counsellor Defence Science, Washington (Doc Data Sheet)
Scientific Adviser to MRDC Thailand (Doc Data Sheet)
Director General Scientific Advisers and Trials/Scientific Adviser Policy and Command (shared copy)
Navy Scientific Adviser
Scientific Adviser - Army (Doc Data Sheet and distribution list only)
Air Force Scientific Adviser
Director Trials

Aeronautical and Maritime Research Laboratory

Director
Research Leader Propulsion
Research Leader Structural Dynamics
Head Machine Dynamics
Brian Rebbechi
Madeleine Burchill
Gareth Coco
David Blunt
Mark Shilo
B. David Forrester
G. Clark
P.K. Sharp
R. Byrnes
N.T. Goldsmith
W. Waldman

DSTO Library

Library Fishermens Bend
Library Maribyrnong
Library Salisbury (2 copies)
Australian Archives
Library, MOD, Pyrmont (Doc Data sheet only)

Capability Development Division

Director General Maritime Development
Director General Land Development (Doc Data Sheet only)
Director General C3I Development (Doc Data Sheet only)

Navy

SO (Science), Director of Naval Warfare, Maritime Headquarters Annex, Garden Island, NSW 2000 (Doc Data Sheet and distribution list only)
Aircraft Maintenance and Flight Trials Unit
Director of Aircraft Engineering-Navy
Director of Aviation Projects-Navy
Chief Aeronautical Engineer, Naval Aircraft Logistics Office
Senior Propulsion Engineer, Naval Aircraft Logistics Office, Locked Bag 12, Naval Support Command, Pyrmont NSW 2009
Director General Force Development (Sea), (Doc Data Sheet only)
Senior Propulsion Engineer, Naval Aircraft Logistics Office, Locked Bag 12, Naval Support Command, Pyrmont NSW 2009

Army

ABCA Office, G-1-34, Russell Offices, Canberra (4 copies)
SO (Science), DJFHQ(L), MILPO Enoggera, Queensland 4051 (Doc Data Sheet only)
NAPOC QWG Engineer NBCD c/- DENGRS-A, HQ Engineer Centre Liverpool Military Area, NSW 2174 (Doc Data Sheet only)
Army Aviation Support Group, Oakey QLD

Air Force

Aircraft Research and Development Unit
Chief Engineer, TFLMSQN (3 copies)
2 OCU (SENGO)
77 SQN (SENGO)
3 SQN (SENGO)
75 SQN (SENGO)
481 WG (OIC EMS)
SCI-4 (DTA-LSA)
RAAF TLO North Island, San Diego
ALLMSQN (CENGR)
SRLMSQN, OIC ENGSPT
501WG ECMF TST L
Directorate of Flying Safety - AF
Army LMSQN Oakey, QLD

Intelligence Program

DGSTA Defence Intelligence Organisation

Corporate Support Program (libraries)

OIC TRS, Defence Regional Library, Canberra
Officer in Charge, Document Exchange Centre (DEC), 1 copy
*US Defence Technical Information Center, 2 copies
*UK Defence Research Information Centre, 2 copies
*Canada Defence Scientific Information Service, 1 copy
*NZ Defence Information Centre, 1 copy
National Library of Australia, 1 copy

UNIVERSITIES AND COLLEGES

Australian Defence Force Academy
Library
Head of Aerospace and Mechanical Engineering
Senior Librarian, Hargrave Library, Monash University
Librarian, Flinders University

OTHER ORGANISATIONS

NASA (Canberra)
AGPS

OUTSIDE AUSTRALIA

ABSTRACTING AND INFORMATION ORGANISATIONS

INSPEC: Acquisitions Section Institution of Electrical Engineers
Library, Chemical Abstracts Reference Service
Engineering Societies Library, US
Materials Information, Cambridge Scientific Abstracts, US
Documents Librarian, The Center for Research Libraries, US

INFORMATION EXCHANGE AGREEMENT PARTNERS

Acquisitions Unit, Science Reference and Information Service, UK
Library - Exchange Desk, National Institute of Standards and Technology, US
National Aerospace Laboratory, Japan
National Aerospace Laboratory, Netherlands

ADDITIONAL DISTRIBUTION

Keith Rowley NADEP, North Island, San Diego
Kevin Widman NAVAIR, Washington
Donald Altobelli (AIR 4.4.6) Naval Air Warfare Center Aircraft Division-Patuxent River Propulsion and power Engineering, 48256 Shaw Road; Unit #4; Building 1461 Patuxent River, Maryland 20670-1900
Lucas Geared Systems, Park City UT (Gregory Perez, JR)
Lucas Power Transmission Company, Utica NY (Dr. J. A. Stocco, R. Iyer)
Mr C. Neubert, Drive Systems and Diagnostics, Naval Air Warfare Center - Aircraft Division, PO Box 7176 Trenton, New Jersey 08628 - 0176 USA
Mr J.J. Coy and D. P. Townsend, Mechanical Systems Technology Branch, Mail Stop 77-10, NASA Lewis, 21000 Brook Park Road, Cleveland, Ohio 44135 USA
Life Cycle Material Manager CF-18/F404 Engines Canadian Forces (WO R. M. Cook)

SPARES (25 copies)

Total number of copies: 114

DEFENCE SCIENCE AND TECHNOLOGY ORGANISATION
DOCUMENT CONTROL DATA

1. PRIVACY MARKING/CAVEAT (OF DOCUMENT)

2. TITLE

An Investigation of F/A-18 AMAD Gearbox Driveshaft Vibration

3. SECURITY CLASSIFICATION (FOR UNCLASSIFIED REPORTS THAT ARE LIMITED RELEASE USE (L) NEXT TO DOCUMENT CLASSIFICATION)

Document (U)
Title (U)
Abstract (U)

4. AUTHOR(S)

Brian Rebbechi, Madeleine Burchill, Gareth Coco

5. CORPORATE AUTHOR

Aeronautical and Maritime Research Laboratory
PO Box 4331
Melbourne Vic 3001 Australia

6a. DSTO NUMBER	6b. AR NUMBER	6c. TYPE OF REPORT	7. DOCUMENT DATE
DSTO-TN-0121	AR-010-389	Technical Note	November 1997

8. FILE NUMBER	9. TASK NUMBER	10. TASK SPONSOR	11. NO. OF PAGES	12. NO. OF REFERENCES
M1/9/146	AIR 94/226	DTA-LC	100	12

13. DOWNGRADING/DELIMITING INSTRUCTIONS

None

14. RELEASE AUTHORITY

Chief, Airframes and Engines Division

15. SECONDARY RELEASE STATEMENT OF THIS DOCUMENT

Approved for public release

OVERSEAS ENQUIRIES OUTSIDE STATED LIMITATIONS SHOULD BE REFERRED THROUGH DOCUMENT EXCHANGE CENTRE, DIS NETWORK OFFICE, DEPT OF DEFENCE, CAMPBELL PARK OFFICES, CANBERRA ACT 2600

16. DELIBERATE ANNOUNCEMENT

No Limitations

17. CASUAL ANNOUNCEMENT Yes

18. DEFTEST DESCRIPTORS

See your Client Liaison Librarian for DEFTEST terms

19. ABSTRACT

The RAAF has experienced several failures of the input bearing of the F/A-18 AMAD (Aircraft Mounted Accessory Drive) gearbox. Two of these failures have resulted in in-flight fires. Measurements of input housing vibration showed very high vibration levels on some aircraft, apparently due to unbalance in the driveshaft assembly. Subsequent measurement of drive-shaft motion confirmed synchronous forward whirl of the driveshaft. The driveshaft system appears to operate below its first critical speed, but there are indications that the first critical speed may not be far above running speed. There is no evidence of significant driveshaft system resonances during the operating speed range of idle to full military power. The unbalance appears to result primarily from clearances in the AMAD gearbox input shaft assembly. These clearances will bring about an initial unbalance of the assembly much greater than specified component tolerances. Partial alleviation of the high vibration has been brought about by rotation of the 19E215-1 driveshaft relative to the input power take-off shaft assembly.

TECHNICAL NOTE DSTO-TN-0121 AR-010-389 NOVEMBER 1997

AERONAUTICAL AND MARITIME RESEARCH LABORATORY
GPO BOX 4331 MELBOURNE VICTORIA 3001
AUSTRALIA, TELEPHONE (03) 9626 7000